

AD-A222 096

WRDC-TR-90-3006

DESIGN OF ROBUST MULTIVARIABLE CONTROLLERS

Borchin C. Chang
Drexel University
Philadelphia, PA

APRIL 1990

FINAL REPORT FOR THE PERIOD APRIL 1988 TO APRIL 1990

APPROVED FOR PUBLIC RELEASE; DISTRIBUTION UNLIMITED

FLIGHT DYNAMICS LABORATORY
WRIGHT RESEARCH AND DEVELOPMENT CENTER
AIR FORCE SYSTEMS COMMAND
WRIGHT-PATTERSON AIR FORCE BASE, OHIO 45433-6553

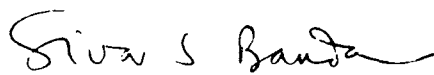


NOTICE

When Government drawings, specifications, or other data are used for any purpose other than in connection with a definitely Government-related procurement, the United States Government incurs no responsibility or any obligation whatsoever. The fact that the Government may have formulated or in any way supplied the said drawings, specifications, or other data, is not to be regarded by implication, or otherwise in any manner construed, as licensing the holder, or any other person or corporation; or as conveying any rights or permission to manufacture, use, or sell any patented invention that may in any way be related thereto.

This report is releasable to the National Technical Information Service (NTIS). At NTIS, it will be available to the general public, including foreign nations.

This technical report has been reviewed and is approved for publication.

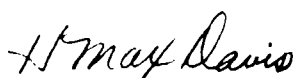


SIVA S. BANDA
Project Engineer
Control Dynamics Branch
Flight Control Division



DAVID K. BOWSER, Chief
Control Dynamics Branch
Flight Control Division

FOR THE COMMANDER



H. MAX DAVIS, Assistant for
Research and Technology
Flight Control Division
Flight Dynamics Laboratory

"If your address has changed, if you wish to be removed from our mailing list, or if the addressee is no longer employed by your organization, please notify WRDC/FIGC, Wright-Patterson AFB, OH 45433-6553 to help us maintain a current mailing list."

Copies of this report should not be returned unless return is required by security considerations, contractual obligations, or notice on a specific document.

REPORT DOCUMENTATION PAGE				Form Approved OMB No. 0704-0188	
1a. REPORT SECURITY CLASSIFICATION UNCLASSIFIED			1b. RESTRICTIVE MARKINGS N/A		
2a. SECURITY CLASSIFICATION AUTHORITY N/A			3. DISTRIBUTION/AVAILABILITY OF REPORT Approved for Public Release, Distribution is Unlimited		
2b. DECLASSIFICATION/DOWNGRADING SCHEDULE N/A					
4. PERFORMING ORGANIZATION REPORT NUMBER(S)			5. MONITORING ORGANIZATION REPORT NUMBER(S) WRDC-TR-90-3006		
6a. NAME OF PERFORMING ORGANIZATION Drexel University		6b. OFFICE SYMBOL (If applicable) N/A	7a. NAME OF MONITORING ORGANIZATION Flight Dynamics Laboratory (WRDC/FIGC) Wright Research and Development Center		
6c. ADDRESS (City, State, and ZIP Code) Philadelphia PA 19104			7b. ADDRESS (City, State, and ZIP Code) Wright-Patterson AFB OH 45433-6553		
8a. NAME OF FUNDING/SPONSORING ORGANIZATION Wright Research and Development Center		8b. OFFICE SYMBOL (If applicable) WRDC/FIGC	9. PROCUREMENT INSTRUMENT IDENTIFICATION NUMBER F33615-88-C-3600		
8c. ADDRESS (City, State, and ZIP Code) Wright-Patterson AFB OH 45433-6553			10. SOURCE OF FUNDING NUMBERS		
PROGRAM ELEMENT NO. 61102F		PROJECT NO. 2304	TASK NO. N2	WORK UNIT ACCESSION NO. 02	
11. TITLE (Include Security Classification) Design of Robust Multivariable Controllers					
12. PERSONAL AUTHOR(S) Borchin C. Chang					
13a. TYPE OF REPORT Final		13b. TIME COVERED FROM 5 Apr 88 TO 13 Apr 90		14. DATE OF REPORT (Year, Month, Day) 1990 April	
15. PAGE COUNT 111					
16. SUPPLEMENTARY NOTATION					
17. COSATI CODES			18. SUBJECT TERMS (Continue on reverse if necessary and identify by block number)		
FIELD	GROUP	SUB-GROUP	Multivariable Systems		
01	04		Unstructured Uncertainty		
			Robust Control		
			H _∞ Optimization		
19. ABSTRACT (Continue on reverse if necessary and identify by block number) Two major problems, the solution of H _∞ optimization problem and the computation of the real structured singular value, are addressed in the report. The observer based controller parameterization, inner-outer factorization, and a state-space size-reduction technique were used to simplify the H _∞ formulation and a fast γ-iteration algorithm was proposed to compute the optimal H _∞ norm of a 2-Block problem. The DGKF's two-Riccati equation method was employed to design a nearly H _∞ optimal controller for a 4-Block problem. An iterative approach for computing the real structured singular value was developed based on a multi-linear mapping from the parameter space to the coefficient space, edge theorem, parameter domain partitioning, and a fast stability checking of the segment of a polytope.					
20. DISTRIBUTION/AVAILABILITY OF ABSTRACT <input checked="" type="checkbox"/> UNCLASSIFIED/UNLIMITED <input type="checkbox"/> SAME AS RPT <input type="checkbox"/> DTIC USERS			21. ABSTRACT SECURITY CLASSIFICATION UNCLASSIFIED		
22a. NAME OF RESPONSIBLE INDIVIDUAL SIVA S. RANDA			22b. TELEPHONE (Include Area Code) (513) 255-8677		22c. OFFICE SYMBOL WRDC/FIGC

FOREWORD

This report was prepared by the Department of Mechanical Engineering and Mechanics, Drexel University, Philadelphia, Pennsylvania, under the Air Force Contract F33615-88-C-3600 sponsored by AFOSR. The work was performed under the direction of Dr. S. S. Banda, Dr. H. H. Yeh of the Flight Dynamics Laboratory, Wright Research & Development Center, Wright-Patterson Air Force Base, Ohio.

The technical work was conducted by Dr. B. C. Chang, Principal Investigator, and his research assistants O. Ekdal, H. Bouguerra, and X. P. Li during the period April 1988 - April 1990.

The investigators in this study would like to thank to Dr. S. S. Banda and Dr. H. H. Yeh for their continuous encouragement and numerous valuable technical discussions.



Accession For	
NTIS GRA&I	<input checked="checked" type="checkbox"/>
DTIC TAB	<input type="checkbox"/>
Unannounced	<input type="checkbox"/>
Justification	
By _____	
Distribution/	
Availability Codes	
Dist	Avail and/or Special
A-1	

Table of Contents

Section	Page
1. Introduction	1
2. H^∞ Formulation of Control Problems	5
2.1 Standard H^∞ Optimization Problem	5
2.2 Formulation of Control Problems as the Standard H^∞ Optimization Problem	6
2.2.1 A Mixed-Sensitivity Optimization Problem	6
2.2.2 A Tracking/Disturbance Reduction Problem	8
3. Stabilization and Observer-based Controller Parametrization	10
3.1 Basic Concept of Controller Parametrization	10
3.2 Youla's Controller Parametrization	13
3.3 Observer-based Controller Parametrization and Its Properties	16
4. Solutions for the Standard H^∞ Optimization Problems	20
4.1 Controller Parametrization and Inner-Outer Factorization	22
4.2 Size Reduction In Four-Block H^∞ Formulation	26
4.3 Fast γ -iteration Algorithm for the Solution of the Two-block H^∞ Optimization Problem	38
4.3.1 Basic Concept of Fast γ -iteration	38
4.3.2 Bounds and Properties of the Function $\mu(\gamma)$	41
4.3.3 Fast γ -Iteration Algorithm	45
4.4 Using DGKF's Solution To Solve A Four-Block H^∞ Optimization Problem	49

Table of Contents (Cont'd)

Section	Page
5. Computation of the Real Structured Singular Value	54
5.1 Definition of the Real Structured Singular Value and Preliminaries	55
5.2 Multilinear Mapping and the Polytopic Polynomials	60
5.3 Algorithm For The Real Structured Singular Value	66
5.4 Fast Algorithm to Check the Stability of Segments	75
6. Conclusion and Further Research	83
6.1 Concluding Remarks	83
6.2 Further Research Suggestions	85
References	88
Appendix A: Proof of Theorems	95
Appendix B: Checking Real Solution Existence by Using Sturm Theorem	104

SECTION 1

INTRODUCTION

Two robustness issues are considered in the research project. One is the command/disturbance input uncertainties and the other is the plant uncertainties. The controller is to be designed such that the closed-loop system remains stable for all possible plant perturbations and the error response is minimized for all disturbances and commands in the prescribed set.

The prescribed set of disturbances and commands is modeled by the designer according to the real-world environment of the system. If the set of disturbances and commands under consideration can be described by a random process then a stochastic design approach like LQG [1] or Wiener-Hopf [2] method can be used to minimize the mean value of the error energy. On the other hand, if we do not have any useful statistical information about the disturbances and the commands, then a new developed H^∞ optimization approach [3-29] is recommended. The H^∞ optimization approach is a minmax design method which minimizes the maximal error energy for all possible disturbances and commands in the prescribed set.

The concept of H^∞ optimization was initiated by G. Zames [3] in 1981. Since then, this new research area has attracted many researchers [4-29]. The popularity of this research area is mainly because this area appears to have a major impact on future engineering practice.

H^∞ optimization technique is a powerful tool which not only allows us to consider a more general class of command and disturbance inputs than those considered by LQG and W-H approaches but also has the ability to handle the plant uncertainties [10-29]. H^∞ optimization technique uses the H^∞ norm of a transfer function matrix as the measure of the error response of a system. This reflects the maximum error energy which may occur in

reality. YJB controller parametrization [2,11,30-32] is employed to characterize the set of the controllers which solve the stabilization problem. Then among the controllers in the set, we will find the one that minimizes the error response subject to control-input and stability-margin constraints.

Two kinds of plant uncertainties are considered. One is the unstructured uncertainty and the other is the real parameter perturbation. The maximum singular value of the complementary sensitivity function is used as a measure of robust stability for the unstructured perturbation and the real structured singular value (or the multivariable stability margin) is used to measure the robust stability for a system under parameter perturbations.

The control problem is formulated in a general way. The models of the plant uncertainties and the reference and disturbance inputs are general enough to reflect the situations found in actual problems and the controller structure is the most general one under linear time-invariance which includes the two-degree-of-freedom controllers.

Although our design basically is a frequency-domain approach, the computation is not necessarily done in frequency domain. As a matter of fact, many algorithms developed on the state-space framework have better numerical properties than their counterparts based on polynomial matrix manipulations. All the computations in our design are implemented on the state-space framework. Furthermore, many pole-zero cancellations can be done theoretically without using any numerical minimal realization technique. This theoretical pole-zero cancellation technique [11,12,21-24] can save a lot of computing time and avoid incomplete cancellation due to rounding errors. It is possible to perform all the computation in a numerically stable, reliable, and efficient way.

Throughout the report, both of the notations $\begin{bmatrix} A & B \\ C & D \end{bmatrix}$ and $\{ A, B, C, D \}$ are

used for the same purpose to represent a state-space realization of a system whose transfer function is $C(sI-A)^{-1}B + D$. $\mathbb{R}(s)^{p \times q}$ is the set of proper rational matrices with real coefficients. $(RH^\infty)^{m \times r}$ is the set of $m \times r$ proper rational matrices with real coefficients which are analytic in the closed right half plane. $(RL^\infty)^{m \times r}$ is the set of $m \times r$ proper rational matrices with real coefficients which are analytic on the imaginary axis.

Section 2 shows how to formulate a control problem into the standard H^∞ optimization problem. A mixed-sensitivity problem and a tracking/disturbance reduction problem are employed to illustrate the formulation procedure.

Section 3 reveals some useful properties of the observer-based controller parametrization. The poles of the closed-loop system with the observer-based controller parametrization are the regulator poles, the observer poles, and the poles of the added parameter matrix. The set of uncontrollable and/or unobservable controller poles is a subset of the regulator and the observer poles. The poles of the closed-loop system with the minimal order controller will include all the poles of the parameter matrix and some of the regulator and the observer poles which are not the removable controller poles. These properties could be useful in controller reduction.

Section 4 presents solutions to the standard H^∞ optimization problem. In Sec. 4.1, the observer-based controller parametrization is used to characterize the set of stabilizing controllers and to reduce the transfer matrix of interest as an affine function of a stable parameter matrix. The affine equation is then reduced further by inner-outer factorizations to a simple linear equation. In Sec.4.2, a size reduction technique is used to reduce the order of the rational matrices involved in the equation. A fast γ -iteration algorithm for the solution of the two-block H^∞ optimization problem is summarized in Sec.4.3. In Sec.4.4,

the recently developed DGKF approach [29] is employed to solve the four-block H^∞ optimization problem. Some numerical difficulties we encountered will be discussed.

Section 5 presents our results in the computation of the real structured singular value (or the real multivariable stability margin). In Sec.5.1, the basic concepts of the proposed algorithm are briefly described. In section 5.2, the mapping properties from the parameter space to the coefficient space and the theories on which the iterative algorithm is developed will be demonstrated. The iterative algorithm for computing the real structured singular value is summarized in Sec.5.3. Sec.5.4 is a summary of the fast segment stability checking algorithm which is used repeatedly in the proposed iterative algorithm in computing the real SSV.

Section 6 is the conclusion and further research suggestions.

SECTION 2

H[∞] FORMULATION OF CONTROL PROBLEMS

2.1 Standard H[∞] Optimization Problem

Most control problems can be formulated as the following standard H[∞] optimization problem. In the standard H[∞] optimization problem formulation, the system representation is rearranged as follows.

$$\begin{bmatrix} z(s) \\ y(s) \end{bmatrix} = \begin{bmatrix} G_{11}(s) & G_{12}(s) \\ G_{21}(s) & G_{22}(s) \end{bmatrix} \begin{bmatrix} v(s) \\ u(s) \end{bmatrix} := G(s) \begin{bmatrix} v(s) \\ u(s) \end{bmatrix} \quad (2.1-1)$$

where $G_{11}(s) \in \mathbb{R}(s)^{p \times q}$, $G_{12}(s) \in \mathbb{R}(s)^{p \times m}$, $G_{21}(s) \in \mathbb{R}(s)^{r \times q}$, and $G_{22}(s) \in \mathbb{R}(s)^{r \times m}$. $\mathbb{R}(s)^{p \times q}$ is the set of proper rational matrices with real coefficients. In (2.1-1), z , y , v , and u are the controlled output, the measured output, the exogenous input, and the control input respectively. The controlled input vector z usually includes the error signal and a weighted control input. The exogenous input v contains the disturbances, the noises, and the commands. The measured output vector y consists of all the signals which can be measured and available for feedback. Through the control input u , the behavior of the system can be modified. The vector y will be used as the input to a controller $K(s)$ and the output of $K(s)$ will be connected to the control input u . That is,

$$u(s) = K(s) y(s) \quad (2.1-2)$$

The standard H[∞] optimization problem is the problem of finding a proper controller $K(s)$ such that the closed-loop system is internally stable and $\|\Phi\|_{\infty}$ is minimized where

$$\|\Phi\|_{\infty} = \sup_{\omega} \bar{\sigma} [\Phi(j\omega)] \quad (2.1-3)$$

and

$$\Phi(s) = G_{11}(s) + G_{12}(s) Q(s) [I - G_{22}(s) Q(s)]^{-1} G_{21}(s) \quad (2.1-3)$$

That is, $\Phi(s)$ is the transfer function of the closed-loop system from v to z . $\bar{\sigma}[\Phi(j\omega)]$ is the maximum singular value of $\Phi(j\omega)$.

2.2 Formulation of Control Problems as the Standard H^∞ Optimization Problem

As mentioned in the previous subsection, most of the control problems can be formulated as the standard H^∞ optimization problem. For the purpose of demonstration, two examples are given in the following. The first is the mixed-sensitivity optimization problem and the second is the tracking and disturbance reduction problem.

2.2.1 A Mixed-Sensitivity Optimization Problem

Consider the system

$$y(s) = P(s)u(s) + v(s) \quad (2.2-1a)$$

$$u(s) = K(s)y(s) \quad (2.2-1b)$$

The nominal plant transfer function $P(s)$ is given and the set of disturbances is assumed to be any signal vector with energy less than or equal to one. One of the objectives of feedback control is to find a controller $K(s)$ such that the closed-loop system is stable and the maximal energy of the disturbance response is minimized subject to stability-robustness and control input constraints.

The transfer function from $v(s)$ to $y(s)$ is given by

$$[I - P(s)K(s)]^{-1} \quad (2.2-2)$$

which is the sensitivity function of the closed-loop system. From [33], we have

$$\| [I - PK]^{-1} \|_\infty := \sup_{\omega} \bar{\sigma} [(I - PK)^{-1} (j\omega)] = \sup \{ \|y\|_2 \mid \|v\|_2 \leq 1 \} \quad (2.2-3)$$

That is, the maximal energy of the disturbance response is equivalent to the H^∞ norm of $[I - PK]^{-1}$.

According to Doyle et. al. [34,35], the stability robustness is inversely proportional to the maximum singular value of the complementary sensitivity function, $\bar{\sigma}[PK(I-PK)^{-1}(j\omega)]$. In other words, the stability robustness is better whenever the H^∞ norm of the weighted complementary sensitivity function is smaller. Usually the H^∞ norms of $W_1(I-PK)^{-1}$ and $W_2PK(I-PK)^{-1}$ cannot be made small at the same time, i.e., if we make one of them smaller then the other will become larger. To have a trade-off between these two quantities, Kwakernaak [14] formulated the mixed-sensitivity problem as the problem of finding a controller $K(s)$ which stabilizes the closed-loop system and minimizes $\|\Phi\|_\infty$ where Φ is given by

$$\Phi = \begin{bmatrix} W_1(I-PK)^{-1} \\ W_2PK(I-PK)^{-1} \end{bmatrix} \quad (2.2-4)$$

W_1 and W_2 are weighting matrices chosen by the designer according to the real-world environment. If the disturbances most likely to occur are low frequency disturbances then $W_1(s)$ is chosen to be a low-pass filter. If the plant uncertainty is a function of frequency, then $W_2(s)$ should be chosen to be frequency-dependent in the same way.

In (2.2-4) only the quantities related to the disturbance reduction and the stability robustness are involved. The control-input constraint has not been brought into the picture. Usually, the control-input energy is reduced when the stability robustness is improved by scaling $W_1(s)$ and $W_2(s)$. If that is not the case, we can add one term to (2.2-4). That is,

$$\Phi = \begin{bmatrix} W_1(I-PK)^{-1} \\ W_2PK(I-PK)^{-1} \\ W_3K(I-PK)^{-1} \end{bmatrix} \quad (2.2-5)$$

where $K(I-PK)^{-1}$ is the transfer function from v to u and W_3 is a weighting matrix.

The problem of finding a $K(s)$ which stabilizes the closed-loop system and minimizes $\|\Phi\|_\infty$ can be rearranged into the standard H^∞ optimization problem. Consider the following system:

$$\begin{bmatrix} z_1 \\ z_2 \\ z_3 \\ y \end{bmatrix} = \begin{bmatrix} W_1 & W_1 P \\ 0 & W_2 P \\ 0 & W_3 \\ I & P \end{bmatrix} \begin{bmatrix} v \\ u \end{bmatrix} \quad (2.2-6a)$$

$$u = K y \quad (2.2-6b)$$

It is easy to show that the matrix Φ defined by (2-8) is just the transfer function from v to $[z_1^T \ z_2^T \ z_3^T]^T$ of the closed-loop system (2.2-6). Comparing (2.2-6a) with (2.1-1), we can see that

$$G_{11} = \begin{bmatrix} W_1 \\ 0 \\ 0 \end{bmatrix}, \quad G_{12} = \begin{bmatrix} W_1 P \\ W_2 P \\ W_3 \end{bmatrix} \quad (2.2-7)$$

$$G_{21} = I, \quad G_{22} = P.$$

2.2.2 A Tracking/Disturbance Reduction Problem

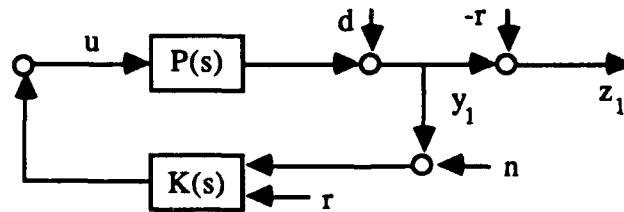


Fig. 2.2-1 Formulating a tracking problem as a standard H^∞ optimization problem.

Consider the system shown in Fig.2.2-1. The objective is to find a controller $K(s)$ such that the closed-loop system is stable and the plant output y_1 follows the command r as closely as possible under the influence of the disturbance d and the measurement noise n . Let the controlled output vector z be

$$z = \begin{bmatrix} z_1 \\ W_1 u \end{bmatrix} \quad (2.2-8)$$

where W_1 is a weighting matrix which is chosen to constrain the control input. The disturbance, command, and noise are assumed unknown, but can be described as

$$\begin{bmatrix} d \\ r \\ n \end{bmatrix} = \begin{bmatrix} W_2 \\ W_3 \\ W_4 \end{bmatrix} v \quad (2.2-9)$$

where v is any signal with bounded energy. The disturbance d and the command r usually are low frequency signals and hence W_2 and W_3 are low-pass filters. The weighting matrix W_4 is a high-pass filter since the measurement noise is a high frequency signal. The measured output y is

$$y = \begin{bmatrix} y_1 + n \\ r \end{bmatrix} \quad (2.2-10)$$

Now, the system can be rearranged as

$$\begin{bmatrix} z \\ y \end{bmatrix} = \begin{bmatrix} W_2 - W_3 & P \\ 0 & W_1 \\ W_2 + W_4 & P \\ W_3 & 0 \end{bmatrix} \begin{bmatrix} v \\ u \end{bmatrix} \quad (2.2-11a)$$

$$u = K y \quad (2.2-11b)$$

and the tracking problem is formulated as the standard H^∞ optimization problem.

SECTION 3

STABILIZATION AND OBSERVER-BASED CONTROLLER PARAMETRIZATION

In Sec.3.1 the basic concept and the historical developments of the controller parametrization will be briefly described. Sec. 3.2 will list the previous results about the controller parametrizations done by Youla et. al., Desoer et. al., Nett et. al., and Doyle et. al.. In Sec. 3.3, some useful properties of the observer-based controller parametrization will be revealed.

Throughout the section, the following notation will be used. The sum, $\mathcal{Q} + \mathcal{B}$, of two sets \mathcal{Q} with p elements and \mathcal{B} with q elements is a set which consists of all elements of \mathcal{Q} and \mathcal{B} . $\mathcal{Q} + \mathcal{B}$ has $p+q$ elements. Assume that $\mathcal{B} \subset \mathcal{Q}$, then the difference, $\mathcal{Q} - \mathcal{B}$, will consist of all the elements of \mathcal{Q} except those in \mathcal{B} . $\mathcal{Q} - \mathcal{B}$ has $p-q$ elements.

3.1 Basic Concept of Controller Parametrization

One of the most fundamental requirements in control systems design is to make the closed-loop system internally stable. In addition to closed-loop stability, usually the closed-loop system is required to meet some other desired performance criteria. Stabilizing controller parametrization is important because of the following reasons: (1) It provides the full set of the controllers which stabilize the closed-loop system. (2) The full set of stabilizing controllers is characterized in terms of a stable parameter matrix and the closed-loop system is internally stable if and only if the parameter matrix is stable. (3) The closed-loop transfer function matrix related to the performance can be written as a simple affine function of the parameter matrix and then the control system design problem becomes that of finding a stable parameter matrix such that the closed-loop transfer function matrix meets the desired performance criteria.

The characterization of the set of all stabilizing controllers in terms of a stable parameter matrix was introduced by Youla et. al. [2] in 1976. Youla's controller characterization was developed based on the fractional factorizations over the ring of polynomial matrices. The only drawback of Youla's characterization is that the stabilizing controller may not be proper. This drawback was removed later by Desoer et. al. [30] in 1980.

Desoer et. al. [30] generalized Youla et. al.'s result based on the fractional factorizations over a general ring. The ring can be chosen as the set of proper stable rational matrices if the given plant is a linear time-invariant system which is represented by a rational matrix. Based on the fractional factorizations over the ring of proper stable rational matrices the set of all proper stabilizing controllers can be characterized in terms of a proper stable parameter matrix.

To use Desoer et. al.'s version of proper stabilizing controller parametrization, it is essential to compute the fractional factorizations over the ring of proper stable rational matrices. Nett et. al. [31] proposed a very convenient state-space method for this computation in 1984. The computation method was developed based on the observer and regulator theories.

Later in 1984, Doyle et. al. [11] showed that the proper stabilizing controller parametrization can be realized as an observer-based controller with an added stable parameter matrix. The structure is simple and easy to implement.

In Sec.3.3 we will show that the observer-based controller parametrization has the following two properties: (1) The poles of the closed-loop system with the observer-based controller parametrization are the regulator poles, the observer poles, together with the poles of the added stable parameter matrix. (2) If the controller is realized by a minimal realization, the closed-loop poles will include all the poles of the added stable parameter matrix and a subset of the regulator and the observer poles.

The concept of stabilizing controller parametrization is briefly described as follows. Consider the block diagram in Fig. 3.1-1 where v is the exogenous input vector which may consist of the disturbances, noises, and the commands, u is the control input vector through which the behavior of the system can be modified, z is the controlled output vector which is composed of all the variables to be controlled, and y is the measured output vector which consists of all the measurable quantities available for feedback. The plant $G(s)$ is given by

$$G(s) = \begin{bmatrix} G_{11}(s) & G_{12}(s) \\ G_{21}(s) & G_{22}(s) \end{bmatrix} = \left[\begin{array}{c|cc} A & B_1 & B_2 \\ \hline C_1 & D_{11} & D_{12} \\ C_2 & D_{21} & D_{22} \end{array} \right] \quad (3.1-1)$$

The objective of a typical control problem is to find a proper controller $K(s)$ which stabilizes the closed-loop system and the H^∞ (or H^2) norm of the closed-loop transfer function matrix $\Phi(s)$ from v to z is minimized. The first step to solve the problem is to find the set of all proper controllers which make the closed-loop system internally stable. Then in the set of all proper stabilizing controllers, one will be chosen such that the H^∞ (or H^2) norm of $\Phi(s)$ is minimized.

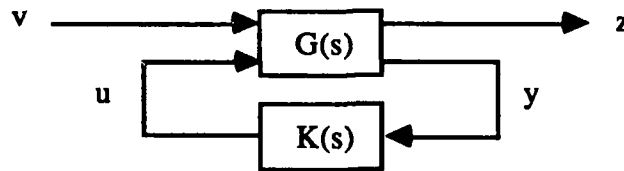


Fig. 3.1-1 Block diagram of a typical control problem.

The stabilizing controller parametrization we are interested in has the following two properties: (1) All the proper stabilizing controllers can be characterized in terms of a proper stable parameter matrix $Q(s)$ and the closed-loop system is internally stable if and only if

$Q(s)$ is stable. (2) The transfer function matrix $\Phi(s)$ is a simple affine function of the parameter matrix $Q(s)$.

After the stabilizing controller parametrization, the above control problem becomes that of finding a proper stable matrix $Q(s)$ such that $\|\Phi\|_{\infty}$ (or $\|\Phi\|_2$) is minimized. Property (2) of the last paragraph is important since it will make the H^{∞} (or H^2) optimization problem easy to solve.

3.2 Youla's Controller Parametrization

The previous results related to the controller parametrization will be briefly reviewed in this subsection. The following theorem was originally developed by Youla et. al. [2] and later modified by Desoer et. al. [30].

Theorem 3.2-1: [2, 30] (Youla's Controller Parametrization)

Consider the system in Fig. 3.1-1. Assume that the realization in (3.1-1) is minimal and the subsystem $G_{22}(s)$ is stabilizable and detectable. Let $M_2(s)$, $N_2(s)$, $X_2(s)$, $Y_2(s)$, $M_1(s)$, $N_1(s)$, $X_1(s)$, and $Y_1(s)$ be proper stable rational matrices such that

$$\begin{bmatrix} M_2(s) & N_2(s) \\ -Y_1(s) & X_1(s) \end{bmatrix} \begin{bmatrix} X_2(s) & -N_1(s) \\ Y_2(s) & M_1(s) \end{bmatrix} = \begin{bmatrix} I & 0 \\ 0 & I \end{bmatrix} \quad (3.2-1)$$

and

$$M_2(s)^{-1} N_2(s) = G_{22}(s) \quad (3.2-2)$$

Then the set of all proper stabilizing controllers can be described as

$$\left\{ K(s) \mid K(s) = [M_1(s)Q(s) + Y_2(s)] [N_1(s)Q(s) - X_2(s)]^{-1} \right. \\ \left. \text{with } Q(s) \text{ proper stable and } |N_1(\infty)Q(\infty) - X_2(\infty)| \neq 0 \right\} \quad (3.2-3)$$

and the closed-loop transfer function matrix $\Phi(s)$ from v to z is an affine function of the parameter matrix $Q(s)$,

$$\Phi(s) = G_{11}(s) - G_{12}(s)Y_2(s)M_2(s)G_{21}(s) - G_{12}(s)M_1(s)Q(s)M_2(s)G_{21}(s) \quad (3.2-4)$$

To use Theorem 3.2-1, we need to construct the proper stable rational matrices in (3.2-1) and (3.2-2). Nett et. al. [31] proposed a convenient state-space approach for this construction. That is, the following realizations

$$\begin{bmatrix} M_2(s) & N_2(s) \\ -Y_1(s) & X_1(s) \end{bmatrix} = \left[\begin{array}{c|cc} A+HC_2 & H & B_2+HD_{22} \\ \hline C_2 & I & D_{22} \\ -F & 0 & I \end{array} \right] \quad (3.2-5a)$$

and

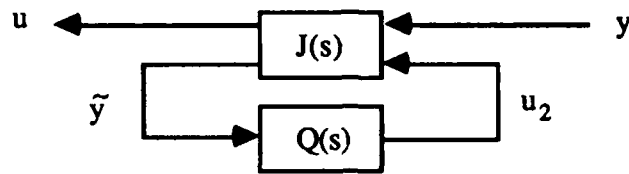
$$\begin{bmatrix} X_2(s) & -N_1(s) \\ Y_2(s) & M_1(s) \end{bmatrix} = \left[\begin{array}{c|cc} A+B_2F & H & B_2 \\ \hline -(C_2+D_{22}F) & I & -D_{22} \\ F & 0 & I \end{array} \right] \quad (3.2-5b)$$

are proper stable and satisfy (3.2-1) and (3.2-2) where F and H can be arbitrarily chosen such that $A+B_2F$ and $A+HC_2$ are stable.

Doyle et. al. [11] showed that if (3.2-5a) and (3.2-5b) are used to realize the proper stable rational matrices in (3.2-1) and (3.2-2) and let

$$J(s) = \begin{bmatrix} J_{11}(s) & J_{12}(s) \\ J_{21}(s) & J_{22}(s) \end{bmatrix} = \left[\begin{array}{c|cc} A+B_2F+HC_2+HD_{22}F & -H & -(B_2+HD_{22}) \\ \hline F & 0 & -I \\ -(C_2+D_{22}F) & I & D_{22} \end{array} \right] \quad (3.2-6)$$

then the set of proper stabilizing controllers described in Theorem 3.2-1 will have a structure as that shown in Fig. 3.2-1.



with $Q(s)$ proper stable and $I - D_{22}Q(\infty)$ invertible.

Fig. 3.2-1 Structure of stabilizing controller parametrization.

Replace the controller $K(s)$ in Fig. 3.1-1 by the structure of Fig. 3.2-1, then the closed-loop system can be redrawn as that shown in Fig. 3.2-2.

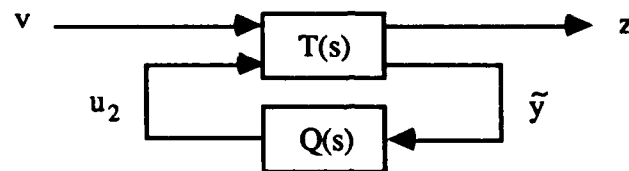
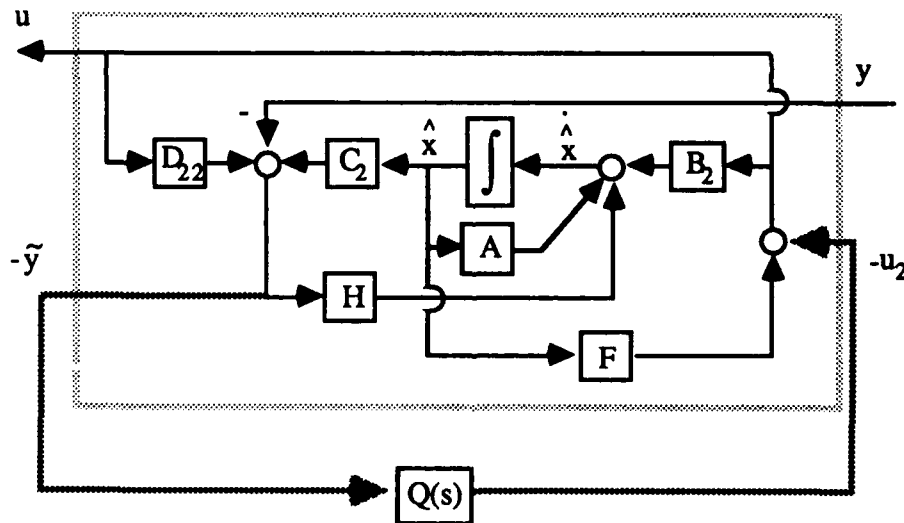


Fig. 3.2-2 The closed-loop system characterized in terms of a parameter matrix $Q(s)$.



with $Q(s)$ proper stable and $I - D_{22}Q(\infty)$ invertible

Fig. 3.2-3 The observer-based controller parametrization.

In Fig. 3.2-2, the open-loop transfer function matrix from u_2 to \tilde{y} , $T_{22}(s)$, is zero. Therefore, the closed-loop transfer function matrix from v to z , i.e., $\Phi(s)$, is a simple affine function of the parameter matrix $Q(s)$. That is,

$$\Phi(s) = T_{11}(s) + T_{12}(s) Q(s) T_{21}(s) \quad (3.2-7)$$

where the realizations of $T_{11}(s)$, $T_{12}(s)$, $T_{21}(s)$ are given by

$$T_{11}(s) = \left[\begin{array}{cc|c} A+B_2F & -B_2F & B_1 \\ 0 & A+HC_2 & B_1+HD_{21} \\ \hline C_1+D_{12}F & -D_{12}F & D_{11} \end{array} \right] \quad (3.2-8a)$$

$$T_{12}(s) = \left[\begin{array}{c|c} A+B_2F & B_2 \\ \hline C_1+D_{12}F & D_{12} \end{array} \right] \quad (3.2-8b)$$

$$T_{21}(s) = \left[\begin{array}{c|c} A+HC_2 & B_1+HD_{21} \\ \hline C_2 & D_{21} \end{array} \right] \quad (3.2-8c)$$

Doyle et. al. [11] also pointed out that the structure of the stabilizing controller parametrization in Fig. 3.2-1 can be realized as an observer-based controller with an added stable dynamics $Q(s)$. The realization is shown in Fig. 3.2-3.

Note that in Fig. 3.2-3 the block diagram inside the dotted-line box is the well-known full-order observer-based controller [1].

3.3 Observer-based Controller Parametrization and Its Properties

In Fig. 3.1-1, the internal stability of the closed-loop system depends only on $G_{22}(s)$ and $K(s)$, i.e., the interconnected system shown in Fig. 3.3-1.

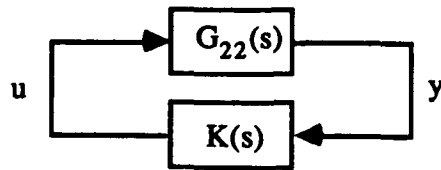


Fig. 3.3-1 Equivalent system to Fig. 3.1-1 for internal stability.

In this subsection, the controller $K(s)$ in Fig. 3.3-1 is replaced by the block diagram of Fig. 3.2-3 which is the observer-based controller with an added dynamics $Q(s)$.

The following theorem shows that the poles of the closed-loop system with the observer-based controller parametrization in Fig. 3.2-3 are the regulator poles (the eigenvalues of $A+B_2F$), the observer poles (the eigenvalues of $A+HC_2$), together with the poles of the parameter matrix $Q(s)$. In the design of the observer-based controller, F and H are chosen such that the eigenvalues of $A+B_2F$ and $A+HC_2$ are stable. Therefore, the closed-loop system is internally stable if and only if the parameter matrix $Q(s)$ is proper stable. The proof is quite straightforward and is done completely in the state space without referring to the derivations used by Youla et. al., Desoer et. al., and Doyle et. al..

Theorem 3.3-1: (Observer-based Controller Parametrization)

Consider the closed-loop system in Fig. 3.3-1. Assume that $G_{22}(s) = \{A, B_2, C_2, D_{22}\}$ with order n is stabilizable and detectable and the controller $K(s)$ is replaced by the observer-based controller with an added m -th order dynamics $Q(s)$ as shown in Fig. 3.2-3. Then the set of the closed-loop poles is composed of the n eigenvalues of $A+B_2F$, the n eigenvalues of $A+HC_2$, and the m poles of the added dynamics $Q(s)$. That is, the set of the closed-loop poles is

$$\mathcal{P}_{\text{closed-loop}} = \mathcal{P}_{\text{regulator}} + \mathcal{P}_{\text{observer}} + \mathcal{P}_{Q(s)} \quad (3.3-1a)$$

where

$$\mathcal{P}_{\text{regulator}} = \{ n \text{ eigenvalues of } A+B_2F \} \quad (3.3-1b)$$

$$\mathcal{P}_{\text{observer}} = \{ n \text{ eigenvalues of } A+HC_2 \} \quad (3.3-1c)$$

and

$$\mathcal{P}_{Q(s)} = \{ m \text{ poles of } Q(s) \} \quad (3.3-1d)$$

Proof: See [65,66]

It is well known that in the observer-based controller design, the closed-loop poles are the regulator poles (the eigenvalues of $A+B_2F$) and the observer poles (the eigenvalues

of $A+HC_2$) [1]. Theorem 3.3-1 shows that the above property still remains when we add a dynamics $Q(s)$ to the observer-based controller as shown in Fig. 3.2-3. The eigenvalues of $A+B_2F$ and $A+HC_2$ are still parts of the closed-loop poles after we add $Q(s)$ to the controller. Adding $Q(s)$ only introduces additional poles to the closed-loop system and the added closed-loop poles are the poles of $Q(s)$. If F and H have been chosen such that $A+B_2F$ and $A+HC_2$ are stable, then the closed-loop system with the observer-based controller parametrization will be internally stable if and only if the parameter matrix $Q(s)$ is proper stable. From Fig. 3.2-3, it is easy to see that the controller $K(s)$ is proper if $Q(s)$ is proper and $I - D_{22}Q(\infty)$ is invertible.

With the observer-based controller parametrization, the closed-loop transfer function matrix from v to z , i.e., $\Phi(s)$, is a simple affine function of the parameter matrix $Q(s)$. That is,

$$\Phi(s) = T_{11}(s) + T_{12}(s) Q(s) T_{21}(s) \quad (3.3-2)$$

where $T_{11}(s)$, $T_{12}(s)$, and $T_{21}(s)$ are given by (3.2-8). The added dynamics $Q(s)$ is a proper stable rational matrix to be chosen such that $I-D_{22}Q(\infty)$ is invertible and $\Phi(s)$ has some desired performance. No matter which $Q(s)$ is to be selected, we always have a clear idea that the closed-loop poles will be the eigenvalues of $A+B_2F$ and $A+HC_2$ together with the poles of the added dynamics $Q(s)$ if the controller is realized as that shown in Fig. 3.2-3.

Assume that the orders of the plant and the parameter matrix $Q(s)$ are n and m respectively. If the controller is realized as that shown in Fig. 3.2-3, then the order of the controller is $n+m$ and the closed-loop system has $2n+m$ poles described by the set $\mathcal{P}_{\text{closed-loop}}$ in (3.3-1). The realization of the controller in Fig. 3.2-3 may not be minimal. Suppose it is not and there are r poles in the controller either uncontrollable or unobservable, then the

controller can be realized by a minimal realization with order $n+m-r$ and the number of closed-loop poles will be reduced to $2n+m-r$.

In the following theorem, we will show that the uncontrollable or unobservable poles of the controller of Fig. 3.2-3 must be the eigenvalues of $A+B_2F$ or $A+HC_2$ and the closed-loop poles will always include all m poles of the added stable dynamics $Q(s)$. If r pole-zero cancellations occur in the controller, then the closed-loop poles will include m poles of $Q(s)$, and $2n-r$ eigenvalues out of the set $\mathcal{P}_{\text{regulator}} + \mathcal{P}_{\text{observer}}$ which was defined in (3.3-1).

Theorem 3.3-2:

Consider the closed-loop system in Fig. 3.3-1. Assume that $G_{22}(s) = \{A, B_2, C_2, D_{22}\}$ with order n is stabilizable and detectable and the controller $K(s)$ is replaced by the observer-based controller with an added m -th order dynamics $Q(s)$ as shown in Fig. 3.2-3. A minimal realization of $Q(s)$ is given as $\{\bar{A}, \bar{B}, \bar{C}, \bar{D}\}$. Define $\mathcal{P}_{\text{regulator}}$, $\mathcal{P}_{\text{observer}}$ and $\mathcal{P}_{Q(s)}$ by (3.3-1b), (3.3-1c), and (3.3-1d) respectively and let

$$\mathcal{P}_{\text{removal}} = \{\text{the controller poles which are either uncontrollable or unobservable}\} \quad (3.3-3)$$

Then

$$\mathcal{P}_{\text{removal}} \subset \mathcal{P}_{\text{regulator}} + \mathcal{P}_{\text{observer}} \quad (3.3-4)$$

and the closed-loop system with the minimal order controller will have a set of poles described by the following

$$\mathcal{P}_{\text{closed-loop with min. controller}} = \mathcal{P}_{Q(s)} + (\mathcal{P}_{\text{regulator}} + \mathcal{P}_{\text{observer}} - \mathcal{P}_{\text{removal}}) \quad (3.3-5)$$

Proof: See Appendix A.

SECTION 4

SOLUTIONS FOR THE STANDARD H^∞ OPTIMIZATION PROBLEMS

Consider the system

$$\begin{bmatrix} z(s) \\ y(s) \end{bmatrix} = \begin{bmatrix} G_{11}(s) & G_{12}(s) \\ G_{21}(s) & G_{22}(s) \end{bmatrix} \begin{bmatrix} v(s) \\ u(s) \end{bmatrix} := G(s) \begin{bmatrix} v(s) \\ u(s) \end{bmatrix} \quad (4-1a)$$

$$u(s) = K(s) y(s) \quad (4-1b)$$

where $G_{11}(s) \in \mathbb{R}(s)^{p \times q}$, $G_{12}(s) \in \mathbb{R}(s)^{p \times m}$, $G_{21}(s) \in \mathbb{R}(s)^{r \times q}$, and $G_{22}(s) \in \mathbb{R}(s)^{r \times m}$.

Recall that the standard H^∞ optimization problem is the problem of finding a proper controller $K(s)$ such that the closed-loop system is internally stable and $\|\Phi\|_\infty$ is minimized where $\Phi(s)$ is the transfer function of the closed-loop system from v to z .

Let

$$G(s) = \left[\begin{array}{c|cc} A & B_1 & B_2 \\ \hline C_1 & D_{11} & D_{12} \\ C_2 & D_{21} & D_{22} \end{array} \right] \quad (4-2)$$

be a minimal realization of $G(s)$. Here

$$G(s) = \left[\begin{array}{c|c} A & B \\ \hline C & D \end{array} \right] = (A, B, C, D) \quad (4-3)$$

implies a state-space realization and $G(s) = D + C(sI - A)^{-1}B$.

According to the dimensions of $G_{11}(s)$, $G_{12}(s)$, $G_{21}(s)$, and $G_{22}(s)$, the standard H^∞ optimization problem has the following cases to consider: (a) $p > m$, $r < q$; (b) $p \leq m$, $r < q$; (c) $p > m$, $r \geq q$; and (d) $p \leq m$, $r \geq q$. Case (a) is referred to as the four-block H^∞ optimization problem. Cases (b) and (c) are referred to as the two-block H^∞ optimization

problem. Case (d) is referred to as the one-block H^∞ optimization problem. The example in Sec. 2.2.1 is a two-block problem and the example in Sec. 2.2.2 is a four-block problem.

The one-block H^∞ optimization problem was solved by Francis, Zames, and Helton [5], Chang and Pearson [6], Safonov and Verma [7] and Glover [8]. A so-called γ -iteration algorithm was originally proposed by Doyle [10] for solving the four-block and two-block H^∞ optimization problems. The major burden of the computation is in the evaluation of the optimal H^∞ norm. Chang, Banda, and McQuade [20] proposed a fast γ -iteration algorithm for computing the optimal H^∞ norm of the two-block problem. For most problems we encountered, the optimal two-block H^∞ norm can be accurately (to a double precision accuracy) obtained within three or four iterations. Once the optimal norm is computed, the two-block problem can be easily transformed into a one-block problem and then Glover's method [8] can be used to construct an optimal controller.

Although Chang and Pearson [17] and Chu and Doyle [18] greatly simplified the original Doyle's four-block H^∞ norm computation algorithm, the simplified γ -iteration algorithms are still not fast enough for practical applications. Recently, Doyle, Glover, Khargonekar, and Francis [29] presented a celebrating Riccati-equation type solution to the four-block H^∞ optimization problem. DGKF's approach characterizes all possible stabilizing suboptimal H^∞ controllers which order is not higher than that of the plant. The major computation involved is the solution of two Riccati equations. There are still some numerical difficulties in the solution of these Riccati equations when the controller is close to the optimal.

In the subsection Sec.4.1, the observer-based controller parametrization is used to characterize the set of stabilizing controllers in terms of a stable parameter matrix. With the controller parametrization, the closed-loop transfer function from v to z is an affine function of the parameter matrix. After inner-outer factorization manipulations, the problem becomes

Find a $\hat{Q}(s) \in (RH^\infty)^{m \times r}$ such that $\|\hat{\Phi}\|_\infty$ is minimized
 where $\hat{\Phi}$ is given by (4-4)

$$\hat{\Phi} = \begin{bmatrix} R_{11} + \hat{Q} & R_{12} \\ R_{21} & R_{22} \end{bmatrix}$$

$(RH^\infty)^{m \times r}$ is the set of $m \times r$ proper rational matrices with real coefficients which are analytic in the closed right half plane. The above problem is referred to as the four-block H^∞ optimization problem. The two-block H^∞ optimization problem is just a special case of problem (4-4) with either $[R_{21} \ R_{22}] = 0$ or $[R_{12}^T \ R_{22}^T] = 0$. When both $[R_{21} \ R_{22}] = 0$ and $[R_{12}^T \ R_{22}^T] = 0$, the problem is one-block problem. In Sec. 4.2, a state-space size reduction method is used to simplify the realizations of R_{11} , R_{12} , R_{21} , and R_{22} . A fast γ -iteration approach for the two-block H^∞ optimization problem is summarized in Sec. 4.3. In Sec.4.4, the numerical difficulties in using the DGKF approach [29] to solve the four-block H^∞ optimization problem will be discussed.

4.1 Controller Parametrization and Inner-Outer Factorization

Suppose the realization $\{ A, B_2, C_2, D_{22} \}$ is stabilizable and detectable, then by using Doyle's version [11,32] of YJB controller parametrization [2,30], the set of stabilizing controllers can be characterized by the structure shown in Fig.3.2-3.

In Fig.3.2-3, the regulator gain matrix F and the observer gain matrix H are chosen such that $A+B_2F$ and $A+HC_2$ have no eigenvalues in the closed right half of s -plane. With the controller $K(s)$ parameterized as above, the closed-loop transfer function matrix from v to z , i.e., $\Phi(s)$, is a simple affine function of the parameter matrix $Q(s)$. That is,

$$\Phi(s) = T_{11}(s) + T_{12}(s) Q(s) T_{21}(s) \quad (4.1-1)$$

where the realizations of $T_{11}(s)$, $T_{12}(s)$, $T_{21}(s)$ are proper stable rational matrices given by (3.2-8).

If $T_{12}(s)$ and $T_{21}(s)$ are thin and fat respectively, i.e., $p > m$ and $r < q$, then they can be decomposed as

$$T_{12}(s) = T_i(s)T_o(s), \quad T_{21}(s) = \tilde{T}_o(s)\tilde{T}_i(s) \quad (4.1-2)$$

where $T_i \in (RH^\infty)^{p \times m}$ is inner, $\tilde{T}_i \in (RH^\infty)^{r \times q}$ is co-inner, $T_o \in (RH^\infty)^{m \times m}$ and $\tilde{T}_o \in (RH^\infty)^{r \times r}$ are outer matrices. Furthermore, we can find a $T_\perp(s) \in (RH^\infty)^{p \times (p-m)}$ such that $[T_i \ T_\perp]$ is square and inner. Similarly, $\tilde{T}_\perp(s) \in (RH^\infty)^{(q-r) \times q}$ can be found such that $[\tilde{T}_i^T \ \tilde{T}_\perp^T]^T$ is square and co-inner. Now, (4.1-1) can be rewritten as

$$\Phi = T_{11} + [T_i \ T_\perp] \begin{bmatrix} \hat{Q} & 0 \\ 0 & 0 \end{bmatrix} \begin{bmatrix} \tilde{T}_i \\ \tilde{T}_\perp \end{bmatrix} \quad (4.1-3)$$

here $\hat{Q} = T_o Q \tilde{T}_o$. Define $\hat{\Phi} = [T_i \ T_\perp]^* \Phi [\tilde{T}_i^* \ \tilde{T}_\perp^*]$, then we have

$$\hat{\Phi} = \begin{bmatrix} T_i^* T_{11} \tilde{T}_i^* + \hat{Q} & T_i^* T_{11} \tilde{T}_\perp^* \\ T_\perp^* T_{11} \tilde{T}_i^* & T_\perp^* T_{11} \tilde{T}_\perp^* \end{bmatrix} := \begin{bmatrix} R_{11} + \hat{Q} & R_{12} \\ R_{21} & R_{22} \end{bmatrix} \quad (4.1-4)$$

Note that $\|\hat{\Phi}\|_\infty = \|\Phi\|_\infty$ and therefore the problem becomes to:

$$\begin{aligned} &\text{Find a } \hat{Q}(s) \in (RH^\infty)^{m \times r} \text{ such that } \|\hat{\Phi}\|_\infty \text{ is minimized} \\ &\text{where } \hat{\Phi} \text{ is given by (4.1-4).} \end{aligned} \quad (4.1-5)$$

Problem (4.1-5) is referred to as the four-block H^∞ optimization problem.

The two-block H^∞ optimization problem is just a special case of problem (4.1-5) and the corresponding $\hat{\Phi}(s)$ is a special case of (4.1-4) with either $[R_{21} \ R_{22}] = 0$ or $[R_{12}^T \ R_{22}^T] = 0$. When both $[R_{21} \ R_{22}] = 0$ and $[R_{12}^T \ R_{22}^T] = 0$, the problem is one-block problem.

In (4.1-4), $R(s)$ is given by

$$R(s) = \begin{bmatrix} R_{11}(s) & R_{12}(s) \\ R_{21}(s) & R_{22}(s) \end{bmatrix} = R_L(s) R_R(s) \quad (4.1-6)$$

The state-space realizations of $R_L(s)$ and $R_R(s)$ are given by [12]

$$R_L(s) = \left[\begin{array}{c|cc} -(A+B_2F)^T & (C_1+D_{12}F)^T & -XH \\ \hline -(B_2R_D^{-1/2})^T & (D_{12}R_D^{-1/2})^T & 0 \\ D_{\perp}^T C_1 X^\dagger & D_{\perp}^T & 0 \end{array} \right] \quad (4.1-7a)$$

$$R_R(s) = \left[\begin{array}{c|cc} -(A+HC_2)^T & -(\tilde{R}_D^{-1/2} C_2)^T & Y^\dagger B_1 \tilde{D}_{\perp}^T \\ \hline C_1 Y + D_{11}(B_1 + HD_{21})^T & D_{11}(\tilde{R}_D^{-1/2} D_{21})^T & D_{11} \tilde{D}_{\perp}^T \\ 0 & \tilde{R}_D^{1/2} & 0 \end{array} \right] \quad (4.1-7b)$$

where

$$F = -R_D^{-1}(D_{12}^T C_1 + B_2^T X) \quad (4.1-8a)$$

$$R_D = D_{12}^T D_{12} \quad (4.1-8b)$$

$$X = \text{Ric} \left[\begin{array}{cc} A - B_2 R_D^{-1} D_{12}^T C_1 & -B_2 R_D^{-1} B_2^T \\ -C_1^T D_{\perp} D_{\perp}^T C_1 & -(A - B_2 R_D^{-1} D_{12}^T C_1)^T \end{array} \right] \quad (4.1-8c)$$

D_{\perp} is the orthogonal complement of $D_{12} R_D^{-1/2}$ so that

$$\begin{bmatrix} D_{12} R_D^{-1/2} & D_{\perp} \end{bmatrix} \text{ is square and orthogonal.} \quad (4.1-8d)$$

$$(R_D^{1/2})^T R_D^{1/2} = R_D \quad (4.1-8e)$$

and

$$K = -(B_1 D_{21}^T + Y C_2^T) \tilde{R}_D^{-1} \quad (4.1-9a)$$

$$\tilde{R}_D = D_{21} D_{21}^T \quad (4.1-9b)$$

$$Y = \text{Ric} \begin{bmatrix} (A - B_1 D_{21}^T \tilde{R}_D^{-1} C_2^T)^T & -C_2^T \tilde{R}_D^{-1} C_2 \\ -B_1 \tilde{D}_\perp^T \tilde{D}_\perp B_1^T & -(A - B_1 \tilde{D}_\perp^T \tilde{R}_D^{-1} C_2^T) \end{bmatrix} \quad (4.1-9c)$$

\tilde{D}_\perp is the orthogonal complement of $\tilde{R}_D^{-1/2} D_{21}$ so that

$$\begin{bmatrix} \tilde{R}_D^{-1/2} D_{21} \\ \tilde{D}_\perp \end{bmatrix} \text{ is square and orthogonal.} \quad (4.1-9d)$$

$$(\tilde{R}_D^{1/2})(\tilde{R}_D^{1/2})^T = \tilde{R}_D \quad (4.1-9e)$$

In (4.1-8c) and (4.1-9c), Ric[H] denotes the solution of the Riccati equation corresponding to the Hamiltonian matrix H.

4.2 Size Reduction In Four-Block H^∞ Formulation

Neither $R_L(s)$ nor $R_R(s)$ in (4.1-7) is a minimal realization. Limebeer and Hung [22] derived a minimal realization of $R_{11}(s)$ in the one-block case (the case with $R_{12}(s)$, $R_{21}(s)$ and $R_{22}(s)$ being zero matrices) for finding a bound on the McMillan degree of the H^∞ optimal controller. This minimal realization process is not numerically reliable although it is adequate for their theoretical purpose. Recently, Postlethwaite, Gu, and O'Young [23] unveiled some useful properties on the solution of the algebraic Riccati equation and used them to develop a numerically reliable algorithm for the minimal realization of $R_{11}(s)$ in the one-block case.

Partitioning $R_L(s)$ and $R_R(s)$ as

$$R_L(s) = \begin{bmatrix} R_{L1}(s) \\ R_{L2}(s) \end{bmatrix}, \quad R_R(s) = \begin{bmatrix} R_{R1}(s) & R_{R2}(s) \end{bmatrix} \quad (4.2-1a)$$

then we have

$$R_{11}(s) = R_{L1}(s) R_{R1}(s), \quad R_{12}(s) = R_{L1}(s) R_{R2}(s) \quad (4.2-1b)$$

$$R_{21}(s) = R_{L2}(s) R_{R1}(s), \quad R_{22}(s) = R_{L2}(s) R_{R2}(s)$$

where

$$R_{L1}(s) = \left[\begin{array}{c|cc} -(A+B_2F)^T & (C_1+D_{12}F)^T & -XH \\ \hline -(B_2R_D^{-1/2})^T & (D_{12}R_D^{-1/2})^T & 0 \end{array} \right] \quad (4.2-1c)$$

$$R_{L2}(s) = \left[\begin{array}{c|cc} -(A+B_2F)^T & (C_1+D_{12}F)^T & -XH \\ \hline D_\perp^T C_1 X^\dagger & D_\perp^T & 0 \end{array} \right] \quad (4.2-1d)$$

$$R_{R1}(s) = \begin{bmatrix} -(A+HC_2)^T & -(\tilde{R}_D^{-1/2}C_2)^T \\ C_1Y+D_{11}(B_1+HD_{21})^T & D_{11}(\tilde{R}_D^{-1/2}D_{21})^T \\ 0 & \tilde{R}_D^{1/2} \end{bmatrix} \quad (4.2-1e)$$

$$R_{R2}(s) = \begin{bmatrix} -(A+HC_2)^T & Y^\dagger B_1 \tilde{D}_\perp^T \\ C_1Y+D_{11}(B_1+HD_{21})^T & D_{11} \tilde{D}_\perp^T \\ 0 & 0 \end{bmatrix} \quad (4.2-1f)$$

The recently discovered properties on the solution of the algebraic Riccati equation by Postlethwaite et. al. [23] and the pole-zero cancellation technique by the similarity transformation are used for constructing the minimal realizations of $R_{L1}(s)$, $R_{L2}(s)$, $R_{R1}(s)$, and $R_{R2}(s)$. Only orthogonal transformations are involved in the computation, so the algorithm is numerically reliable. The new result of Postlethwaite et. al. is listed as follows.

Theorem 4.2-1: [23]

Consider the algebraic Riccati equation,

$$A^T X + X A - X B B^T X + C^T C = 0 \quad (4.2-2a)$$

There exists an orthogonal matrix $U = \begin{bmatrix} U_1 & U_2 \end{bmatrix}$ such that

$$U^T A U = \begin{bmatrix} A_1 & A_2 \\ 0 & A_3 \end{bmatrix} \quad (4.2-2b)$$

$$U^T B = \begin{bmatrix} U_1^T B \\ U_2^T B \end{bmatrix}, \quad C U = \begin{bmatrix} 0 & C U_2 \end{bmatrix} \quad (4.2-2c)$$

and

$$U^T X U = \begin{bmatrix} 0 & 0 \\ 0 & X_2 \end{bmatrix} \quad (4.2-2d)$$

The eigenvalues of A_1 are unobservable but stable. That is, the set of eigenvalues of A_3 includes all the observable and all the unstable eigenvalues of A . The rank of X_2 , and therefore the rank of X , equals the dimension of A_3 . $X_2 > 0$ satisfies the following algebraic Riccati equation (ARE),

$$A_3^T X_2 + X_2 A_3 - X_2 U_2^T B B^T U_2 X_2 + U_2^T C^T C U_2 = 0 \quad (4.2-2e)$$

The algorithm we developed is different from that of Postlethwaite et. al.. The advantage of the decomposition $R(s) = R_L(s)R_R(s)$ is taken to simplify the size reduction process for $R_{11}(s)$, $R_{12}(s)$, $R_{21}(s)$ and $R_{22}(s)$. Although we do not try to construct minimal realizations for $R_{ij}(s)$, we do have minimal realizations for $R_{Li}(s)$ and $R_{Rj}(s)$, $i,j=1,2$, and there is no possible mathematically identical pole-zero cancellation between $R_{Li}(s)$ and $R_{Rj}(s)$.

In the following, we will derive minimal state-space realizations for $R_{L1}(s)$ and $R_{L2}(s)$. Minimal realizations of $R_{R1}(s)$ and $R_{R2}(s)$ can be obtained in a similar way. First of all, let us consider $R_{L1}(s)$.

Minimal Realization of $R_{L1}(s)$

The first step is to apply Theorem 4.2-1 to the solution of the algebraic Riccati equation (4.1-8c). There exists an orthogonal matrix

$$U = \begin{bmatrix} U_1 & U_2 \end{bmatrix} \quad (4.2-3a)$$

such that

$$U^T (A - B_2 R_D^{-1} D_{12}^T C_1) U = \begin{bmatrix} A_1 & A_{12} \\ 0 & A_2 \end{bmatrix} \quad (4.2-3b)$$

$$U^T B_2 R_D^{-1/2} = \begin{bmatrix} L_1 \\ L_2 \end{bmatrix}, \quad D_{\perp}^T C_1 U = \begin{bmatrix} 0 & W_2 \end{bmatrix} \quad (4.2-3c)$$

and

$$U^T X U = \begin{bmatrix} 0 & 0 \\ 0 & X_2 \end{bmatrix} \quad (4.2-3d)$$

where X_2 is the positive definite solution of the following reduced-order algebraic Riccati equation

$$A_2^T X_2 + X_2 A_2 - X_2 L_2 L_2^T X_2 + W_2^T W_2 = 0 \quad (4.2-3e)$$

Applying the similarity transformation (U^T, U) to the realization of $R_{L_1}(s)$ in (4.2-1c) and then using (4.1-8) and (4.2-3), we have

$$\begin{aligned} R_{L_1}(s) &= \left[\begin{array}{cc|cc} -A_1^T & 0 & 0 & 0 \\ \hline -(A_{12} - L_1 L_2^T X_2)^T & -(A_2 - L_2 L_2^T X_2)^T & (D_{\perp} W_2 - D_{12} R_D^{-1} B_2^T U_2 X_2)^T & -X_2 U_2^T H \\ \hline -L_1^T & -L_2^T & (D_{12} R_D^{-1/2})^T & 0 \end{array} \right] \\ &= \left[\begin{array}{c|cc} -(A_2 - L_2 L_2^T X_2)^T & (D_{\perp} W_2 - D_{12} R_D^{-1} B_2^T U_2 X_2)^T & -X_2 U_2^T H \\ \hline -L_2^T & (D_{12} R_D^{-1/2})^T & 0 \end{array} \right] \quad (4.2-4) \end{aligned}$$

The size of the state-space realization of $R_{L_1}(s)$ has been reduced from the dimension of A to that of A_2 and the realization in (4.2-4) is controllable according to the following.

Remark 4.2-1:

The state-space realization of $R_{L_1}(s)$ in (4.2-4) is controllable.

Proof: See Appendix A.

Remark 4.2-2:

If $R_{L2}(s) = 0$, i.e., $D_L = 0$, then it is easy to prove that the pair $\{L_2^T, (A_2 - L_2 L_2^T X_2)^T\}$ is observable. In this case, the realization of $R_{L1}(s)$ in (4.2-4) is already a minimal realization.

Now the realization of $R_{L1}(s)$ in (4.2-4) is controllable but not necessarily observable if $R_{L2}(s) \neq 0$. By using the Van Dooren's version [36] of Rosenbrock's algorithm [37], we can find an orthogonal matrix

$$V = \begin{bmatrix} V_1 & V_2 \end{bmatrix} \quad (4.2-5a)$$

such that

$$\begin{aligned} & -V^T(A_2 - L_2 L_2^T X_2)^T V \\ &= \begin{bmatrix} -V_1^T(A_2 - L_2 L_2^T X_2)^T V_1 & 0 \\ -V_2^T(A_2 - L_2 L_2^T X_2)^T V_1 & -V_2^T(A_2 - L_2 L_2^T X_2)^T V_2 \end{bmatrix} \end{aligned} \quad (4.2-5b)$$

and

$$-L_2^T V = \begin{bmatrix} -L_2^T V_1 & 0 \end{bmatrix} \quad (4.2-5c)$$

and the pair

$$\{ -L_2^T V_1, -V_1^T(A_2 - L_2 L_2^T X_2)^T V_1 \} \quad (4.2-5d)$$

is observable.

Applying the similarity transformation (V^T, V) to the realization of $R_{L1}(s)$ in (4.2-4) and eliminating the unobservable part, we have the following minimal realization

$$R_{L1}(s) = \left[\begin{array}{c|c} -V_1^T(A_2 - L_2 L_2^T X_2)^T V_1 & V_1^T(D_1 W_2 - D_{12} R_D^{-1} B_2^T U_2 X_2)^T - V_1^T X_2 U_2^T H \\ \hline -L_2^T V_1 & (D_{12} R_D^{-1/2})^T \quad 0 \end{array} \right] \quad (4.2-6)$$

Minimal Realization of $R_{L2}(s)$

The first step is just similar to that of the minimal realization of $R_{L1}(s)$. Applying the similarity transformation (U^T, U) to the realization of $R_{L2}(s)$ in (4.2-1d), and then using (4.1-8) and (4.2-3), we have

$$\begin{aligned} R_{L2}(s) &= \left[\begin{array}{cc|cc} -A_1^T & 0 & 0 & 0 \\ \hline -(A_{12} - L_1 L_2^T X_2)^T - (A_2 - L_2 L_2^T X_2)^T & (D_1 W_2 - D_{12} R_D^{-1} B_2^T U_2 X_2)^T - X_2 U_2^T H \\ \hline 0 & W_2 X_2^{-1} & D_1^T & 0 \end{array} \right] \\ &= \left[\begin{array}{c|c} -(A_2 - L_2 L_2^T X_2)^T & (D_1 W_2 - D_{12} R_D^{-1} B_2^T U_2 X_2)^T - X_2 U_2^T H \\ \hline W_2 X_2^{-1} & D_1^T \quad 0 \end{array} \right] \quad (4.2-7) \end{aligned}$$

For the same reason of Remark 4.2-1, the realization of $R_{L2}(s)$ in (4.2-7) is controllable. Next, we can find an orthogonal matrix

$$S = [S_1 \quad S_2] \quad (4.2-8a)$$

such that

$$\begin{aligned} &-S^T(A_2 - L_2 L_2^T X_2)^T S \\ &= \left[\begin{array}{cc} -S_1^T(A_2 - L_2 L_2^T X_2)^T S_1 & 0 \\ -S_2^T(A_2 - L_2 L_2^T X_2)^T S_1 & -S_2^T(A_2 - L_2 L_2^T X_2)^T S_2 \end{array} \right] \quad (4.2-8b) \end{aligned}$$

and

$$W_2 X_2^{-1} S = \begin{bmatrix} W_2 X_2^{-1} S_1 & 0 \end{bmatrix} \quad (4.2-8c)$$

and the pair

$$\{ W_2 X_2^{-1} S_1, -S_1^T (A_2 - L_2 L_2^T X_2)^T S_1 \} \quad (4.2-8d)$$

is observable.

Applying the similarity transformation (S^T, S) to the realization of $R_{L2}(s)$ in (4.2-7) and eliminating the unobservable part, we have the following minimal realization:

$$R_{L2}(s) = \left[\begin{array}{c|cc} -S_1^T (A_2 - L_2 L_2^T X_2)^T S_1 & S_1^T (D_{\perp} W_2 - D_{12} R_D^{-1} B_2^T U_2 X_2)^T - S_1^T X_2 U_2^T H & \\ \hline W_2 X_2^{-1} S_1 & D_{\perp}^T & 0 \end{array} \right] \quad (4.2-9)$$

Minimal Realization of $R_{R1}(s)$

The procedure is similar to that of $R_{L1}(s)$. Theorem 4.2-1 will be applied to the solution of the algebraic Riccati equation (4.1-9c). There exists an orthogonal matrix

$$\bar{U} = \begin{bmatrix} U_3 & U_4 \end{bmatrix} \quad (4.2-10a)$$

such that

$$\bar{U}^T (A - B_1 D_{21}^T \tilde{R}_D^T C_2)^T \bar{U} = \begin{bmatrix} A_3 & A_{34} \\ 0 & A_4 \end{bmatrix} \quad (4.2-10b)$$

$$\bar{U}^T (\tilde{R}_D^{-1/2} C_2)^T = \begin{bmatrix} L_3 \\ L_4 \end{bmatrix}, \quad \tilde{D}_{\perp} B_1^T \bar{U} = \begin{bmatrix} 0 & W_4 \end{bmatrix} \quad (4.2-10c)$$

and

$$\bar{U}^T Y \bar{U} = \begin{bmatrix} 0 & 0 \\ 0 & Y_2 \end{bmatrix} \quad (4.2-10d)$$

where Y_2 is positive definite solution of the following reduced-order algebraic Riccati equation

$$A_4^T Y_2 + Y_2 A_4 - Y_2 L_4 L_4^T Y_2 + W_4^T W_4 = 0 \quad (4.2-10e)$$

Applying the similarity transformation (\bar{U}^T, \bar{U}) to the realization of $R_{R1}(s)$ in (4.2-1e) and then using (4.1-9) and (4.2-10), we have

$$R_{R1}(s) = \left[\begin{array}{cc|c} -A_3 & -A_{34} + L_3 L_4^T Y_2 & -L_3 \\ 0 & -A_4 + L_4 L_4^T Y_2 & -L_4 \\ \hline 0 & \# & D_{11}(\tilde{R}_D^{-1/2} D_{21})^T \\ 0 & 0 & \tilde{R}_D^{1/2} \end{array} \right] \\ = \left[\begin{array}{c|c} -A_4 + L_4 L_4^T Y_2 & -L_4 \\ \hline \# & D_{11}(\tilde{R}_D^{-1/2} D_{21})^T \\ 0 & \tilde{R}_D^{1/2} \end{array} \right] \quad (4.2-11a)$$

where

$$\# = C_1 U_4 Y_2 + D_{11}(\tilde{D}_\perp^T W_4 - D_{21}^T \tilde{R}_D^{-1} C_2 U_4 Y_2) \quad (4.2-11b)$$

The size of the state-space realization of $R_{R1}(s)$ has been reduced from the dimension of A to that of A_4 although the realization in (4.2-11) in general is neither controllable nor observable.

Remark 4.2-3:

If $R_{R2}(s) = 0$, i.e., $\tilde{D}_\perp = 0$, then it is easy to prove that the pair

$$\{ (A_4 - L_4 L_4^T Y_2), L_4 \}$$

is controllable. In this case, the realization of $R_{R1}(s)$ in (4.2-11) is controllable.

There exists an orthogonal matrix

$$\bar{V} = \begin{bmatrix} V_3 & V_4 \end{bmatrix} \quad (4.2-12a)$$

such that

$$\begin{aligned} & -\bar{V}^T(A_4 - L_4 L_4^T Y_2) \bar{V} \\ &= \begin{bmatrix} -V_3^T(A_4 - L_4 L_4^T Y_2) V_3 & 0 \\ -V_4^T(A_4 - L_4 L_4^T Y_2) V_3 & -V_4^T(A_4 - L_4 L_4^T Y_2) V_4 \end{bmatrix} \end{aligned} \quad (4.2-12b)$$

and

$$\begin{bmatrix} \# \\ 0 \end{bmatrix} \bar{V} = \begin{bmatrix} \#V_3 & 0 \\ 0 & 0 \end{bmatrix} \quad (4.2-12c)$$

and the pair

$$\{ \#V_3, -V_3^T(A_4 - L_4 L_4^T Y_2) V_3 \} \quad (4.2-12d)$$

is observable.

Applying the similarity transformation (\bar{V}^T, \bar{V}) to the realization of $R_{R1}(s)$ in (4.2-11) and eliminating the unobservable part, we have the following realization which is observable

$$R_{R1}(s) = \left[\begin{array}{c|c} -V_3^T(A_4 - L_4 L_4^T Y_2) V_3 & -V_3^T L_4 \\ \hline \#V_3 & D_{11}(\tilde{R}_D^{-1/2} D_{21})^T \\ 0 & \tilde{R}_D^{1/2} \end{array} \right] \quad (4.2-13)$$

If $R_{R2}(s) = 0$, then from Remark 4.2-3 the realization of $R_{R1}(s)$ in (4.2-13) is controllable and therefore is minimal. Otherwise, we can find an orthogonal matrix

$$\bar{S} = \begin{bmatrix} S_3 & S_4 \end{bmatrix} \quad (4.2-14a)$$

such that

$$\begin{aligned}
& -\bar{S}^T V_3^T (A_4 - L_4 L_4^T Y_2) V_3 \bar{S} \\
& = \begin{bmatrix} -S_3^T V_3^T (A_4 - L_4 L_4^T Y_2) V_3 S_3 & -S_3^T V_3^T (A_4 - L_4 L_4^T Y_2) V_3 S_4 \\ 0 & -S_4^T V_3^T (A_4 - L_4 L_4^T Y_2) V_3 S_4 \end{bmatrix}
\end{aligned} \tag{4.2-14b}$$

and

$$-\bar{S}^T V_3^T L_4 = \begin{bmatrix} -S_3^T V_3^T L_4 \\ 0 \end{bmatrix} \tag{4.2-14c}$$

and the pair

$$\{ -S_3^T V_3^T (A_4 - L_4 L_4^T Y_2) V_3 S_3, -S_3^T V_3^T L_4 \} \tag{4.2-14d}$$

is controllable.

Applying the similarity transformation (\bar{S}^T, \bar{S}) to the realization of $R_{R1}(s)$ in (4.2-13) and eliminating the uncontrollable part, we have the following minimal realization:

$$R_{R1}(s) = \left[\begin{array}{c|c} -S_3^T V_3^T (A_4 - L_4 L_4^T Y_2) V_3 S_3 & -S_3^T V_3^T L_4 \\ \hline \# V_3 S_3 & D_{11} (\tilde{R}_D^{-1/2} D_{21})^T \\ 0 & \tilde{R}_D^{1/2} \end{array} \right] \tag{4.2-15}$$

Minimal Realization of $R_{R2}(s)$

Applying the similarity transformations (\bar{U}^T, \bar{U}) and then (\bar{V}^T, \bar{V}) to the realization of $R_{R2}(s)$ in (4.2-1f) and eliminating the unobservable part, we have the following realization which is observable:

$$R_{R2}(s) = \left[\begin{array}{c|c} -V_3^T (A_4 - L_4 L_4^T Y_2) V_3 & V_3^T Y_2^{-1} W_4^T \\ \hline \# V_3 & D_{11} \tilde{D}_\perp^T \\ 0 & 0 \end{array} \right] \quad (4.2-16)$$

Furthermore, we can find an orthogonal matrix

$$\bar{T} = \begin{bmatrix} T_3 & T_4 \end{bmatrix} \quad (4.2-17a)$$

such that

$$\begin{aligned} & -\bar{T}^T V_3^T (A_4 - L_4 L_4^T Y_2) V_3 \bar{T} \\ &= \begin{bmatrix} -T_3^T V_3^T (A_4 - L_4 L_4^T Y_2) V_3 T_3 & -T_3^T V_3^T (A_4 - L_4 L_4^T Y_2) V_3 T_4 \\ 0 & -T_4^T V_3^T (A_4 - L_4 L_4^T Y_2) V_3 T_4 \end{bmatrix} \end{aligned} \quad (4.2-17b)$$

and

$$\bar{T}^T V_3^T Y_2^{-1} W_4^T = \begin{bmatrix} T_3^T V_3^T Y_2^{-1} W_4^T \\ 0 \end{bmatrix} \quad (4.2-17c)$$

and the pair

$$\{ -T_3^T V_3^T (A_4 - L_4 L_4^T Y_2) V_3 T_3, \quad T_3^T V_3^T Y_2^{-1} W_4^T \} \quad (4.2-17d)$$

is controllable.

Applying the similarity transformation (\bar{T}^T, \bar{T}) to the realization of $R_{R2}(s)$ in (4.2-16) and eliminating the uncontrollable part, we have the following minimal realization:

$$R_{R2}(s) = \left[\begin{array}{c|c} -T_3^T V_3^T (A_4 - L_4 L_4^T Y_2) V_3 T_3 & T_3^T V_3^T Y_2^{-1} W_4^T \\ \hline \# V_3 T_3 & D_{11} \tilde{D}_1^T \\ 0 & 0 \end{array} \right] \quad (4.2-18)$$

4.3 Fast γ -iteration Algorithm for the Solution of the Two-block H^∞ Optimization Problem

4.3.1 Basic Concept of Fast γ -iteration

In (4.1-4), if $\begin{bmatrix} R_{12}^T & R_{22}^T \end{bmatrix} = 0$, i.e.,

$$\hat{\Phi}(s) = \begin{bmatrix} R_{11}(s) + \hat{Q}(s) \\ R_{21}(s) \end{bmatrix} \quad (4.3-1)$$

then we have the two-block H^∞ optimization problem described as follows,

$$\begin{aligned} &\text{Find a } \hat{Q}(s) \in (RH^\infty)^{m \times r} \text{ such that } \|\hat{\Phi}\|_\infty \text{ is minimized} \\ &\text{where } \hat{\Phi} \text{ is given by (4.3-1).} \end{aligned} \quad (4.3-2)$$

The two-block H^∞ optimization problem arises in the optimal disturbance attenuation with control weighting, the minimization of a weighted sum involving both the sensitivity function and its complement, and any control problems with more controlled outputs than control inputs. The two-block H^∞ optimization problem usually is solved in two steps. The first step is the computation of the optimal H^∞ norm $\|\hat{\Phi}\|_\infty$ which is the most time-consuming job. The second step is the construction of an optimal $\hat{Q}(s)$ and then an optimal controller.

In this section, a very fast iterative algorithm was developed for the computation of the optimal two-block H^∞ norm, i.e., the computation of

$$\inf_{\hat{Q} \in (RH^\infty)^{m \times r}} \left\| \begin{bmatrix} R_{11} + \hat{Q} \\ R_{21} \end{bmatrix} \right\|_\infty := \gamma_0 \quad (4.3-3)$$

$R_{11}(s)$ and $R_{21}(s)$ are in $(RL^\infty)^{m \times r}$ and $(RL^\infty)^{q \times r}$ respectively. $(RL^\infty)^{m \times r}$ is the set of proper rational matrices with real coefficients which are analytic on the imaginary axis.

In the two-block H^∞ optimization problem, the most computationally demanding work is the computation of the optimal H^∞ norm γ_0 . Define

$$\mu(\gamma) = \inf_{\hat{Q} \in (RH^\infty)^{m \times r}} \left\| \left[R_{11}(s) + \hat{Q}(s) \right] M(s, \gamma)^{-1} \right\|_\infty \quad (4.3-4a)$$

where

$$\gamma^2 I - R_{21}(-s)^T R_{21}(s) = M(-s, \gamma)^T M(s, \gamma) \quad (4.3-4b)$$

Then the problem of computing γ_0 can be considered as that of finding a γ such that $\mu(\gamma)$ equals to 1.

In γ -iteration approach, an initial guess of the optimal norm γ_0 , say γ , is made and the computations of the spectral factorization (4.3-4b) and the one-block optimal H^∞ norm computation (4.3-4a) are performed to determine what the next guess shall be. The next guess of γ is determined by the value of $\mu(\gamma)$. This guess and computation loop is repeated until $\mu(\gamma) = 1$. Numerically, this computation ends when $|\mu(\gamma) - 1| < \epsilon$, where ϵ is a very small number. This search scheme works all right if $|\mu(\gamma) - 1| < \epsilon$ implies that $|\gamma - \gamma_0| < \epsilon$, i.e., the absolute value of the slope of $\mu(\gamma)$ at γ is large enough. On the other hand, if the absolute value of the slope is small, we may have $|\gamma - \gamma_0| \gg \epsilon$. In other words, the accuracy of γ may be very poor although the accuracy of $\mu(\gamma)$ is good.

A simple bisection search scheme can be used. Starting from a lower bound γ_L and an upper bound γ_U , one can define $\gamma = (\gamma_L + \gamma_U)/2$ and evaluate $\mu(\gamma)$. If $\mu(\gamma) > 1$, then γ_L is updated by γ . Otherwise, γ_U is replaced by γ . This process is repeated until the gap between γ_L and γ_U is small enough. This search scheme is straightforward, but the convergence rate is slow. Say, the initial gap between γ_L and γ_U is 1. To reduce the gap to be less than 10^{-15} , the number of iterations required is

$$n > 15 / (\log_{10} 2) = 49.8$$

In Sec.4.3.3 a very fast iterative algorithm is developed for the computation of the optimal H^∞ norm γ_0 in (4.3-3). To achieve this objective, three tasks have been done. The first task is to find better initial lower and upper bounds of γ_0 . Here "initial lower and upper bounds" means the lower and upper bounds which can be easily computed without doing any spectral factorization. The second task is to reduce the computation amount in each iteration. The last, but the most important task is to find a fast search scheme by which the number of iterations is greatly reduced.

In Sec.4.3.2 we present an easy way of computing a new initial lower bound and showed some useful properties of $\mu(\gamma)$ which had just been discovered. Together with the well-known properties of $\mu(\gamma)$, these discoveries are of great help in developing a sophisticated and fast search scheme for γ_0 . The initial lower and upper bounds are denoted by γ_1 and γ_2 respectively.

Before entering the iteration loop, we compute $\mu(\gamma_1)$, and $\mu(\gamma_2)$. With the knowledge of γ_1 , $\mu(\gamma_1)$, γ_2 , and $\mu(\gamma_2)$, we can generate three new upper-bound candidates and two new lower-bound candidates very easily. A new greatest lower bound, denoted by γ_3 , and a new least upper bound, denoted by γ_4 , can be found.

Now we are starting the iteration loop with the input data: γ_1 , $\mu(\gamma_1)$, γ_2 , $\mu(\gamma_2)$, γ_3 , and γ_4 . Let $\gamma = (\gamma_3 + \gamma_4)/2$, and evaluate $\mu(\gamma)$. If $\mu(\gamma)$ is exactly equal to 1, then γ is the optimal norm γ_0 . Otherwise, $\mu(\gamma)$ may be greater or less than 1. In either case, we can easily generate two new lower-bound candidates and two new upper-bound candidates by using the information of γ , $\mu(\gamma)$, γ_1 , $\mu(\gamma_1)$, γ_2 , and $\mu(\gamma_2)$. The bounds γ_3 , and γ_4 can be updated by the new greatest lower bound and the new least upper bound respectively. Depending on the sign of $\mu(\gamma)-1$, either the pair $\{\gamma_1, \mu(\gamma_1)\}$ or the pair $\{\gamma_2, \mu(\gamma_2)\}$ will be updated by $\{\gamma, \mu(\gamma)\}$. The iteration loop is repeated until the difference $\gamma_4 - \gamma_3$ is small enough.

The proposed fast γ -iteration search scheme is much faster than any other existing γ -iteration search scheme. We only require one evaluation of $\mu(\gamma)$ per iteration. In each iteration, two new lower-bound and two new upper-bound candidates are generated. In several examples we have encountered, the gap of lower and upper bounds can be reduced from 1 to 10^{-15} in only 2 or 3 iterations.

4.3.2 Bounds and Properties of the Function $\mu(\gamma)$

For notational simplicity, we will omit the indeterminates s or $j\omega$ when there is no confusion. A^* is the conjugate transpose of A if A is a constant matrix. The same notation A^* is also used as a short-hand notation for $A^T(-s)$ when A is a rational matrix.

First of all, we need to find the initial lower and upper bounds of γ_0 . The initial bounds are those which can be easily obtained without doing any heavy computation like spectral factorization or Hankel-Toeplitz approximation. The initial bounds which appeared in the literatures [17,18,67] are listed as follows. The initial upper bounds are

$$\gamma_{U1} := \left\| \begin{bmatrix} R_{11} \\ R_{21} \end{bmatrix} \right\|_{\infty} \geq \gamma_0 \quad (4.3-5a)$$

$$\gamma_{U2} := \bar{\sigma} \begin{bmatrix} a \\ b \end{bmatrix} \geq \gamma_0 \quad (4.3-5b)$$

where

$$a = \inf_{\hat{Q} \in (RH^{\infty})^{m \times r}} \| R_{11} + \hat{Q} \|_{\infty} \quad (4.3-5c)$$

and

$$b = \| R_{21} \|_{\infty} \quad (4.3-5d)$$

The initial lower bounds are

$$\gamma_{L1} := b \leq \gamma_0 \quad (4.3-6a)$$

$$\gamma_{L2} := a \leq \gamma_0 \quad (4.3-6b)$$

$$\gamma_{L3} := \inf_{\substack{\hat{Q} \in (RH^\infty)^{m \times r} \\ \hat{Q}_1 \in (RH^\infty)^{q \times r}} \left\| \begin{bmatrix} R_{11} \\ R_{21} \end{bmatrix} + \begin{bmatrix} \hat{Q} \\ \hat{Q}_1 \end{bmatrix} \right\|_\infty \leq \gamma_0 \quad (4.3-6c)$$

where a and b are given in (4.3-5c) and (4.3-5d) respectively. The lower bound γ_{L3} is greater or equal to γ_{L2} .

Now we have the best pair of initial lower and upper bounds as follows.

$$\gamma_L = \max \{ \gamma_{L1}, \gamma_{L3} \} \quad (4.3-7a)$$

and

$$\gamma_U = \min \{ \gamma_{U1}, \gamma_{U2} \} \quad (4.3-7b)$$

To design a fast and effective iterative algorithm for the computation of γ_0 , it is important to have enough knowledge about the properties of the function $\mu(\gamma)$ which is defined in (4.3-4). Chu, Doyle and Lee [18], and Wang and Pearson [68] have made great contributions in this. Their results are listed in the following.

Theorem 4.3-1: [18]

The function $\mu(\gamma)$ is a continuous, convex, and strictly monotonically decreasing function of γ .

Theorem 4.3-2: [18]

Define

$$f(\alpha, \gamma) = \mu(\alpha) \sqrt{\alpha^2 - b^2} / \sqrt{\gamma^2 - b^2} \quad (4.3-8)$$

for some $\alpha > b$, where $b = \|R_{21}\|_\infty$. Then

$$\text{i) } \mu(\gamma) < f(\alpha, \gamma) \text{ if } \gamma < \alpha. \quad (4.3-9a)$$

$$\text{ii) } \mu(\gamma) = f(\alpha, \gamma) \text{ if } \gamma = \alpha. \quad (4.3-9b)$$

$$\text{iii) } \mu(\gamma) > f(\alpha, \gamma) \text{ if } \gamma > \alpha. \quad (4.3-9c)$$

Theorem 4.3-3: [68]

$$\text{If } \mu(\gamma) > 1, \text{ then} \quad \gamma_0 < \mu(\gamma) \gamma \quad (4.3-10)$$

Theorem 4.3-4: [68]

If $\mu(\gamma) < 1$, then

$$\gamma_0 < \sqrt{\mu^2(\gamma) \gamma^2 + [1 - \mu^2(\gamma)] b^2} \quad (4.3-11)$$

where $b = \|R_{21}\|_\infty$.

The bound in Theorem 4.3-4 can also be derived from Theorem 4.3-2. However, Wang and Pearson found this bound before Chu, Doyle and Lee obtained Theorem 4.3-2. Chu, Doyle and Lee never used this bound in their algorithm. From Theorem 4.3-2, it is easy to have the following corollary.

Corollary 4.3-5:

If $\mu(\gamma) > 1$, then

$$\gamma_0 > \sqrt{\mu^2(\gamma) \gamma^2 + [1 - \mu^2(\gamma)] b^2} \quad (4.3-12)$$

where $b = \|R_{21}\|_\infty$.

Proof of Corollary 4.3-5:

$\mu(\gamma) > 1 \Rightarrow \gamma < \gamma_0 \Rightarrow$ from Theorem 4.3-2 (i) we have

$$\mu^2(\gamma) (\gamma^2 - b^2) < \gamma_0^2 - b^2 \Rightarrow (4.3-12).$$

The following theorem is a modified version of Theorem 4.3-3. The proof is similar to that of Theorem 4.3-3 and therefore is omitted.

Theorem 4.3-6:

$$\text{If } \mu(\gamma) > 1, \text{ then} \quad \gamma_0 \leq \sqrt{\mu^2(\gamma) \gamma^2 + [1 - \mu^2(\gamma)] c^2} \quad (4.3-13a)$$

where

$$c = \inf_{\omega} \sigma[R_{21}(j\omega)] \quad (4.3-13b)$$

$\sigma(A)$ is the minimum singular value of A .

Theorem 4.3-6 is very useful in speeding up the convergence rate. Notice that Theorem 4.3-4 and Corollary 4.3-5 are so alike that the only difference is the direction of the inequality arrows. Corollary 4.3-5 can be obtained by reversing the inequality arrows in Theorem 4.3-4. This inequality-arrow-reversing property motivated us that Theorem 4.3-6 may have its counterpart as follows.

Theorem 4.3-7:

If $\mu(\gamma) < 1$, then

$$\gamma_o \geq \sqrt{\mu^2(\gamma) \gamma^2 + [1 - \mu^2(\gamma)] c^2} \quad (4.3-14)$$

where c is given by (4.3-13b).

Proof : See Appendix A.

The following corollary plays an important role in our algorithm. This corollary can be easily derived by using the properties in Theorem 4.3-1.

Corollary 4.3-8:

Given γ_1 , γ_2 , $\mu(\gamma_1)$, and $\mu(\gamma_2)$ and $\gamma_1 < \gamma_2$. The optimal norm γ_o lies between γ_1 and γ_2 , i.e., $\gamma_1 < \gamma_o < \gamma_2$. Suppose γ_5 is a point such that $\gamma_1 < \gamma_5 < \gamma_2$, and the value $\mu(\gamma_5)$ is known.

i) If $\mu(\gamma_5) > 1$, then

$$\gamma_o > \gamma_5 + [\mu(\gamma_5) - 1][\gamma_5 - \gamma_1] / [\mu(\gamma_1) - \mu(\gamma_5)] \quad (4.3-15)$$

and

$$\gamma_o < \gamma_5 + [\mu(\gamma_5) - 1][\gamma_5 - \gamma_2] / [\mu(\gamma_2) - \mu(\gamma_5)] \quad (4.3-16)$$

ii) If $\mu(\gamma_5) < 1$, then

$$\gamma_o < \gamma_5 + [\mu(\gamma_5) - 1][\gamma_5 - \gamma_1] / [\mu(\gamma_1) - \mu(\gamma_5)] \quad (4.3-17)$$

and

$$\gamma_o > \gamma_5 + [\mu(\gamma_5) - 1][\gamma_5 - \gamma_2] / [\mu(\gamma_2) - \mu(\gamma_5)] \quad (4.3-18)$$

Proof of Corollary 4.3-8: See Appendix A.

4.3.3 Fast γ -Iteration Algorithm

We will start with the initial lower and upper bounds of γ . The initial lower and upper bound are

$$\gamma_L = \max \{ \gamma_{L1}, \gamma_{L3} \} \quad (4.3-19)$$

and

$$\gamma_U = \min \{ \gamma_{U1}, \gamma_{U2} \} \quad (4.3-20)$$

where γ_{U1} , γ_{U2} , γ_{L1} , and γ_{L3} are given by (4.3-5a), (4.3-5b), (4.3-6a), and (4.3-6c) respectively.

Before entering the iteration loop, some initialization should be done. Let

$$\gamma_1 = \gamma_L \quad \text{and} \quad \gamma_2 = \gamma_U \quad (4.3-21)$$

and evaluate $\mu(\gamma_1)$ and $\mu(\gamma_2)$. Since $\gamma_1 < \gamma_o < \gamma_2$, we have

$$\mu(\gamma_1) > 1 \quad \text{and} \quad \mu(\gamma_2) < 1 \quad (4.3-22)$$

From Theorem 4.3-4, Theorem 4.3-6, Corollary 4.3-5, and Theorem 4.3-7, we have the following:

$$\gamma_o \leq \sqrt{\mu^2(\gamma_1) \gamma_1^2 + [1 - \mu^2(\gamma_1)] c^2} := \alpha_{U1} \quad (4.3-23)$$

$$\gamma_o < \sqrt{\mu^2(\gamma_2) \gamma_2^2 + [1 - \mu^2(\gamma_2)] b^2} := \alpha_{U2} \quad (4.3-24)$$

$$\gamma_o > \sqrt{\mu^2(\gamma_1) \gamma_1^2 + [1 - \mu^2(\gamma_1)] b^2} := \alpha_{L2} \quad (4.3-25)$$

and

$$\gamma_0 \geq \sqrt{\mu^2(\gamma_2) \gamma_2^2 + [1 - \mu^2(\gamma_2)] c^2} := \alpha_{L1} \quad (4.3-26)$$

where $b = \|R_{21}\|_\infty$ and $c = \inf_{\omega} \sigma[R_{21}(j\omega)]$.

It is easy to see that the intersection of the horizontal line $y = 1$ and the straight line connecting the two points $(\gamma_1, \mu(\gamma_1))$ and $(\gamma_2, \mu(\gamma_2))$ is at the right of the point $(\gamma_0, 1)$. That is,

$$\gamma_0 < \gamma_2 + [\mu(\gamma_2) - 1][\gamma_2 - \gamma_1] / [\mu(\gamma_1) - \mu(\gamma_2)] := \alpha_{U3} \quad (4.3-27)$$

Let

$$\gamma_3 = \max \{ \alpha_{L1}, \alpha_{L2} \} \quad (4.3-28)$$

$$\gamma_4 = \min \{ \alpha_{U1}, \alpha_{U2}, \alpha_{U3} \} \quad (4.3-29)$$

where $\alpha_{L1}, \alpha_{L2}, \alpha_{U1}, \alpha_{U2}$, and α_{U3} are given by (4.3-23) - (4.3-27). It is easy to see that

$$\gamma_1 < \gamma_3 \leq \gamma_0 \leq \gamma_4 < \gamma_2 \quad (4.3-30)$$

After the initialization of $\gamma_1, \mu(\gamma_1), \gamma_2, \mu(\gamma_2), \gamma_3$, and γ_4 , we are ready to enter into the iteration loop. The first step of the iteration loop is to let

$$\gamma_5 = (\gamma_3 + \gamma_4) / 2 \quad (4.3-31)$$

and compute $\mu(\gamma_5)$. Define

$$\beta_1 := \sqrt{\mu^2(\gamma_5) \gamma_5^2 + [1 - \mu^2(\gamma_5)] c^2} \quad (4.3-32)$$

$$\beta_2 := \sqrt{\mu^2(\gamma_5) \gamma_5^2 + [1 - \mu^2(\gamma_5)] b^2} \quad (4.3-33)$$

$$\beta_3 := \gamma_5 + [\mu(\gamma_5) - 1][\gamma_5 - \gamma_1] / [\mu(\gamma_1) - \mu(\gamma_5)] \quad (4.3-34)$$

$$\beta_4 := \gamma_5 + [\mu(\gamma_5) - 1][\gamma_5 - \gamma_2] / [\mu(\gamma_2) - \mu(\gamma_5)] \quad (4.3-35)$$

where $b = \|R_{21}\|_\infty$ and $c = \inf_{\omega} \sigma[R_{21}(j\omega)]$.

Now we compare $\mu(\gamma_5)$ with 1. If $\mu(\gamma_5) > 1$, then from Theorem 4.3-6, Corollary 4.3-5, and Corollary 4.3-8, we have

$$\gamma_0 \leq \beta_1, \quad \gamma_0 > \beta_2, \quad \gamma_0 > \beta_3, \quad \gamma_0 < \beta_4 \quad (4.3-36)$$

Thus, $\gamma_3, \gamma_4, \gamma_1$, and $\mu(\gamma_1)$ are updated as follows

$$\begin{aligned} \gamma_3 &= \max \{ \beta_2, \beta_3 \}, & \gamma_4 &= \min \{ \beta_1, \beta_4, \gamma_4 \}, \\ \gamma_1 &= \gamma_5, & \mu(\gamma_1) &= \mu(\gamma_5) \end{aligned} \quad (4.3-37)$$

where $\beta_1, \beta_2, \beta_3$, and β_4 are given by (4.3-32) - (4.3-35).

If $\mu(\gamma_5) < 1$, then from Theorem 4.3-4, Theorem 4.3-7, and Corollary 4.3-8, we have

$$\gamma_0 < \beta_2, \quad \gamma_0 \geq \beta_1, \quad \gamma_0 < \beta_3, \quad \gamma_0 > \beta_4 \quad (4.3-38)$$

Thus, $\gamma_3, \gamma_4, \gamma_2$, and $\mu(\gamma_2)$ are updated as follows

$$\begin{aligned} \gamma_3 &= \max \{ \beta_1, \beta_4, \gamma_3 \}, & \gamma_4 &= \min \{ \beta_2, \beta_3 \}, \\ \gamma_2 &= \gamma_5, & \mu(\gamma_2) &= \mu(\gamma_5) \end{aligned} \quad (4.3-39)$$

where $\beta_1, \beta_2, \beta_3$, and β_4 are given by (4.3-32) - (4.3-35).

The iteration loop is repeated until the difference $\gamma_4 - \gamma_3$ is small enough. The accuracy of γ_0 , i.e., $(\gamma_4 - \gamma_3) / 2$, can be arbitrarily small by simply increasing the number of iterations.

The fast iterative algorithm for the computation of γ_0 in (4.3-3) is summarized as follows.

Fast γ -iteration Algorithm:

(1) Compute the initial lower and upper bounds

$$\gamma_1 = \max \{ \gamma_{L1}, \gamma_{L3} \}, \quad \gamma_2 = \min \{ \gamma_{U1}, \gamma_{U2} \}$$

where γ_{U1} , γ_{U2} , γ_{L1} , and γ_{L3} are given by (4.3-5a), (4.3-5b), (4.3-6a), and (4.3-6c) respectively.

- (2) Evaluate $\mu(\gamma_1)$ and $\mu(\gamma_2)$.
- (3) If $\mu(\gamma_1)$ or $\mu(\gamma_2)$ equals to 1, then $\gamma_o = \mu(\gamma_1)$ or $\gamma_o = \mu(\gamma_2)$ and go to (11).
- (4) Compute the bounds γ_3 and γ_4 .

$$\gamma_3 = \max \{ \alpha_{L1}, \alpha_{L2} \}, \quad \gamma_4 = \min \{ \alpha_{U1}, \alpha_{U2}, \alpha_{U3} \}$$

where α_{L1} , α_{L2} , α_{U1} , α_{U2} , and α_{U3} are given by (4.3-23) - (4.3-27).

- (5) If $|\gamma_4 - \gamma_3| < \epsilon$, then $\gamma_o = (\gamma_3 + \gamma_4) / 2$ and go to (11). (ϵ is the acceptable accuracy.)
- (6) Let $\gamma_5 = (\gamma_3 + \gamma_4) / 2$ and evaluate $\mu(\gamma_5)$.
- (7) If $\mu(\gamma_5) = 1$, then $\gamma_o = \gamma_5$ and go to (11).
- (8) If $\mu(\gamma_5) < 1$, then go to (10).
- (9) If $\mu(\gamma_5) > 1$, then update $\gamma_3, \gamma_4, \gamma_1$ and $\mu(\gamma_1)$ as

$$\begin{aligned} \gamma_3 &= \max \{ \beta_2, \beta_3 \}, & \gamma_4 &= \min \{ \beta_1, \beta_4, \gamma_4 \} \\ \gamma_1 &= \gamma_5, & \mu(\gamma_1) &= \mu(\gamma_5) \end{aligned}$$

and then go to (5), where $\beta_1, \beta_2, \beta_3$, and β_4 are given by (4.3-32) - (4.3-35).

- (10) Update $\gamma_3, \gamma_4, \gamma_2$ and $\mu(\gamma_2)$ as

$$\begin{aligned} \gamma_3 &= \max \{ \beta_1, \beta_4, \gamma_3 \}, & \gamma_4 &= \min \{ \beta_2, \beta_3 \} \\ \gamma_2 &= \gamma_5, & \mu(\gamma_2) &= \mu(\gamma_5) \end{aligned}$$

and then go to (5), where $\beta_1, \beta_2, \beta_3$, and β_4 are given by (4.3-32) - (4.3-35).

- (11) Stop.

4.4 Using DGKF's Solution To Solve A Four-Block H^∞ Optimization Problem

In [29], DGKF assume the realization of $G(s)$ is given by

$$G(s) = \left[\begin{array}{c|cc} A & B_1 & B_2 \\ \hline C_1 & 0 & D_{12} \\ C_2 & D_{21} & 0 \end{array} \right] \quad (4.4-1)$$

with the following assumptions.

$$(i) \quad (A, B_1) \text{ is stabilizable and } (C_1, A) \text{ is detectable.} \quad (4.4-2a)$$

$$(ii) \quad (A, B_2) \text{ is stabilizable and } (C_2, A) \text{ is detectable.} \quad (4.4-2b)$$

$$(iii) \quad D_{12}^T [C_1 \ D_{12}] = [0 \ I]. \quad (4.4-2c)$$

$$(iv) \quad \begin{bmatrix} B_1 \\ D_{21} \end{bmatrix} D_{21}^T = \begin{bmatrix} 0 \\ I \end{bmatrix}. \quad (4.4-2d)$$

Define two Hamiltonian matrices as follows,

$$H_\infty := \begin{bmatrix} A & \gamma^2 B_1 B_1^T - B_2 B_2^T \\ -C_1^T C_1 & -A^T \end{bmatrix}, \quad (4.4-3a)$$

and

$$J_\infty := \begin{bmatrix} A^T & \gamma^2 C_1^T C_1 - C_2^T C_2 \\ -B_1 B_1^T & -A \end{bmatrix} \quad (4.4-3b)$$

Then the following theorems will characterize the set of suboptimal stabilizing controllers such that $\|\Phi\|_\infty < \gamma$ where Φ is the closed-loop transfer matrix from v to z .

Theorem 4.4-1: [29]

There exists a stabilizing controller such that $\|\Phi\|_\infty < \gamma$ if and only if the following three conditions hold.

$$(i) \quad H_\infty \in \text{dom}(\text{Ric}) \text{ and } X_\infty := \text{Ric}(H_\infty) \geq 0. \quad (4.4-4a)$$

$$(ii) \quad J_\infty \in \text{dom}(\text{Ric}) \text{ and } Y_\infty := \text{Ric}(J_\infty) \geq 0. \quad (4.4-4b)$$

$$(iii) \quad \rho(X_\infty Y_\infty) < \gamma^2. \quad (4.4-4c)$$

Moreover, when these conditions hold, one such controller is

$$K_{\text{sub}}(s) = \left[\begin{array}{c|c} \hat{A}_\infty & -Z_\infty L_\infty \\ \hline F_\infty & 0 \end{array} \right] \quad (4.4-5a)$$

where

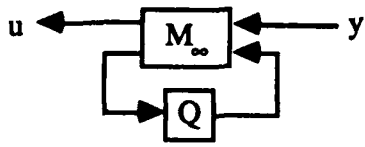
$$\hat{A}_\infty = A + \gamma^2 B_1 B_1^T X_\infty + B_2 F_\infty + Z_\infty L_\infty C_2 \quad (4.4-5b)$$

$$F_\infty := -B_2^T X_\infty, \quad L_\infty := -Y_\infty C_2^T, \quad Z_\infty := (I - \gamma^2 Y_\infty X_\infty)^{-1}. \quad (4.4-5c)$$

In the above theorem, condition (i) means that there exists a nonnegative definite solution X_∞ to the Riccati equation corresponding to the Hamiltonian H_∞ . Condition (iii) means that the spectral radius of $X_\infty Y_\infty$ is less than γ^2 .

Theorem 4.4-2: [29]

If conditions (i) to (iii) in Theorem 4.4-1 are satisfied, the set of all stabilizing controllers such that $\|\Phi\|_\infty < \gamma$ equals the set of all transfer matrices from y to u in



$$M_\infty(s) = \left[\begin{array}{c|cc} \hat{A}_\infty & -Z_\infty L_\infty & Z_\infty B_2 \\ \hline F_\infty & 0 & I \\ -C_2 & I & 0 \end{array} \right] \quad (4.4-6)$$

where $Q \in \text{RH}^\infty$, $\|Q\|_\infty < \gamma$.

The above two theorems show an easy state-space approach in constructing a stabilizing suboptimal controller such that $\|\Phi\|_\infty < \gamma$. The order of the suboptimal controller

can be the same as that of the plant $G(s)$. The major computation involved is the solution of two Riccati equations which are easy to solve if solution exist.

The DGKF approach is a great break-through in the solution of H^∞ optimization problem. However, if we try to reduce the value of γ to the minimum we will encounter numerical difficulty before γ reaches the minimum. The optimum occurs when γ^2 equals to $\rho(X_\infty Y_\infty)$. When γ^2 is close to $\rho(X_\infty Y_\infty)$, the matrix $(I - \gamma^2 Y_\infty X_\infty)$ becomes ill-conditioned and the inversion $Z_\infty = (I - \gamma^2 Y_\infty X_\infty)^{-1}$ will not be numerically reliable. In (4.4-5a), both A and B matrices of $K_{\text{sub}}(s)$, i.e., \hat{A}_∞ and $-Z_\infty L_\infty$, rely on the computation of Z_∞ and therefore on the the inversion of $(I - \gamma^2 Y_\infty X_\infty)$.

In [38], we attempted to use DGKF approach to design an optimal controller for a four-block H^∞ optimization problem. We started from a large $\gamma = \gamma_U$ which guarantees solution existence of Riccati equations and $\rho(X_\infty Y_\infty) < \gamma^2$. Then γ is updated as $\gamma \leftarrow \sqrt{\rho(X_\infty Y_\infty)}$, the new Riccati equation solutions X_∞ and Y_∞ will make $\rho(X_\infty Y_\infty) > \gamma^2$. Let $\gamma_L \leftarrow \gamma$ and $\gamma \leftarrow \sqrt{\rho(X_\infty Y_\infty)}$, the new Riccati equation solutions X_∞ and Y_∞ will make $\rho(X_\infty Y_\infty) < \gamma^2$. Let $\gamma_U \leftarrow \gamma$ and $\gamma \leftarrow \sqrt{\rho(X_\infty Y_\infty)}$. The iterative process is repeated until the gap $\gamma_U - \gamma_L$ is small enough. The convergence rate is fast. For many examples, it only takes 8 to 10 iterations to reduce the gap from 100 to 10^{-10} .

As γ is close to the optimum, i.e., the gap $\gamma_U - \gamma_L$ is approaching to zero, the matrix $(I - \gamma^2 Y_\infty X_\infty)$ will be nearly singular and then the elements of Z_∞ and \hat{A}_∞ will approach to infinity. It looks like that there is no way to design a controller such that $\|\Phi\|_\infty$ is close to the optimum since the elements of A and B matrices of the controller will all approach to infinity. Nevertheless, the gain of the controller is not really infinite. If we do partial fraction expansion for the controller we will find that only some of the controller poles and their corresponding gains will approach to infinity and the rest will remain finite when γ is close to the optimum. These terms with infinite poles and gains can be approximated by

finite directly feedthrough terms. In other words, the practical optimal controllers will be proper with direct feedthrough terms instead of strictly proper.

The numerical difficulty is mainly caused by the restriction of the controller to be strictly proper. Most of optimal H^∞ controllers are proper with direct feedthrough. If a proper with direct feedthrough optimal controller is forced to be represented in a strictly proper form, some poles and their corresponding gains will be forced to be infinity.

The following is a simple four-block H^∞ optimization problem which is used to illustrate our numerical experience in using the DGKF's approach to design an H^∞ optimal controller. A realization of the plant $G(s)$ is given by

$$G(s) = \left[\begin{array}{c|cc} A & B_1 & B_2 \\ \hline C_1 & D_{11} & D_{12} \\ C_2 & D_{21} & D_{22} \end{array} \right] = \left[\begin{array}{cc|cc|c} -1 & 0 & 1 & 0 & 0 \\ 0 & 2 & 0 & 0 & 1 \\ \hline 1 & 1 & 0 & 0 & 0 \\ 0 & 0 & 0 & 0 & 1 \\ \hline 1 & 1 & 0 & 1 & 0 \end{array} \right] \quad (4.4-7)$$

The assumptions in (4.4-2) are all satisfied except assumption (i) which we believe is too restrictive. However, Theorems 4.4-1 and 4.4-2 are still applicable to this example even (A, B_1) is not stabilizable.

We started from $\gamma = 100$. Conditions (i) to (iii) are all satisfied and $\sqrt{\rho(X_\infty Y_\infty)} = 4.6476411024$ which is less than $\gamma = 100$. Update γ to be 4.6476411024 and compute the new Riccati equation solutions X_∞ and Y_∞ and $\sqrt{\rho(X_\infty Y_\infty)} = 4.7375420092$ which is greater than $\gamma = 4.6476411024$ and condition (iii) is not satisfied. The new value of $\sqrt{\rho(X_\infty Y_\infty)}$, i.e., 4.7375420092 is used to update γ . Now, just two iterations after the initial guess $\gamma = 100$, we find that the optimal $\|\Phi\|_\infty$, γ_0 , is between 4.6476411024 and 4.7375420092. After six more iterations, we have

$$4.7341604761 < \gamma_0 < 4.7341604768 \quad (4.4-8)$$

With $\gamma = 4.7341604768$ which is very close to the optimum, from (4.4-5) we have a state-space realization of the controller as follows:

$$K(s) = \left[\begin{array}{c|c} A_K & B_K \\ \hline C_K & 0 \end{array} \right] \quad (4.4-9a)$$

with

$$A_K = \begin{bmatrix} 2.7785374772e+09 & 2.7785374782e+09 \\ -2.4722482140e+10 & -2.4722482142e+10 \end{bmatrix} \quad (4.4-9b)$$

$$B_K = \begin{bmatrix} -2.7785374782e+09 \\ 2.4722482140e+10 \end{bmatrix} \quad (4.4-9c)$$

$$C_K = [-3.1088034728e-01 \quad -4.2370320107e+00] \quad (4.4-9d)$$

The eigenvalues of A_K are $-8.7542343140e-01$ and $-2.1943944664e+10$. Notice that one of the controller poles is pretty far away. When γ is nearly optimal, this pole will move further to the infinity. Do a partial fraction expansion for the above second order strictly proper controller $K(s)$, we have

$$K(s) = \frac{-8.9043458823e+00}{s+8.7542343140e-01} + \frac{1.0388615552e+11}{s+2.1943944664e+10} \quad (4.4-10)$$

The second term of the above expression is a wide band low-pass filter which can be approximated by a direct feedthrough term; therefore, $K(s)$ can be approximated by the following:

$$K_r(s) = \frac{-8.9043458823e+00}{s+8.7542343140e-01} + 4.7341604762 \quad (4.4-11)$$

With the controller $K_r(s)$, the closed-loop system is internally stable and the H^∞ norm of the closed-loop system from v to z , $\|\Phi\|_\infty$ is 4.7341604762 which is very close to the optimum up to the accuracy of 10^{-10} . This nearly optimal controller is proper with direct feedthrough and is first order which is one order less than that of the plant.

SECTION 5

COMPUTATION OF THE REAL STRUCTURED SINGULAR VALUE

Stability robustness is an important issue in the analysis and design of control systems. Currently, there are two major approaches to stability robustness analysis. One is the structured-singular-value (SSV) [39-45] or the multivariable-stability-margin (MSM) [46-50] approach and the other is the perturbed-characteristic-polynomials approach [51-56]. Several significant progresses have been made in both approaches.

For a large class of linear time-invariant systems with real parametric perturbations, the coefficient vector of the characteristic polynomial is a multilinear function of the real parameter vector. Based on this multilinear mapping together with the recent results by De Gaston and Safonov [48], Sideris and Pena [50], Bartlett, Hollot, and Lin [52], and Bouguerra, Chang, Yeh, and Banda [57], an algorithm for computing the real structured singular value is proposed. The algorithm requires neither frequency search nor Routh's array symbolic manipulations and allows the dependency among the elements of the parameter vector. Moreover, the number of the independent parameters in the parameter vector is not limited to three, as is required by many existing structured singular value computation algorithms.

In Sec.5.1, the definition of the real structured singular value is reviewed, and the basic concepts of the proposed algorithm are briefly described. In section 5.2, the mapping properties from the parameter space to the coefficient space and the theories on which the iterative algorithm is developed will be demonstrated. The detailed iterative algorithm for computing the real structured singular value is summarized in Sec.5.3. Sec.5.4 is a summary of the fast segment stability checking algorithm which is used repeatedly in the proposed iterative algorithm in computing the real SSV.

5.1 Definition of the Real Structured Singular Value and Preliminaries

According to Doyle and Safonov [39-40,46-47], all the plant uncertainties, structured or unstructured, unmodeled dynamics or parametric perturbations, can be described by the block diagram shown in Fig.5.1-1. In Fig.5.1-1, $\Delta(s)$ = block diag $\{\Delta_1(s), \Delta_2(s), \dots, \Delta_m(s)\}$ and $M(s)$ is the nominal system which includes the nominal plant and the stabilizing controller. Doyle [39-40] and Safonov [46-47] defined the structured singular value (SSV) and the multivariable stability margin (MSM) respectively based on the above perturbation structure and used them as analysis tools for robust stability. The SSV and the MSM are nonconservative scalar stability-margin measures for multivariable systems.

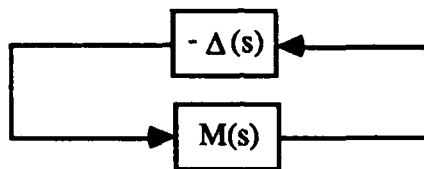


Fig.5.1-1 Standard structure for a perturbed closed-loop system.

Algorithms [39-45] to compute the SSV are available only for those cases where the number of perturbation blocks are less than or equal to three. The computational problem for the cases with more than three perturbation blocks is still an unsolved problem.

One important special case of plant uncertainties is the real parametric perturbation. In this case the perturbation matrix $\Delta(s)$ is a real diagonal matrix. The SSV defined for this case is called the real SSV. Algorithms of computing the real SSV [44-45] are also only available for those cases where the number of independent perturbation parameters are less than or equal to three. The MSM defined for this case is called the real MSM. An iterative algorithm of computing the real MSM for real diagonal Δ was developed by De Gaston and Safonov [48] and generalized by Pena and Sideris [49]. There is no limitation on the number of perturbation parameters. However, this iterative algorithm is complicated since

an extensive frequency search is required. In [50], Sideris and Pena eliminated the need of frequency search by requiring the first column of the Routh's array to be positive. This approach requires symbolic manipulations. Besides, the first-column elements of the Routh's array are not multilinear functions of the parameter vector even though the original characteristic coefficients are. For those elements to be multilinear functions of the parameters, more dependent parameters need to be created which will cause unnecessary complexity.

In the following we assume that the perturbation matrix Δ in Fig.5.1-1 is real diagonal, i.e., $\Delta = \text{diag} \{ \bar{\delta}_1, \bar{\delta}_2, \dots, \bar{\delta}_m \}$ and the nominal system $M(s)$ is a rational matrix with real coefficients. If the parameters vary independently and $-1 \leq \bar{\delta}_i \leq 1$, $i = 1, 2, \dots, m$, the parameter perturbation domain \mathcal{D} can be described as a hyper-cube $\bar{\mathcal{D}}$ with 2^m vertices $(\pm 1, \dots, \pm 1)$ in the m -dimensional real space. In general, the perturbation matrix Δ can be written as $\Delta = \text{diag} \{ \delta_1 I_{m_1}, \delta_2 I_{m_2}, \dots, \delta_r I_{m_r} \}$ where I_{m_i} is the identity matrix of order m_i and $m_1 + m_2 + \dots + m_r = m$. That is, $\bar{\delta}_1 = \bar{\delta}_2 = \dots = \bar{\delta}_{m_1} = \delta_1$, $\bar{\delta}_{m_1+1} = \bar{\delta}_{m_1+2} = \dots = \bar{\delta}_{m_1+m_2} = \delta_2$, ..., etc. In this case, the parameter perturbation domain \mathcal{D} is an r -dimensional hyperrectangle inside the m -dimensional hypercube $\bar{\mathcal{D}}$. The system is said to be robustly stable in \mathcal{D} if and only if it is stable for every parameter vector $\bar{\delta} = [\bar{\delta}_1 \ \bar{\delta}_2 \ \dots \ \bar{\delta}_m]^T$ in \mathcal{D} . Throughout the report, we may use " \mathcal{D} is stable" to replace "the system is robustly stable in \mathcal{D} " whenever there is no confusion.

The real multivariable stability margin (real MSM) k_M is defined as the largest real constant k such that the closed-loop system remains robustly stable in $k\mathcal{D}$ where $k\mathcal{D}$ is the enlarged (or shrunk) parameter perturbation domain of \mathcal{D} , i.e.,

$$k\mathcal{D} := \{ \bar{\delta} : \bar{\delta} = [\delta_1, \dots, \delta_1, \delta_2, \dots, \delta_2, \dots, \delta_r, \dots, \delta_r] \in \mathbb{R}^m \text{ and } |\delta_i| \leq k, i=1, 2, \dots, r \} \quad (5.1-1)$$

The enlarged (or shrunk) hypercube of $\bar{\mathcal{D}}$, $k\bar{\mathcal{D}}$ is

$$k\bar{\mathcal{D}} := \{ \bar{\delta} : \bar{\delta} \in \mathbb{R}^m \text{ and } |\delta_i| \leq k, i=1, 2, \dots, m \}. \quad (5.1-2)$$

Recall that the real structured singular value (real SSV) μ is defined as

$$\mu := [\min \{ k \mid \det [I + M(j\omega)\Delta] = 0 \text{ for some } \omega \text{ and } \Delta \in \mathbf{X}(k) \}]^{-1} \quad (5.1-3)$$

where

$$\mathbf{X}(k) = \{ \Delta \mid \text{diag} \{ \delta_1 I_{m_1}, \delta_2 I_{m_2}, \dots, \delta_r I_{m_r} \} \text{ with } |\delta_i| \leq k, \text{ for all } i \} \quad (5.1-4)$$

That is, the real SSV μ is the reciprocal of the smallest k such that the system is unstable in $k\mathcal{D}$. It is easy to see that the relation between the real SSV μ and the real MSM k_M is

$$\mu = 1 / k_M \quad (5.1-5)$$

Several significant results [51-56] have been obtained in the perturbed-characteristic-polynomials approach. Probably the most famous are the Kharitonov's theorems [51] which apply to the special case with a hyper-rectangular perturbed region in the coefficient space. In this special case, the coefficients of the characteristic polynomial vary independently and the robust stability of the system can be easily determined by four bounding characteristic polynomials. Unfortunately, the Kharitonov's theorems cannot be applied to our problem since the coefficient variations of the characteristic polynomial are not independent.

Bartlett, Hollot, and Lin [52] developed an important theorem which is applicable to the case when the coefficients of characteristic polynomial are linearly dependent. The theorem is now well known as the Edge Theorem: For the set of characteristic polynomials inside a polytope \mathcal{P} in the coefficient space, every polynomial in \mathcal{P} is stable if and only if all the exposed edges of \mathcal{P} are stable. This simplifies the stability checking tremendously since checking the stability of exposed edges is much simpler than checking that of the full \mathcal{P} . The exposed-edge stability checking is done by sweeping t from 0 to 1 such that

$$t \alpha^i + (1-t) \alpha^j \quad (5.1-6)$$

are all stable for all vertices α^i and α^j of \mathcal{P} .

Bialas [54] and Fu and Barmish [53] reduced the checking of the exposed-edge sweep stability to a one-shot test. They showed that $t \alpha^i + (1-t) \alpha^j$ is stable for all $t \in [0,1]$ if and only if the real eigenvalues of $-H_i H_j^{-1}$ are all negative where α^i and α^j are assumed to be stable and H_i and H_j are the Hurwitz matrices for α^i and α^j respectively. Recently, a fast algorithm based on Chapellat and Bhattacharyya's Segment Lemma [58] was proposed by Bouguerra, Chang, Yeh, and Banda [57] for checking the stability of the exposed edges. The computation in the algorithm mainly depends on the number of vertices instead of the edges and therefore reduces the computation burden due to the "combinatoric explosion."

There are no such celebrated properties in the parameter space as those in the coefficient space discovered by Kharitonov [51], Bartlett, Hollot, and Lin [52]. The closed-loop system may be unstable inside $\bar{\mathcal{D}}$ although it is stable at all the edges of the hypercube $\bar{\mathcal{D}}$ [59]. So far, there is no easy way of checking robust stability in the parameter space.

For each parameter vector $\bar{\delta}$ in the parameter perturbation domain \mathcal{D} , there is a corresponding characteristic polynomial, i.e., a coefficient vector α in the coefficient space. Let $\mathcal{I}(\mathcal{D})$ be the image of \mathcal{D} in the coefficient space. The closed-loop system is robustly stable in \mathcal{D} if and only if every characteristic polynomial in $\mathcal{I}(\mathcal{D})$ is stable. Although several significant results for robust stability have been obtained in the coefficient space, there is no efficient way to check robust stability for $\mathcal{I}(\mathcal{D})$ since $\mathcal{I}(\mathcal{D})$ usually is neither a Kharitonov's hyper-rectangle [51] nor a polytope considered by Bartlett, Hollot, and Lin [52].

Define the polytope $\mathcal{P}(\bar{\mathcal{D}})$ as the convex hull of the 2^m image points in the $(n+1)$ -dimensional coefficient space mapped from the vertices of $\bar{\mathcal{D}}$ where n is the degree of the characteristic polynomial. If the mapping is multilinear, then the image of the edges of the hypercube $\bar{\mathcal{D}}$ will be the straight line segments connecting the corresponding mapped

vertices. The image of \mathcal{D} , $\mathcal{I}(\mathcal{D})$, is a subset of $\mathcal{I}(\bar{\mathcal{D}})$ and therefore is a subset of the polytope $\mathcal{P}(\bar{\mathcal{D}})$. Under the condition of the multilinear mapping, the stability of the edges of $\mathcal{P}(\bar{\mathcal{D}})$ will guarantee the robust stability in $\bar{\mathcal{D}}$. The multilinear mapping can be easily achieved by assuming that the nominal system $M(s)$ in Fig.5.1-1 is a rational matrix with real coefficients.

Now, we have an easy way to check the sufficient condition for the robust stability in \mathcal{D} by using its corresponding polytope $\mathcal{P}(\bar{\mathcal{D}})$. The sufficient condition is still not enough to determine the real MSM k_M . Any k such that the polytope $\mathcal{P}(k\bar{\mathcal{D}})$ remains stable, say k_L , can be served as a lower bound for k_M . However, there may exist some $k > k_L$ such that $k\mathcal{D}$ is stable although the corresponding polytope $\mathcal{P}(k\bar{\mathcal{D}})$ is unstable.

Any k which cause instability of $k\mathcal{D}$ or $\mathcal{I}(k\mathcal{D})$ qualifies as an upper bound for k_M . To facilitate the description of the relations between the parameter space and the coefficient space, let the edges (vertices, resp.) of $\mathcal{P}(k\bar{\mathcal{D}})$ which are mapped from the edges (vertices, resp.) that are parallel to an axis of coordinates of $k\mathcal{D}$ be called the crucial edges (vertices, resp.) and those which are not crucial be called noncrucial edges (vertices, resp.). The noncrucial edges include two kinds of edges: supplemental edges and fictitious edges. The supplemental edges are the image of the edges of $k\bar{\mathcal{D}}$ which are not in $k\mathcal{D}$. The fictitious edges are the edges of $\mathcal{P}(k\bar{\mathcal{D}})$ which are not mapped from the edges of $k\bar{\mathcal{D}}$. The crucial edges are all in $\mathcal{I}(k\mathcal{D})$. Thus, some k which causes instability at the crucial edges of $\mathcal{P}(k\bar{\mathcal{D}})$, say k_U , may be used as an upper bound for k_M . If the lower and the upper bounds coincide or are close enough, we have the real MSM k_M and the real SSV μ . The objective of the iterative algorithm is to reduce the gap of the lower and the upper bounds. When the gap is smaller than the desired accuracy ϵ , i.e., $|k_U - k_L| \leq \epsilon$, we have the real MSM $k_M = k_L$ and the real SSV $\mu = 1/k_M$.

5.2 Multilinear Mapping and the Polytopic Polynomials

The robust stability of the perturbed system in Fig.5.1-1 is determined by $\det[I+M(s)\Delta]$. There are two lemmas available for checking the robust stability. They are listed as follows.

Lemma 5.2-1:

The closed-loop system is robustly stable in \mathcal{D} if and only if $M(s)$ is asymptotically stable and

$$\det [I + M(j\omega)\Delta] \neq 0 \quad \text{for all } \omega \text{ and all } \bar{\delta} \text{ in } \mathcal{D}. \quad (5.2-1)$$

Lemma 5.2-2:

The closed-loop system is robustly stable in \mathcal{D} if and only if all the zeros of

$$\det [I + M(s)\Delta] \quad \text{for all } \bar{\delta} \text{ in } \mathcal{D} \quad (5.2-2)$$

are in the open left half of s-plane.

The existing computational algorithms for the SSV and the MSM are all developed based on Lemma 5.2-1 while the approach to be presented in Sec.5.3 is based on Lemma 5.2-2.

Recall that $\Delta = \text{diag} \{ \delta_1 I_{m1}, \delta_2 I_{m2}, \dots, \delta_r I_{mr} \} = \text{diag} \{ \bar{\delta}_1, \bar{\delta}_2, \dots, \bar{\delta}_m \}$ where I_{mi} is the identity matrix of order m_i and $m_1+m_2+\dots+m_r = m$. That is, $\bar{\delta}_1 = \bar{\delta}_2 = \dots = \bar{\delta}_{m1} = \delta_1$, $\bar{\delta}_{m1+1} = \bar{\delta}_{m1+2} = \dots = \bar{\delta}_{m1+m2} = \delta_2$, ..., etc. The parameters $\delta_1, \delta_2, \dots, \delta_r$ are assumed independent and $-1 \leq \delta_i \leq 1$, $i = 1, 2, \dots, r$. The parameter perturbation domain \mathcal{D} is an r -dimensional hyperrectangle inside the m -dimensional hypercube $\bar{\mathcal{D}}$ with 2^m vertices $(\pm 1, \dots, \pm 1)$ in the m -dimensional real space.

First of all, we will establish the relationship between the coefficients $\{\alpha_0, \alpha_1, \alpha_2, \dots, \alpha_n\}$ of the characteristic polynomial

$$\alpha_0 s^n + \alpha_1 s^{n-1} + \alpha_2 s^{n-2} + \dots + \alpha_n \quad (5.2-3)$$

and the perturbation parameters. It is interesting to note that if $M(s)$ is a rational matrix with real coefficients then the coefficient vector $\alpha = [\alpha_0 \ \alpha_1 \ \alpha_2 \ \dots \ \alpha_n]^T$ is a multilinear function of the parameter vector $\bar{\delta} = [\bar{\delta}_1 \ \bar{\delta}_2 \ \dots \ \bar{\delta}_m]^T$. That is, if we only allow one of the $\bar{\delta}_i$'s, say $\bar{\delta}_j$, to vary and keep the rest $m-1$ of the $\bar{\delta}_i$'s constant then α is a linear function of $\bar{\delta}_j$.

Theorem 5.2-3:

Consider the perturbed system in Fig.5.1-1 where $\Delta = \text{diag} \{ \bar{\delta}_1, \bar{\delta}_2, \dots, \bar{\delta}_m \}$ and $M(s)$ is rational with real coefficients. The coefficients α_i 's, $i=0,1,2,\dots,n$, of the characteristic polynomial of the perturbed system are multilinear functions of $\bar{\delta}_i$'s.

Proof: See Appendix A.

Remark 5.2-4:

The coefficients α_i 's, $i=0,1,2,\dots,n$, of the characteristic polynomial of the perturbed system in general are **not** multilinear functions of δ_i 's unless $\mathcal{D} = \bar{\mathcal{D}}$.

The following lemma is a direct consequence of the multilinear mapping between $\bar{\delta}$ and α .

Lemma 5.2-5:

In the parameter space, draw a line segment with ending points E_1 and E_2 and the line is parallel to an axis of coordinates. The images of these two ending points are denoted by $\mathcal{I}(E_1)$ and $\mathcal{I}(E_2)$ respectively. The image of the line segment in the coefficient space is a straight line segment which connects $\mathcal{I}(E_1)$ and $\mathcal{I}(E_2)$ if the mapping from the parameter space to the coefficient space is multilinear.

The parameter perturbation domain \mathcal{D} is an r -dimensional hyperplane inside the m -dimensional hypercube $\bar{\mathcal{D}}$ with 2^m vertices whose edges are parallel to the axes of coordinates. $\mathcal{I}(\mathcal{D})$ and $\mathcal{I}(\bar{\mathcal{D}})$ are the images of \mathcal{D} and $\bar{\mathcal{D}}$ respectively in the coefficient space. The polytope $\mathcal{P}(\bar{\mathcal{D}})$ is the convex hull of the 2^m image points in the $(n+1)$ -

dimensional coefficient space mapped from the vertices of $\bar{\mathcal{D}}$. In the following, we will show that if the mapping is multilinear, the image of $\bar{\mathcal{D}}$, i.e., $\mathcal{I}(\bar{\mathcal{D}})$, is a subset of the polytope $\mathcal{P}(\bar{\mathcal{D}})$.

Theorem 5.2-6:

$$\mathcal{I}(\bar{\mathcal{D}}) \subset \mathcal{P}(\bar{\mathcal{D}}). \quad (5.2-4)$$

Proof: See Appendix A.

Theorem 5.2-7:

If $\bar{\mathcal{D}}_1 \subset \bar{\mathcal{D}}_2$, then

$$\mathcal{I}(\bar{\mathcal{D}}_1) \subset \mathcal{I}(\bar{\mathcal{D}}_2) \quad (5.2-5)$$

and

$$\mathcal{P}(\bar{\mathcal{D}}_1) \subset \mathcal{P}(\bar{\mathcal{D}}_2). \quad (5.2-6)$$

Proof: See Appendix A.

Theorem 5.2-8:

The hypercube or hyperrectangle $\bar{\mathcal{D}}$ is cut into two equal subdomains $\bar{\mathcal{D}}_1$ and $\bar{\mathcal{D}}_2$ by a hyperplane which is orthogonal to an axis of coordinates. Then

$$\mathcal{I}(\bar{\mathcal{D}}) \subset \mathcal{P}(\bar{\mathcal{D}}_1) \cup \mathcal{P}(\bar{\mathcal{D}}_2) \subset \mathcal{P}(\bar{\mathcal{D}}) \quad (5.2-7)$$

Proof: See Appendix A.

In the following, a simple case with 2-dimensional parameter space and 3-dimensional coefficient space will be used to illustrate the basic concept on which our algorithm is developed.

In Fig.5.2-1(a), the hypercube $\bar{\mathcal{D}}$ is a square with edges V_1V_2 , V_2V_3 , V_3V_4 , and V_4V_1 parallel to either $\bar{\delta}_1$ -axis or $\bar{\delta}_2$ -axis and the perturbed parameter domain \mathcal{D} is the straight line segment connecting V_2 and V_4 . In Fig.5.2-1(b), X_1 , X_2 , X_3 , and X_4 are the images of the vertices V_1 , V_2 , V_3 , and V_4 of $\bar{\mathcal{D}}$ respectively in the 3-dimensional coefficient space. The polytope $\mathcal{P}(\bar{\mathcal{D}})$, i.e., the convex hull of the four image points X_1 ,

X_2, X_3 , and X_4 , is a pyramid with six edges. X_2 and X_4 are crucial vertices since they are in $\mathcal{I}(\bar{\mathcal{D}})$. From Theorem 5.2-3, the four edges X_1X_2, X_2X_3, X_3X_4 , and X_4X_1 are the images of V_1V_2, V_2V_3, V_3V_4 , and V_4V_1 respectively and therefore are supplemental edges. The other two edges of the polytope, X_1X_3 and X_4X_2 , are fictitious edges which may not even be in the image of $\bar{\mathcal{D}}$.

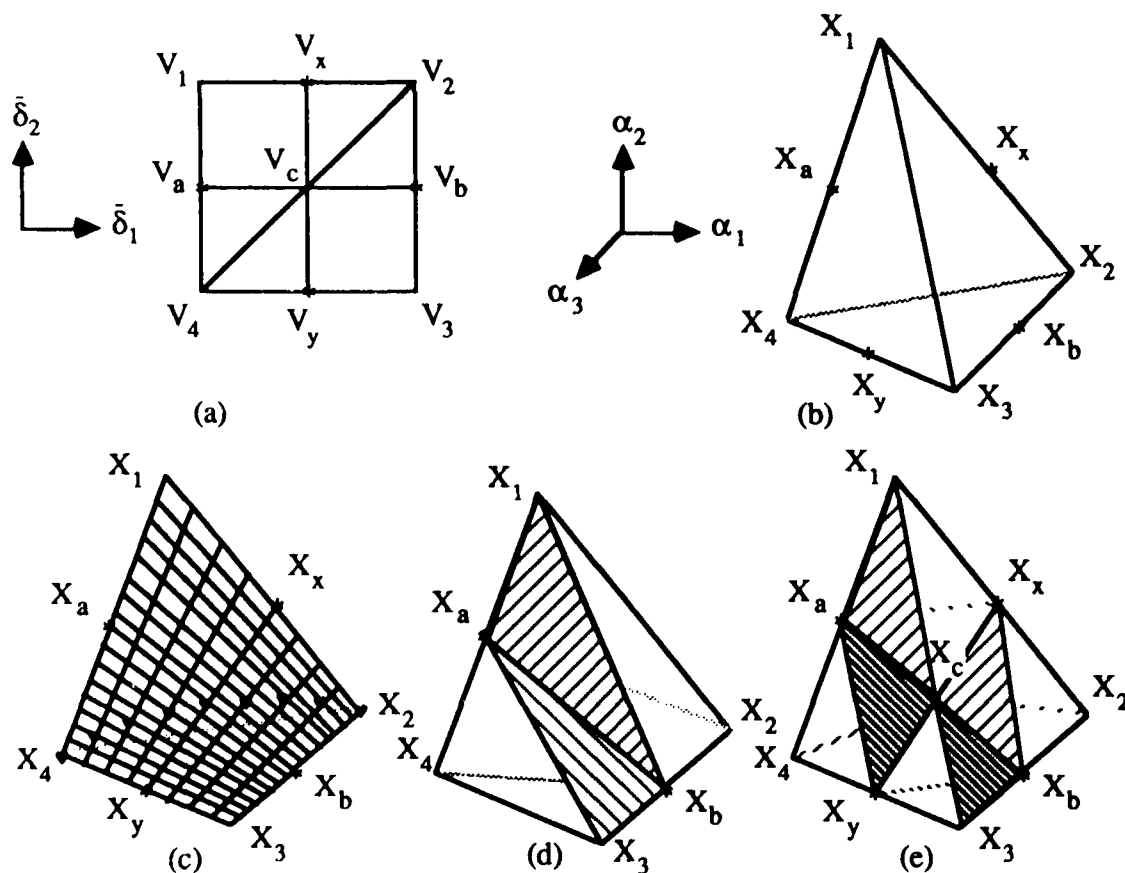


Fig.5.2-1 Multilinear mapping, polytopes, and $\bar{\mathcal{D}}_i$ partition technique.

The image of $\bar{\mathcal{D}}$ (\mathcal{D} resp.), $\mathcal{I}(\bar{\mathcal{D}})$ ($\mathcal{I}(\mathcal{D})$ resp.), can be constructed as follows. Let V_a and V_b be the center points of the line segments V_1V_4 and V_2V_3 respectively. It is easy to see that the line segment drawn between V_a and V_b , i.e., V_aV_b , is parallel to V_1V_2 and V_4V_3 , and therefore parallel to the $\bar{\delta}_1$ -axis. Since the mapping is multilinear, $\mathcal{I}(V_aV_b)$ will be the straight line segment X_aX_b , where $X_a = \mathcal{I}(V_a)$ and $X_b = \mathcal{I}(V_b)$ are the center points

of the line segments X_1X_4 and X_2X_3 respectively. Similarly, $\mathcal{I}(V_xV_y)$ will be the straight line segment X_xX_y , where $X_x = \mathcal{I}(V_x)$ and $X_y = \mathcal{I}(V_y)$ are the center points of the line segments X_1X_2 and X_4X_3 respectively. It is easy to see that X_aX_b and X_xX_y are both in $\mathcal{I}(\bar{\mathcal{D}})$ and the intersection point of X_aX_b and X_xX_y , i.e., X_c is in $\mathcal{I}(\mathcal{D})$. Repeating the above mapping, we can see that $\mathcal{I}(\bar{\mathcal{D}})$ and $\mathcal{I}(\mathcal{D})$ can be constructed as that shown in Fig.5.2-1(c). In Fig.5.2-1(c), $\mathcal{I}(\bar{\mathcal{D}})$ is a saddle-shaped surface and is inside the pyramid $X_1X_2X_3X_4$, i.e., $\mathcal{P}(\bar{\mathcal{D}})$. The \heartsuit curve in $\mathcal{I}(\bar{\mathcal{D}})$ is the image of \mathcal{D} .

Note that $\mathcal{I}(\mathcal{D}) \subset \mathcal{I}(\bar{\mathcal{D}}) \subset \mathcal{P}(\bar{\mathcal{D}})$. There is an easy way to check the stability of $\mathcal{P}(\bar{\mathcal{D}})$ and therefore a sufficient condition for the stability of $\mathcal{I}(\mathcal{D})$ can be determined without too much effort. That is, $\mathcal{I}(\mathcal{D})$ is stable if all the six edges of $\mathcal{P}(\bar{\mathcal{D}})$: X_1X_2 , X_2X_3 , X_3X_4 , X_4X_1 , X_1X_3 and X_4X_2 are stable [52]. The stability of the line segment X_iX_j is determined by using the fast segment stability checking algorithm which will be summarized in Sec.5.4.

In the proposed algorithm for computing the stability margin k_M , we need to check whether a subdomain \mathcal{D}_i is stable. Consider \mathcal{D}_i as the line segment V_2V_4 in Fig.5.2-1(a) and its corresponding polytope $\mathcal{P}(\bar{\mathcal{D}}_i)$ as shown in Fig.5.2-1(b). \mathcal{D}_i is stable if $\mathcal{P}(\bar{\mathcal{D}}_i)$ is stable. If $\mathcal{P}(\bar{\mathcal{D}}_i)$ is unstable and the instability is caused by the crucial edges or vertices, then \mathcal{D}_i is unstable. If $\mathcal{P}(\bar{\mathcal{D}}_i)$ is unstable but the instability is not caused by the crucial edges or vertices, then the information is not enough to determine the stability of \mathcal{D}_i . In this case, a partition technique should be used and repeated until the stability of \mathcal{D}_i is determined. The partition technique is illustrated briefly as follows.

The hypercube $\bar{\mathcal{D}}_i$ (square $V_1V_2V_3V_4$) is partitioned equally into four hyperrectangles $\bar{\mathcal{D}}_{i1}$ (square $V_4V_aV_cV_y$), $\bar{\mathcal{D}}_{i2}$ (square $V_cV_xV_2V_b$), $\bar{\mathcal{D}}_{i3}$ (square $V_aV_1V_xV_c$), and $\bar{\mathcal{D}}_{i4}$ (square $V_yV_cV_bV_3$), by two hyperplanes (line V_aV_b and line V_xV_y) which are orthogonal to the axes $\bar{\delta}_1$ and $\bar{\delta}_2$. From Fig.5.2-1, it is easy to see that $\mathcal{I}(\mathcal{D}_i) \subset \mathcal{I}(\bar{\mathcal{D}}_{i1}) \cup \mathcal{I}(\bar{\mathcal{D}}_{i2}) \subset \mathcal{P}(\bar{\mathcal{D}}_{i1}) \cup \mathcal{P}(\bar{\mathcal{D}}_{i2})$ where the polytopes $\mathcal{P}(\bar{\mathcal{D}}_{i1})$ and $\mathcal{P}(\bar{\mathcal{D}}_{i2})$ are the

pyramids $X_4X_aX_cX_y$ and $X_cX_xX_2X_b$ respectively. If both $\mathcal{P}(\bar{\mathcal{D}}_{i1})$ and $\mathcal{P}(\bar{\mathcal{D}}_{i2})$ are stable then \mathcal{D}_i is stable. If either $\mathcal{P}(\bar{\mathcal{D}}_{i1})$ or $\mathcal{P}(\bar{\mathcal{D}}_{i2})$ is unstable and the instability is caused by the crucial edges or vertices (note that X_4 , X_2 , and X_c are a crucial vertices), then \mathcal{D}_i is unstable. If $\mathcal{P}(\bar{\mathcal{D}}_{i1})$ or $\mathcal{P}(\bar{\mathcal{D}}_{i2})$ is unstable but the instability is not caused by the crucial vertices or edges, then the $\bar{\mathcal{D}}_{ij}$'s corresponding to the unstable $\mathcal{P}(\bar{\mathcal{D}}_{ij})$'s should be partitioned further and the partition process is continued until the stability of \mathcal{D}_i is determined.

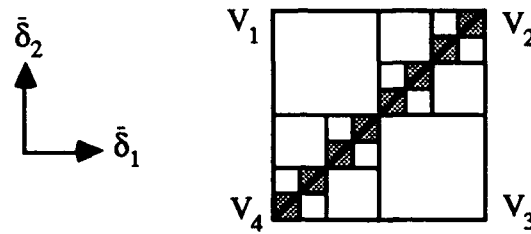


Fig.5.2-2 Further partitioning in the parameter space.

From Fig.5.2.2 we can see that the perturbed parameter domain \mathcal{D}_i (line V_4V_2) is inside the shaded hyperrectangles (squares) and as the number of the shaded hyperrectangles become very large the image of \mathcal{D}_i will be close to the union of the polytopes corresponding to the shaded hyperrectangles. In our algorithm, the number of partitioning usually is small since the partition process is terminated whenever all $\mathcal{P}(\bar{\mathcal{D}}_{ij})$'s are stable or some crucial vertex or edge is unstable. The partition process needs to continue only if some $\mathcal{P}(\bar{\mathcal{D}}_{ij})$'s are unstable and the instability is not caused by the crucial vertices or edges. Besides, only the $\bar{\mathcal{D}}_{ij}$'s related to the unstable $\mathcal{P}(\bar{\mathcal{D}}_{ij})$'s need to be partitioned further.

In the next section, an algorithm based on the above theorems for computing the real MSM k_M and the real SSV μ will be summarized.

5.3 Algorithm For The Real Structured Singular Value

The algorithm is developed based on the multilinear mapping between the parameter and the coefficient spaces. Some recent results by De Gaston and Safonov [48], Sideris and Pena [50], Bartlett, Hollot, and Lin [52], and Bouguerra, Chang, Yeh, and Banda [57] are used in the algorithm. The iterative algorithm is designed to find the largest positive real number k , i.e., the real MSM k_M , such that the system in Fig.5.1-1 remains robustly stable for every possible perturbation in $k_M \mathcal{D}$. Then the real SSV μ can be obtained from $\mu = 1 / k_M$.

Recall that $\bar{\mathcal{D}}$ is the hypercube with 2^m vertices $(\pm 1, \dots, \pm 1)$ in the m -dimensional real space and the parameter perturbation domain \mathcal{D} is an r -dimensional hyperplane inside the m -dimensional hypercube $\bar{\mathcal{D}}$. In Fig.5.1-1, the nominal system $M(s)$ is fixed and the shape of the perturbation domain \mathcal{D} is also fixed. In the computation of stability margin, we will just enlarge or shrink the perturbation domain \mathcal{D} by a factor k until k is the largest positive real number such that the system in Fig.5.1-1 remains robustly stable for every possible perturbation in $k\mathcal{D}$. Recall that " $k\mathcal{D}$ is stable" means "the system in Fig.5.1-1 remains robustly stable for every possible perturbation in $k\mathcal{D}$ " and " $\mathcal{I}(k\mathcal{D})$ (resp. $\mathcal{P}(k\bar{\mathcal{D}})$) is stable" means "every characteristic polynomial in $\mathcal{I}(k\mathcal{D})$ (resp. $\mathcal{P}(k\bar{\mathcal{D}})$) is stable."

Since $\mathcal{I}(k\mathcal{D})$ is a coefficient-space image of $k\mathcal{D}$, $k\mathcal{D}$ is stable if and only if $\mathcal{I}(k\mathcal{D})$ is stable. From Theorems 2.6 and 2.7, we have $\mathcal{I}(k\mathcal{D}) \subset \mathcal{I}(k\bar{\mathcal{D}}) \subset \mathcal{P}(k\bar{\mathcal{D}})$ which implies that if $\mathcal{P}(k\bar{\mathcal{D}})$ is stable then $\mathcal{I}(k\mathcal{D})$ is stable and therefore so is $k\mathcal{D}$. Hence, any k such that the polytope $\mathcal{P}(k\mathcal{D})$ remains stable, say k_L , can be served as a lower bound for k_M . The stability of the polytope $\mathcal{P}(k\mathcal{D})$ can be easily checked by using the recent results developed by Bartlett, Hollot, and Lin [52], and Bouguerra, Chang, Yeh, and Banda [57].

Any k which causes instability of $k\mathcal{D}$ or $\mathcal{I}(k\mathcal{D})$ qualifies as an upper bound for k_M . In the proposed algorithm, some k which causes instability at the crucial vertices or edges of the polytopes corresponding to $k\bar{\mathcal{D}}$ or its subdomains, say k_U , will be used as an

upper bound for k_M . If the lower and the upper bounds coincide or close enough, we have the stability margin k_M . Otherwise, the iterative algorithm needs to continue until the gap of the lower and the upper bounds is small enough.

In an iteration loop of the algorithm, for a given k we construct a polytope $\mathcal{P}(k\bar{\mathcal{D}})$. If $\mathcal{P}(k\bar{\mathcal{D}})$ is stable, k_L is updated by k . In the case of unstable $\mathcal{P}(k\bar{\mathcal{D}})$, the instability may be caused by the crucial or the noncrucial edges. If it is caused by the crucial vertices or edges the upper bound k_U shall be updated by k . On the other hand, the instability is caused by the noncrucial edges, no information can be used to update k_L or k_U . In this situation, the perturbation domain partition technique [48,50] is employed.

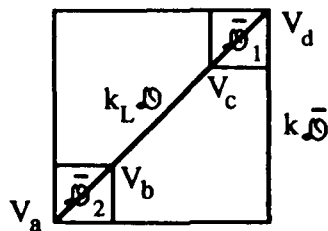


Fig.5.3-1 Partitioning in the parameter space.

The domain partition procedure is described as follows. Refer to Fig.5.3-1, the perturbation domain $k\mathcal{D}$ is the line segment $V_a V_d$ and $k\bar{\mathcal{D}}$ is the hypercube (square) which encloses $k\mathcal{D}$. Assume $k_L\mathcal{D}$ (line segment $V_b V_c$) is stable and $k\bar{\mathcal{D}}$ is unstable and the instability is caused by noncrucial vertices or edges. To determine the stability of $k\mathcal{D}$, the following partition technique is used. The domain $k\mathcal{D}$ is partitioned into three parts: $k_L\mathcal{D}$ (line segment $V_b V_c$), \mathcal{D}_1 (line segment $V_a V_b$), and \mathcal{D}_2 (line segment $V_c V_d$). Enclose \mathcal{D}_1 and \mathcal{D}_2 by hyperrectangles $\bar{\mathcal{D}}_1$ and $\bar{\mathcal{D}}_2$ respectively. Now, there are three possibilities: (1) Both $\mathcal{P}(\bar{\mathcal{D}}_1)$ and $\mathcal{P}(\bar{\mathcal{D}}_2)$ are stable, then $k\mathcal{D}$ is stable and the lower bound k_L shall be updated by k . (2) Some crucial vertex or edge of $\mathcal{P}(\bar{\mathcal{D}}_1)$ or $\mathcal{P}(\bar{\mathcal{D}}_2)$ is unstable, then $k\mathcal{D}$ is unstable and the upper bound k_U shall be updated by k . (3) Either or both of $\mathcal{P}(\bar{\mathcal{D}}_1)$ and $\mathcal{P}(\bar{\mathcal{D}}_2)$ is unstable and the instability is not caused by crucial vertices or edges, then no

information can be used to update k_L or k_U and therefore the $\bar{\mathcal{D}}_i$'s with unstable $\mathcal{P}(\bar{\mathcal{D}}_i)$ shall be partitioned further until all polytopes which contain parts of $\mathcal{D}(k\mathcal{D})$ are stable (update the lower bound k_L by k) or some crucial vertex or edge is unstable (update the upper bound k_U by k). The iterative procedure is repeated with a new $k = (k_U + k_L)/2$ or $k = 2k_L$ (if k_U is not available) until $k_U - k_L$ is negligible and then the stability margin is $k_M = k_L$.

The algorithm for computing the real MSM k_M and the real SSV μ is listed as follows.

ALGORITHM 5.3-1:

1. Initialize both the lower and the upper bounds $k_L = k_U = 0$. Set the partition indicator $p = 0$. Set ϵ for the accuracy of k_M . Set initial trial value at $k=1$.
2. Check the stability of the corresponding polytope $\mathcal{P}(k\bar{\mathcal{D}})$. If it is stable, go to 3. Otherwise, go to 5.
3. Update k_L by k and check k_U . If $k_U = 0$, update k by $2k_L$ and go to 2. If $k_U \neq 0$, (it must have been updated and must $k_U > k_L$) go to 4.
4. Set $k = (k_U + k_L)/2$. If $p = 0$, then go to 2. Otherwise go to 5.
5. If the instability of the polytope $\mathcal{P}(k\bar{\mathcal{D}})$ (or the polytopes of the relevant sub-hyperrectangles as resulted from the partitioning in 7) is due to crucial vertices or crucial edges ($k\mathcal{D}$ is unstable), go to 8. Otherwise, go to 6.
6. Partition the hyperrectangles with unstable polytopes by the hyperplanes orthogonal to the axes of coordinates. Only the sub-hyperrectangles which enclose $k\mathcal{D} - k_L\mathcal{D}$ (we call these the relevant sub-hyperrectangles) need to be considered.
7. If the polytopes of the relevant sub-hyperrectangles under consideration are all stable, set $p = 1$ and go to 3. Otherwise, go to 5.
8. $k\mathcal{D}$ is unstable. Update k_U by k and check $k_U - k_L$. If $k_U - k_L > \epsilon$, go to 4. Otherwise, set $k_M = k_L$ and stop.

In the algorithm, ϵ , the tolerable gap between the lower bound k_L and the upper bound k_U , is a small number preset to determine the computation accuracy. The algorithm is employed to determine the stability margin k_M by narrowing down the gap between the lower bound k_L and the upper bound k_U . The perturbation domain partitioning loop is described in step 6. Only the hyperrectangles enclosing $k\mathcal{D} - k_L\mathcal{D}$ and corresponding to unstable polytopes whose crucial vertices and edges are stable need to be partitioned further and the domain partitioning loop is terminated whenever all the polytopes under consideration are stable or any crucial vertex or edge is unstable. The set $k\mathcal{D} - k_L\mathcal{D}$ consists all the points in $k\mathcal{D}$ which is not in $k_L\mathcal{D}$. Theoretically, the domain partitioning loop should be terminated in finite steps unless the unstable region is of measure zero (e.g. a singular point) inside $k\mathcal{D}$. However, in practical computation a preset counter can be placed in the loop to avoid the loop from repeating too many times for a given k . The partition indicator p initially is set as zero and is set to be one in step 7 whenever $k\mathcal{D}$ is determined to be stable after partitioning. If a $k_L\mathcal{D}$ is determined to be stable after partitioning, then the polytope $\mathcal{P}(k\bar{\mathcal{D}})$ is unstable for $k > k_L$. Therefore, in step 4 after setting a new k we go to 5 instead of 2 if $p \neq 0$.

Two examples are used to illustrate our algorithm. The first example is from De Gaston and Safonov [48] in which $\mathcal{D} = \bar{\mathcal{D}}$, i.e., the elements in the parameter vector $\bar{\delta}$ are independent and the other example has dependency among the entries of $\bar{\delta}$. In the following, the vertices of the hypercube $k\bar{\mathcal{D}}$ and their image points in the coefficient space are denoted by V_i 's and X_i 's respectively. The line segment between X_i and X_j is represented by X_iX_j . Note that both V_i 's and X_i 's are functions of k .

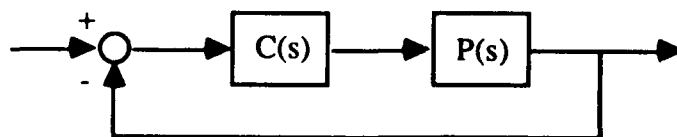


Fig. 5.3-2 A closed-loop system considered in Example 5.3-1.

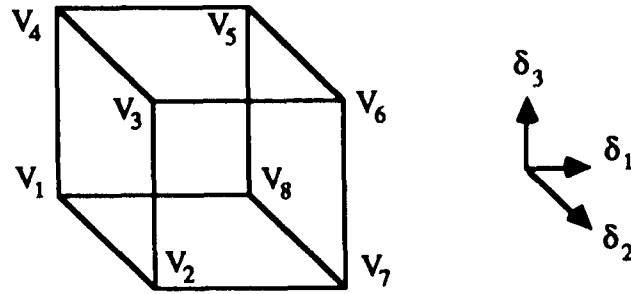


Fig. 5.3-3 Perturbation domain of Example 5.3-1

Example 5.3-1 :

De Gaston and Safonov [48] developed an algorithm for computing the stability margin based on the multilinear mapping between the parameter space and the complex plane [61]. They used an example to illustrate their algorithm. We will use exactly the same example to illustrate our algorithm and then the solutions of both approaches can be compared.

The system to be considered is shown in Fig.5.3-2 where the plant $P(s)$ and the controller $C(s)$ are described by

$$P(s) = \frac{\delta_{1a}}{s(s + \delta_{2a})(s + \delta_{3a})} \quad \text{and} \quad C(s) = \frac{s + z_1}{s + p_1}$$

respectively. The parameters in the above expressions are given by

$z_1 = 2 \text{ rad/sec}$	$p_1 = 10 \text{ rad/sec}$	
$\delta_{1a} = \delta_{10}(1 + \delta_1)$	$\delta_{10} = 800$	$ \delta_1 \leq 0.1$
$\delta_{2a} = \delta_{20} + \delta_2$	$\delta_{20} = 4 \text{ rad/sec}$	$ \delta_2 \leq 0.2 \text{ rad/sec}$
$\delta_{3a} = \delta_{30} + \delta_3$	$\delta_{30} = 6 \text{ rad/sec}$	$ \delta_3 \leq 0.3 \text{ rad/sec}$

The perturbation part of the perturbed closed-loop system can be pulled out and represented by a diagonal matrix and therefore the perturbed closed-loop system in Fig. 5.3-2 can be

restructured as that in Fig.5.1-1, where $\Delta = \text{diag} \{ \delta_1, \delta_2, \delta_3 \}$ and the nominal closed-loop system $M(s)$ has a realization (A, B, C) as follows:

$$A = \begin{bmatrix} 0 & 1 & 0 & 0 \\ 0 & -10 & -800 & 3200 \\ 1 & 0 & -4 & 0 \\ 0 & 0 & 1 & -6 \end{bmatrix}, \quad B = \begin{bmatrix} 0 & 0 & 0 \\ 0 & 0 & -800 \\ -1 & 1 & 0 \\ 0 & 0 & 1 \end{bmatrix}, \quad C = \begin{bmatrix} 1 & 0 & 0 & 0 \\ 0 & 0 & 1 & 0 \\ 0 & 0 & 0 & 1 \end{bmatrix}.$$

The vertices of the perturbation domain $k\mathcal{D}$ in the 3-dimensional parameter space are numbered as shown in Fig.5.3-3. Recall that the vertices of $k\mathcal{D}$ are denoted by V_i 's.

The vertices of $k\mathcal{D}$ with $k = 1$ are

$$\begin{aligned} V_1 &= (-.1, -.2, -.3), & V_2 &= (-.1, .2, -.3), & V_3 &= (-.1, .2, .3), & V_4 &= (-.1, -.2, .3), \\ V_5 &= (.1, -.2, .3), & V_6 &= (.1, .2, .3), & V_7 &= (.1, .2, -.3), & V_8 &= (.1, -.2, -.3). \end{aligned}$$

Since $M(s)$ is a rational matrix with real coefficients, the coefficients of the characteristic polynomial are multilinear functions of the parameters δ_1, δ_2 , and δ_3 . The characteristic polynomial

$$\alpha_0 s^4 + \alpha_1 s^3 + \alpha_2 s^2 + \alpha_3 s + \alpha_4$$

can be obtained from $\det [sI - (A - B\Delta C)]$ and then

$$\alpha_0 = 1$$

$$\alpha_1 = 20 + \delta_2 + \delta_3$$

$$\alpha_2 = 124 + 16\delta_2 + 14\delta_3 + \delta_2\delta_3$$

$$\alpha_3 = 1040 + 800\delta_1 + 60\delta_2 + 40\delta_3 + 10\delta_2\delta_3$$

$$\alpha_4 = 1600 + 1600\delta_1$$

As we expect, the coefficient vector $\alpha = [\alpha_0 \ \alpha_1 \ \alpha_2 \ \alpha_3 \ \alpha_4]^T$ is a multilinear function of the parameter vector $\delta = [\delta_1 \ \delta_2 \ \delta_3]^T$.

The objective is to compute the stability margin k_M which is the largest k such that $k\mathcal{D}$ is stable, i.e., the closed-loop system remains robustly stable in $k\mathcal{D}$. For each k , we map the eight vertices of $k\mathcal{D}$ into the coefficient space as X_i , $i=1,2,\dots,8$ from which the polytope $\mathcal{P}(k\mathcal{D})$ can be constructed. It is easy to see that the polytope $\mathcal{P}(k\mathcal{D})$ has 12 crucial edges and 16 fictitious edges. If these 28 edges are all stable, i.e., $\mathcal{P}(k\mathcal{D})$ is stable, then $k\mathcal{D}$ is stable. If any of the crucial edges is unstable, then so is $k\mathcal{D}$. Note that unstable $\mathcal{P}(k\mathcal{D})$ does not imply unstable $k\mathcal{D}$, since the instability may be only caused by some fictitious edges which are not in $\mathcal{I}(k\mathcal{D})$.

Let's go through the algorithm listed in the previous section. First of all, we initialize both the lower and the upper bounds $k_L = k_U = 0$ and set the accuracy $\epsilon = 10^{-6}$. For $k=1$, $\mathcal{P}(k\mathcal{D})$ is stable and we have $k_L = 1$ and update k to 2. For $k=2$, again $\mathcal{P}(k\mathcal{D})$ is stable and therefore we update k_L to 2 and k to 4 respectively. For $k=4$, $\mathcal{P}(k\mathcal{D})$ is unstable and the instability occurs at X_8 which is crucial and k_U is updated to 4.

Now, we are in the loop of bisection to narrow down the gap between k_L and k_U to be less than ϵ . After 21 iterations we have $k_L = 3.417395$ and $k_U = 3.417396$ such that $\mathcal{P}(k_L\mathcal{D})$ is stable while $\mathcal{P}(k_U\mathcal{D})$ is unstable and the instability occurs at X_8 . Therefore, we have the real MSM $k_M = 3.417395$.

From the above computation, we find that the no. 8 vertex of the perturbation domain is the critical point. Thus, we can check our solution at V_8 of the parameter space. When $k = k_M = 3.417395$, the closed-loop system at V_8 is stable since its characteristic values are

$$\begin{aligned} & -16.3521921088081 \\ & \quad -0.00000016598452 + 8.2282006559442I \\ & \quad -0.00000016598452 - 8.2282006559442I \\ & -1.93911005922287 \end{aligned}$$

If we increase k a little bit to $k = k_U = 3.417396$, the closed-loop system at V_8 becomes unstable since its characteristic values are

$$\begin{aligned}
& -16.352192213492 \\
& .00000014646442 + 8.228200893344I \\
& .00000014646442 - 8.228200893344I \\
& -1.9391100794366
\end{aligned}$$

In [48], De Gaston and Safonov obtain a margin $k = 3.44$ which is close to our result. However, when $k = 3.44$, the closed-loop system at V_g is unstable since its characteristic values are

$$\begin{aligned}
& -16.354555659044 \\
& .00706068635988 + 8.2335635562319I \\
& .00706068635988 - 8.2335635562319I \\
& -1.9395657136757
\end{aligned}$$

That means 3.44 could not be a correct margin. One of the major reasons that De Gaston and Safonov's algorithm [48] is complicated is that it requires frequency ω sweep. For the same example, they found that at $\omega = 8.22$ rad/sec, $\det[I + kM(j\omega)\Delta]$ approximately equals to zero at V_g when $k = 3.44$. To have an accuracy of 10^{-6} for the stability margin, they need a more accurate ω , say $\omega = 8.2282$ rad/sec, which needs extensive frequency ω search. Our approach does not require frequency ω search.

The real SSV μ for the system is $\mu = 1 / k_M = 1 / 3.417395 = .29262055$.

Example 5.3-2 :

Assume that the nominal system $M(s)$ in Fig.5.1-1 has a state-space representation (A, B, C) as

$$A = \begin{bmatrix} -2.7 & -2 & -1.5 & -0.5 \\ -1.5 & -4 & -1.5 & -1.5 \\ -0.2 & 0 & -3 & 0 \\ 1.5 & 2 & 3.5 & -0.7 \end{bmatrix}, \quad B = \begin{bmatrix} 1 & 0 & 0 \\ 0 & 0 & 0 \\ 0 & 0 & 1 \\ 0 & 1 & 0 \end{bmatrix}, \quad C = \begin{bmatrix} -0.3 & 0 & 0 & 0 \\ 0 & 0 & 0 & -0.3 \\ -0.3 & 0 & 0 & 0 \end{bmatrix}$$

and the perturbation matrix Δ in Fig.5.1-1 is given by

$$\Delta = \text{diag} \{ \bar{\delta}_1, \bar{\delta}_2, \bar{\delta}_3 \}$$

where

and

$$\bar{\delta}_1 = \delta_1, \quad \bar{\delta}_2 = \bar{\delta}_3 = \delta_2$$

$$-1 \leq \delta_1 \leq 1, \quad -1 \leq \delta_2 \leq 1$$

The set of the characteristic polynomials of the perturbed system can be described by

$$\alpha_0 s^4 + \alpha_1 s^3 + \alpha_2 s^2 + \alpha_3 s + \alpha_4$$

where

$$\alpha_0 = 1$$

$$\alpha_1 = 10.4 - 0.3 \bar{\delta}_1 - 0.3 \bar{\delta}_2$$

$$\alpha_2 = 38.14 - 2.31 \bar{\delta}_1 - 2.91 \bar{\delta}_2 + 0.45 \bar{\delta}_3 + 0.09 \bar{\delta}_1 \bar{\delta}_2$$

$$\alpha_3 = 58.12 - 5.97 \bar{\delta}_1 - 8.28 \bar{\delta}_2 + 1.74 \bar{\delta}_3 + 0.63 \bar{\delta}_1 \bar{\delta}_2 - 0.135 \bar{\delta}_2 \bar{\delta}_3$$

$$\alpha_4 = 31.36 - 5.22 \bar{\delta}_1 - 6.84 \bar{\delta}_2 + 0.48 \bar{\delta}_3 + 1.08 \bar{\delta}_1 \bar{\delta}_2 - 0.27 \bar{\delta}_2 \bar{\delta}_3$$

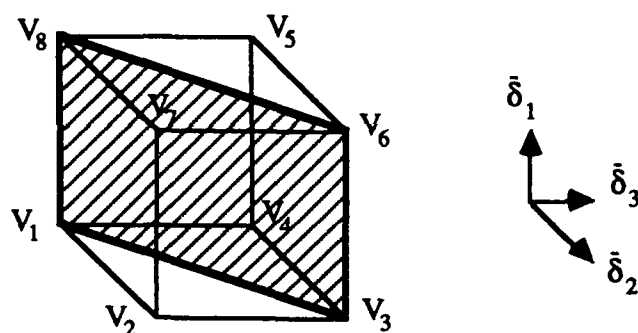


Fig.5.3-4 Perturbation domain of Example 5.3-2.

The parameter perturbation domain is shown in Fig.5.3-4. The shaded area $V_1 V_8 V_6 V_3$ is the perturbation domain \mathcal{D} in which $\bar{\delta}_1 = \delta_1$, $\bar{\delta}_2 = \bar{\delta}_3 = \delta_2$ and the hypercube $V_1 V_2 V_3 V_4 V_5 V_6 V_7 V_8$ is $\bar{\mathcal{D}}$. In the following we will use the proposed iterative algorithm to compute k_M . Initially, $k_L = k_U = 0$ and ϵ is set as 10^{-4} . $\mathcal{P}(k, \bar{\mathcal{D}})$ is stable for $k=1$ and therefore k_L is updated to 1. For $k=5$, the polytope $\mathcal{P}(k, \bar{\mathcal{D}})$ is unstable and the instability is caused by the crucial vertices X_3, X_6 and by the noncrucial vertex X_7 .

Therefore k_U is updated to 5. As a next step k is chosen as $(1+5)/2 = 3$. $\mathcal{P}(k, \bar{\mathcal{D}})$ is stable for $k=3$ and therefore k_L is updated to 3. Following the iteration steps, $k=(3+5)/2=4$, we find that the polytope $\mathcal{P}(k, \bar{\mathcal{D}})$ is unstable for the value of $k = 4$ and the instability is caused by the crucial vertex X_6 . Therefore k_U is updated to 4. Iterating k between 3 and 4 as it is suggested in steps 2-8 we find that the polytope $\mathcal{P}(k, \bar{\mathcal{D}})$ is unstable for the value of $k = 3.6297$ and the instability is caused by the crucial vertex X_6 . Hence, $k_U = 3.6297$. $\mathcal{P}(k, \bar{\mathcal{D}})$ is stable at for $k=3.6296$ and we have $k_L = 3.6296$. Now, $|k_U - k_L| \leq \varepsilon$ and therefore we have the real MSM $k_M = 3.6296$. The real SSV is $\mu = 1 / k_M = 1 / 3.6296 = 0.2755$.

5.4 Fast Algorithm to Check the Stability of Segments

In the previous subsection, an iterative algorithm for computing the real SSV based on polytopic-polynomial approach was presented. In this algorithm, the major computation is checking the stability of edges of polytopes.

There are several different computational methods available to verify the stability of an exposed edge of a polytope. However, in practical problems, these methods are found to impose a heavy computational burden due to the fact of the "combinatoric explosion" of the number of edges of the polytope whose stability needs to be checked. To illustrate this phenomenon, we consider a system with m perturbation parameters. The corresponding polytope in the coefficient space has 2^m vertices. There are $2^{m-1}(2^m-1)$ edges joining these vertices; note that the number of edges which depend on m can be very large compared to the number of vertices. This is a fact that will be exploited later on in our algorithm in order to reduce the computations to a minimum.

These existing methods to verify the stability of these edges usually require laborious computations that need to be performed independently for each edge. For instance, there is the roots locus technique which consists of representing the edge of a

polytope as a convex combination of two polynomials $\alpha(s)$ and $\beta(s)$ of degree n . The characteristic polynomial of this convex combination can be written as $1 + k\beta(s)/\alpha(s)$, where k takes on the values from zero to infinity. The necessity to sweep the infinite interval for k makes this method unattractable. Another widely used test for the stability of the convex combination of two stable polynomials was developed by Bialas [54]. He showed that the convex combination of two stable polynomials of degree n is stable if and only if all the real eigenvalues of $-H(\alpha)H^{-1}(\beta)$ are negative, where $H(\alpha)$ is the Hurwitz matrix associated with the polynomial $\alpha(s)$. Although Bialas' test does not require the sweep of k , the computations involved, i.e. computations of eigenvalues of an $n \times n$ matrix, must be carried out for each edge of the polytope independently. Hence, in the case of combinatoric explosion alluded to earlier, this technique can be found to be computer time consuming. The iterative algorithm proposed by [60] for computing the multivariable stability margin needs to check the stability of polytopes for each iteration. Therefore, a more efficient computational tool for checking the stability of the edges of a polytope is necessary.

In this section, we propose a fast algorithm for checking the stability of the edges of a polytope where most of the computations involved depend on the number of vertices rather than on the number of edges. This algorithm was developed based on "the segment lemma" derived by Chapellat and Bhattacharyya [56]. Although the segment lemma is a great result, no explicit algorithm was given in [58]. We will reveal some magnificent properties of the lemma and show how these will lead to a fast algorithm. In the proposed algorithm, the major computation involved is the solution of the positive real roots of two polynomials with degree less than or equal to $n/2$ for each vertex. The computation required by the algorithm is mainly vertex-dependent, and the burden of the combinatoric explosion of the number of edges is greatly reduced.

The major computations in the algorithm are vertex dependent, and the edge dependent computations involved are trivial. Therefore the combinatoric explosion is not fatal if the proposed algorithm is used.

As mentioned earlier, the problem of checking robust stability of a system can be reduced to that of checking the stability of the edges of polytopes. However, an edge of a polytope is nothing but a line segment in the coefficient space which can be represented as the convex combination of two vertices corresponding to two polynomials. If the two end points of the line segment are designated by α and β , hence corresponding to two polynomials $\alpha(s)$ and $\beta(s)$ of degree n , then every point on the line segment corresponds to a polynomial is given by

$$t \alpha(s) + (1-t)\beta(s) \quad (5.4-1)$$

for some $t \in [0,1]$. In the following, $\alpha(s)$ and $\beta(s)$ are assumed stable. Let the polynomials $\alpha(s)$ and $\beta(s)$ of degree n be written as

$$\alpha(s) = a(s) + s b(s) \quad (5.4-2a)$$

$$\beta(s) = c(s) + s d(s) \quad (5.4-2b)$$

where the polynomials $a(s)$, $b(s)$, $c(s)$, $d(s)$ are of the form

$$p(s) = p_0 + p_1 s^2 + p_2 s^4 + p_3 s^6 + \dots \quad (5.4-3)$$

Instability of the line segment occurs when the roots of (5.4-1) cross the imaginary axis. Therefore, letting $s = j\omega$ and substituting x for ω^2 , (5.4-3) becomes

$$\hat{p}(x) = p_0 - p_1 x + p_2 x^2 - p_3 x^3 + \dots \quad (5.4-4)$$

where the degree of $\hat{p}(x)$ is now only half of that of $p(s)$. Setting (5.4-1) equal to zero, substituting (5.4-2) and (5.4-4) and equating real and imaginary parts on both sides of the resulting equation, yields

$$\frac{t}{1-t} = - \frac{\hat{c}(x)}{\hat{a}(x)} \quad (5.4-5a)$$

$$\frac{t}{1-t} = - \frac{\hat{d}(x)}{\hat{b}(x)} \quad (5.4-5b)$$

and therefore

$$\hat{a}(x) \hat{d}(x) - \hat{b}(x) \hat{c}(x) = 0 \quad (5.4-6)$$

where, for n even, the polynomials $\hat{a}(x)$, $\hat{b}(x)$, $\hat{c}(x)$, and $\hat{d}(x)$ are expressed as:

$$\hat{a}(x) = \sum_{k=0}^{n/2} (-1)^k a_k x^k \quad (5.4-7)$$

$$\hat{b}(x) = \sum_{k=0}^{n/2-1} (-1)^k b_k x^k \quad (5.4-8)$$

$$\hat{c}(x) = \sum_{k=0}^{n/2} (-1)^k c_k x^k \quad (5.4-9)$$

$$\hat{d}(x) = \sum_{k=0}^{n/2-1} (-1)^k d_k x^k \quad (5.4-10)$$

when n is odd the summation in the above four equations is carried out up to $(n-1)/2$.

Equation (5.4-6) then becomes

$$\sum_{k=0}^{n-1} \sum_{i=0}^k (-1)^k (a_i d_{k-i} - b_{k-i} c_i) x^k = 0 \quad (5.4-11)$$

note that equation (5.4-11) is of order $n-1$.

Now, according to the segment lemma [58], the line segment (edge) connecting the two stable points α and β in the coefficient space is unstable if and only if there exists a positive real x which satisfies (5.4-6) and (5.4-5) simultaneously. One can solve the positive real roots of the $(n-1)$ -th order polynomial equation (5.4-6) first and then plug

these roots into either (5.4-5a) or (5.4-5b). If one of these roots make the left handed side of (5.4-5), i.e., $t/(1-t)$, positive, then the edge is unstable. Otherwise, the edge is stable. This approach is quite straightforward but it is still not efficient.

Recall that by using Bialas' method [54], one has to construct a Hurwitz matrix H_i of size n and invert the matrix for each vertex, then compute the product $H_i H_j^{-1}$ and find the eigenvalues of the $n \times n$ matrix for each edge. It is easy to see that the approach we mentioned in the previous paragraph is slightly better than Bialas' since solving positive real roots of an $(n-1)$ -th order polynomial equation is easier than computing the eigenvalues of an $n \times n$ matrix. However, both approaches require nontrivial computations for each edge of the polytope and hence they will become impractical when the combinatoric explosion of the number of edges occurs.

In the proposed algorithm, first of all, we solve the positive real roots for the four polynomials $\hat{a}(x)$, $\hat{b}(x)$, $\hat{c}(x)$, and $\hat{d}(x)$. Then from these positive roots, the intervals such that both $\hat{a}(x)\hat{c}(x)$ and $\hat{d}(x)\hat{b}(x)$ are negative can be easily found. If such intervals do exist one needs to check for the existence of roots of equation (5.4-6) inside these intervals. If (5.4-6) admits roots inside these intervals then the edge is unstable and stable otherwise. Note that when such intervals are empty one needs not continue and can conclude that the edge is stable. Recall that when n is even $\hat{a}(x)$ and $\hat{c}(x)$ are of order $n/2$ and $\hat{b}(x)$ and $\hat{d}(x)$ are of order $n/2-1$. When n is odd, $\hat{a}(x)$, $\hat{b}(x)$, $\hat{c}(x)$, and $\hat{d}(x)$ are all of order $(n-1)/2$. One of the significant features of this method is revealed in the fact that the polynomials $\hat{a}(x)$, $\hat{b}(x)$, $\hat{c}(x)$, and $\hat{d}(x)$ are of at most degree $n/2$, hence it is computationally easier to deal with. In fact, if $n=4$, $\hat{a}(x)$ and $\hat{c}(x)$ are second-order polynomials and $\hat{b}(x)$ and $\hat{d}(x)$ are first-order polynomials. If $n=9$, $\hat{a}(x)$, $\hat{c}(x)$, $\hat{b}(x)$, and $\hat{d}(x)$ are fourth-order polynomials. From [63], we can have closed-form solutions for the polynomial equations with order less than or equal to four. Also, the problem of determining whether or not (5.4-6) has positive real

roots inside an interval is a trivial one since it can be easily checked by using the Sturm Theorem [see App. B] without solving the equation.

The most significant feature of the proposed algorithm is that the computation involved is mainly determined by the number of vertices instead of that of edges. To see why the algorithm is more efficient than Bialas', let us assume the number of the perturbation parameters $m=10$ and the order of the characteristic polynomials $n=9$. Now in the coefficient space, the polytope has $2^{10}=1024$ vertices and more than a half million (523,776) edges. By using Bialas' method to check the stability of the polytope, we need to construct a 9×9 Hurwitz matrices H_i and its inverse H_i^{-1} for every vertex and then do the matrix multiplication $H_i H_j^{-1}$ and find the eigenvalues of the 9×9 matrix $H_i H_j^{-1}$ for each edge. By using the new algorithm, for each vertex we only need to solve two 4-th order polynomials for positive real roots and then for each edge find the intervals such that both $\hat{a}(x)\hat{c}(x)$ and $\hat{d}(x)\hat{b}(x)$ are negative which can be easily found. If such intervals are empty, the edge is stable. On the other hand, if such intervals do exist we need to use the Sturm theorem to check if the 8-th order equation (5.4-11) has any roots inside these intervals. Now we can see that the major computation effort in the new algorithm is finding the positive real roots for 2,048 4-th order polynomial equations while Bialas' method requires finding the eigenvalues for more than a half million 9-th order matrices.

Three examples are used to illustrate the segment stability checking algorithm.

Example 5.4-1:

Consider the two stable polynomials given as:

$$\alpha(s) = s^4 + 5s^3 + 3s^2 + 2s + 1$$

$$\beta(s) = s^4 + s^3 + 5s^2 + s + 3$$

The polynomials in equations (5.4-7) - (5.4-10) become

$$\hat{a}(x) = 1 - 3x + x^2$$

$$\hat{b}(x) = 2 - 5x$$

$$\hat{c}(x) = 3 - 5x + x^2$$

$$\hat{d}(x) = 1 - x$$

Upon substitution into equation (5.4-11), one obtains

$$4x^3 - 23x^2 + 21x - 5 = 0$$

Instability of the convex combination occurs whenever there are positive values of x that satisfy both equations (5.4-5a) and (5.4-5b) as well equation (5.4-6). For this example, one can see that equations (5.4-5) are satisfied, i.e., both $\hat{a}(x)\hat{c}(x)$ and $\hat{d}(x)\hat{b}(x)$ are negative over the interval $[.4, .697]$. To see whether (5.4-6) admits any roots inside this interval, the following Sturm sequence is formed:

$$f_0(x) = 4x^3 - 23x^2 + 21x - 5$$

$$f_1(x) = 12x^2 - 46x + 21$$

$$f_2(x) = 554x - 303$$

$$f_3(x) = 87354$$

Therefore the number of real roots of (5.4-6) inside $[.4, .697]$ is the difference in sign variation of the sequence when evaluated at both end points, i.e. in this example there are two roots inside the interval and so the edge is unstable.

Example 5.4-2:

As a second example we now consider the following two polynomials:

$$\alpha(s) = s^4 + 5s^3 + 10s^2 + 5s + 1$$

$$\beta(s) = s^4 + 2s^3 + 15s^2 + s + 3$$

The polynomials in equations (5.4-7) - (5.4-10) become

$$\hat{a}(x) = 1 - 10x + x^2$$

$$\hat{b}(x) = 5 - 5x$$

$$\hat{c}(x) = 3 - 15x + x^2$$

$$\hat{d}(x) = 1 - 2x$$

Upon substitution into equations (5.4-5), one can see that $\hat{a}(x)\hat{c}(x)$ is negative over [.101, .203] and [9.9, 14.79] whereas $\hat{d}(x)\hat{b}(x)$ is negative over [.5, 1]. Hence there are no values of x that satisfy both equations (5.4-5a) and (5.4-5b) at the same time and therefore the edge is stable. Note that checking for the existence of roots of equation (5.4-6) is not required for this example.

Example 5.4-3:

In this third example, we apply our algorithm to the perturbed plant in Example 5.3-1. In Example 5.3-1, we found that for $k=3.417396$ the characteristic polynomial corresponding to V_8 is unstable. For $k=3.417395$ the polytope corresponding to $k\mathcal{D}$ is stable. This polytope has 8 vertices and 28 edges. Recall that if we use Bialas' method to check the stability of the polytope, we need to construct a Hurwitz matrix H_i and its inverse H_i^{-1} for each vertex, do the multiplication $H_i H_j^{-1}$ and find the eigenvalues of a 4×4 matrix $H_i H_j^{-1}$ for each edge. In the following, we will use our fast algorithm to verify that this polytope is stable. We first solve a first-order and a second-order equations associated with each vertex. Then, for each pair of vertices (each edge) the intervals of x such that (5.4-5) are satisfied can be easily found. It turns out that in this example such intervals are all empty and so all the edges of the polytope are stable. The stability of $k\mathcal{D}$ is then inferred by the edge theorem. Note that since no intervals satisfying equations (5.4-5) were found, one needs not bother with checking the conditions required by equation (5.4-6). With this, we conclude that the new approach can be used effectively to greatly reduce the amount of computations required especially when one is faced with a large number of perturbation parameters in the plant.

SECTION 6

CONCLUSION AND FURTHER RESEARCH

6.1 Concluding Remarks

As demonstrated in Section 2, most robust control problems can be formulated as the standard H^∞ optimization problem. The standard H^∞ optimization problem consists of two subproblems. One is stabilization and the other is H^∞ optimization. The observer-based controller parametrization is employed to characterize the set of all stabilizing controllers in terms of a proper stable parameter matrix. Then among this set of stabilizing controllers, some will be chosen to solve the H^∞ optimization.

The poles of the closed-loop system with the observer-based controller parametrization can be classified into three groups, and each group of poles can be independently determined. These three groups of poles are the regulator poles, the observer poles, and the poles of the added parameter matrix. The regulator gain, the observer gain, and the added parameter matrix are free parameters to be chosen such that the closed-loop transfer function matrix has some optimal performance with the constraint that the regulator poles, the observer poles, and the poles of the parameter matrix are stable. Furthermore, these parameters can be chosen such that the controller is uncontrollable and/or unobservable and then the uncontrollable and/or unobservable controller poles can be removed and the order of the controller can be reduced. The set of these removable controller poles is a subset of the regulator and the observer poles. The poles of the closed-loop system with the minimal order controller will include all the poles of the parameter matrix and some of the regulator and the observer poles which are not the removable controller poles.

There is very few, if there is any, one-block problems. Most of practical control problems are either two-block or four-block problems. To reduce the order of the optimal

controller, we require low order realizations of $R_{11}(s)$, $R_{12}(s)$, $R_{21}(s)$, and $R_{22}(s)$ instead of a minimal realization of $R(s)$. In Sec.4.2, a numerically reliable algorithm for constructing the minimal realizations of $R_{L1}(s)$, $R_{L2}(s)$, $R_{R1}(s)$, and $R_{R2}(s)$ has been presented. From these realizations, the rational matrices $R_{ij}(s) = R_{Li}(s)R_{Rj}(s)$, $i,j=1,2$, can be easily obtained. There is no possible mathematically identical pole-zero cancellation between $R_{Li}(s)$ and $R_{Rj}(s)$, therefore, the order of the realization of $R_{ij}(s)$ constructed by our algorithm is minimal in most practical cases.

The two-block H^∞ optimization problem can be solved by using the proposed fast γ -iteration algorithm in Sec.4.3 to compute the optimal H^∞ norm. The fast γ -iteration algorithm converges extremely fast. The optimal H^∞ norm can be obtained with accuracy up to double precision within four iterations. Once the optimal H^∞ norm is available, the two-block H^∞ optimization problem can be converted into a one-block H^∞ optimization problem and then an optimal controller can be easily constructed by using Glover's method.

For the four-block H^∞ optimization problem, the easiest solution is probably the two-Riccati-equation approach proposed by Doyle, Glover, Khargonekar, and Francis. Strictly speaking, the two-Riccati-equation approach only gives suboptimal controllers such that the H^∞ norm of the closed-loop system is less than a number γ which is larger than the optimal norm. In Sec.4.4, we attempted to use the two-Riccati-equation approach to design a nearly H^∞ optimal controller. A simple iterative scheme can be used to reduce γ to a number which is very close to the optimum. However, as γ is close to the optimum, the elements of the state-space realization of the controller will approach to infinity. The remedy to this difficulty is to do partial fraction expansion for the controller and to approximate the wide-band low-pass terms by direct feedthrough terms. Then the elements of the realization of the controller will be all finite, and the order of the nearly H^∞ optimal controller is at least one less than that of the plant.

The real structured singular value computation algorithm presented in Sec.5.3 was developed based on the multilinear mapping, the edge theorem, the fast segment stability checking algorithm in Sec.5.4, and the perturbation domain partition technique. The computational burden due to the combinatoric explosion of the number of edges has been reduced a lot by using the fast segment stability checking algorithm. The convergence usually is not a problem unless a singular unstable region is inside or very close to the perturbation domain which hardly happens in the real world. If that happens, we just simply shrink the perturbation domain and try to find the largest lower bound k_L at which the computer can handle in finite steps. Although the algorithm requires no frequency search, the frequency at which the system becomes unstable can be computed from the real structured singular value and the critical point at which the stable perturbation domain touches the unstable region. This critical point can be evaluated by using the fast segment stability checking algorithm.

6.2 Further Research Suggestions

The two-Riccati-equation approach is a great break-through in the solution of H^∞ optimization problem. However, it only gives suboptimal solutions. If we try to have a suboptimal solution which is very close to the optimum, an inevitable numerical difficulty will occur. This numerical difficulty is caused by an unnecessary restriction that the controller be strictly proper. The first further research suggestion is to develop two-Riccati-equation like state-space formulae for optimal (instead of suboptimal) H^∞ controllers which are allowed to have direct feedthrough terms.

The second further research suggestion is related to the M- Δ structure shown in Fig.5.1-1. M- Δ structure is important since all the SSV analysis and design techniques are developed based on this structure. The construction of an M- Δ structure for a perturbed system is not difficult at all. However, it is by no means an easy task to find a minimal M- Δ structure. Here "minimal" means that the dimension of Δ (or M) is minimal. We can

easily construct an $M-\Delta$ structure for a given perturbed system, but the dimension of the structure may be unnecessarily large. Although theoretically the structured singular values of all $M-\Delta$ structures of the same perturbed system should be identical, a minimal $M-\Delta$ structure is much easier to handle than those with high dimension in computation. A minimal $M-\Delta$ structure is essential in the computation of the structured singular value.

The third further research suggestion is the development of a controller design updating scheme. The H^∞ optimization technique, fast computational algorithm for the real SSV, and the controller updating procedure are employed in the proposed design approach for robust optimal controllers. The H^∞ optimization technique allows us to consider a larger and more realistic set of disturbances, noises, and commands than those considered by LQG and Wiener-Hopf methods. The robust-stability constraint for the unstructured plant uncertainty and the control-input constraint are also incorporated in the H^∞ cost function. The controller which minimizes the H^∞ cost function is a tentative robust optimal controller. For the closed-loop system with the tentative robust optimal controller, we will check all performance measures like the real SSV, the H^∞ norm of the sensitivity function, the H^∞ norm of the complementary sensitivity function, and the amplitude of the control input, etc. These performance measures will be used to update the H^∞ cost function (and therefore the controller) and the updating procedure is repeated until a satisfactory trade-off is reached. In the proposed design approach, the uncertain disturbances and commands are modelled in a realistic way. Furthermore, the control-input constraint and the robust stability constraints for both of the unstructured and parametric plant uncertainties are also taken into account.

The fourth further research suggestion is fast computational algorithm for the real SSV. Parametric perturbation is a kind of plant uncertainties which occurs very often. The closed-loop system is required to be stable for all possible parametric perturbations. It is essential to have a robust-stability checking tool for testing if the closed-loop system is stable for all possible perturbations in a given parameter domain. The real SSV is not only

a robust-stability checking tool but also a stability-margin measure which gives the maximal allowable parameter perturbation domain in which the system remains stable. In the design of robust optimal controller, we need to compute the real SSV repeatedly until the controller updating loop is terminated. A fast computational algorithm for the real SSV is indispensable in the analysis and design of robust control systems.

For easy controller implementation, we would like the order of the controller to be as small as possible. The fifth further research suggestion is the development of a controller order reduction technique which guarantees the closed-loop performance. Most of the existing controller order reduction techniques are indirect methods in which the basic concept is to find a reduced-order controller which approximates the robust optimal controller and then check the closed-loop characteristics of the reduced-order controller. The drawback of these indirect methods is that the closed-loop properties are not considered during the controller reduction. The proposed approach is to characterize the set of all reduced-order stabilizing controllers and then to find a controller in this set such that the H^∞ cost function is minimized. This approach is a direct method in which the closed-loop properties are always guaranteed.

REFERENCES

- [1] H. Kwakernaak and R. Sivan, Linear Optimal Control Systems, John Wiley & Sons, Inc., 1972.
- [2] D. C. Youla, J. J. Bongiorno, and H. A. Jabr, "Modern Wiener-Hopf Design of Optimal Controllers, Part II: The Multivariable Case," IEEE Trans. A-C. AC-21, pp.319-338, 1976.
- [3] G. Zames, "Feedback and Optimal Sensitivity: Model Reference Transformations, Multiplicative Seminorms, and Approximate Inverses," IEEE Trans. A-C. AC-26, pp. 301-320, 1981.
- [4] B. A. Francis and G. Zames, "On H^∞ -Optimal Sensitivity Theory for SISO Feedback Systems," IEEE Trans. A-C. AC-29, pp.9-16, Jan. 1984.
- [5] B. A. Francis, J. W. Helton, and G. Zames, " H^∞ -Optimal Feedback Controllers for Linear Multivariable Systems," IEEE Trans. A-C. AC-29, pp.888-900, Oct. 1984.
- [6] B. C. Chang and J. B. Pearson, "Optimal Disturbance Reduction in Linear Multivariable Systems," IEEE Trans. A-C. AC-29, pp.880-887, Oct. 1984.
- [7] M. G. Safonov and M. S. Verma, " L^∞ -sensitivity Optimization via Hankel-norm Approximation," Proceedings of American Control Conference, San Francisco, June 1983.
- [8] K. Glover, "All Optimal Hankel-norm Approximations of Linear Multivariable Systems and Their L^∞ -error Bounds," International Journal of Control. Vol. 39. No. 6, pp.1115-1193, 1984.
- [9] A. C. Allison and N. J. Young, "Numerical Algorithms for the Nevanlinna-Pick Problem," Numerische Mathematik. Vol. 42, pp.125-145, 1983.
- [10] J. Doyle, "Synthesis of Robust Controllers and Filters," Proceedings of 22nd Conference on Decision and Control, Dec. 1983.

- [11] J. Doyle, Lectures Notes, ONR/Honeywell Workshop on Advances in Multivariable Control, Minneapolis, Minnesota, Oct. 1984.
- [12] C-C Chu, H. Optimization and Robust Multivariable Control, Ph.D. Dissertation, University of Minnesota, Sept. 1985.
- [13] H. Kimura, "Robust Stabilization for a Class of Transfer Functions," IEEE Trans. A-C. AC-29, pp.788-793, Sept. 1984.
- [14] H. Kwakernaak, "Minimax Frequency Domain Performance and Robustness Optimization of Linear Feedback Systems," IEEE Trans. A-C. AC-30, pp.994-1004, Oct. 1985.
- [15] B. A. Francis, A Course in H^∞ Control Theory, Springer-Verlag, 1987.
- [16] A. Feintuch and B. A. Francis, "Uniformly Optimal Control of Linear Feedback Systems," Automatica, vol.21, No.5, pp.563-574, 1985.
- [17] B. C. Chang and J. B. Pearson, "Iterative Computation of Minimal H^∞ Norm," Proceedings of 24th Conference on Decision and Control, Dec. 1985.
- [18] C-C Chu, J. Doyle, and E. B. Lee, "The General Distance Problem in H_∞ Optimal Control Theory," International Journal of Control, Vol. 44, No. 2, pp.565-596, 1986.
- [19] E. A. Jonckheere and J. C. Juang, "Fast Computation on Achievable Feedback Performance in Mixed Sensitivity H^∞ Design," IEEE Transactions on Automatic Control, Vol. AC-32, pp.896-906, Oct. 1987.
- [20] B. C. Chang, S. S. Banda, and T. E. McQuade, "Fast Iterative Computation of Optimal Two-block H^∞ Norm," IEEE Transactions on Automatic Control, Vol. AC-34, No.7, pp.738-743, July 1989.
- [21] B. C. Chang, "A Stable State-Space Realization in the Formulation of H^∞ Norm Computation," IEEE Trans. on A-C. AC-32, pp.811-815, Sept. 1987.

- [22] D. J. N. Limebeer and Y. S. Hung, "An Analysis of the Pole-zero Cancellations in H^∞ Optimal Control Problems of the First Kind," *SIAM J. Control and Optimization*, Vol. 25, No. 6, pp.1457-1493, Nov. 1987.
- [23] I. Postlethwaite, D. W. Gu, and S. D. O'Young, "Some Computational Results on Size Reduction in H^∞ Design," *IEEE Trans. on A-C. AC-33*, pp.177-185, Feb. 1988.
- [24] B. C. Chang, "Size Reduction in Four-Block H^∞ Formulation," *Proceedings of the 26th Conference on Decision and Control*, Dec. 1987.
- [25] B. C. Chang and S. S. Banda, "Optimal H^∞ Norm Computation for MIMO Systems with Multiple Zeros," *IEEE Transactions on Automatic Control*, Vol. AC-34, No. 5, pp.553-557, May 1989.
- [26] K. Glover and J.C. Doyle, "State Space Formulae for All Stabilizing Controllers that Satisfy an H_∞ -Norm Bound and Relations to Risk Sensitivity," *Systems & Control Letters* Vol. 11, pp.167-172, 1988.
- [27] K. Zhou and P.P. Khargonekar, "An Algebraic Riccati Equation Approach to H^∞ Optimization," *Systems & Control Letters* Vol. 11, pp.85-91, 1988.
- [28] M.G. Safonov and D.J.N. Limebeer, "Simplifying the H^∞ Theory via Loop Shifting," *Proceedings of the 27th Conference on Decision and Control*, Dec. 1988.
- [29] J.C. Doyle, K. Glover, P.P. Khargonekar, and B.A. Francis, "State-space Solutions to Standard H_2 and H_∞ Control Problems," *IEEE Transactions on Automatic Control*, Vol. AC-34, No. 8, pp.831-847, Aug. 1989.
- [30] C.A. Desoer, R.W. Liu, J. Murray, and R. Saeks, "Feedback System Design: The Fractional Representation Approach," *IEEE Trans. A-C. AC-25*, pp.399-412, 1980.
- [31] C. N. Nett, C. A. Jacobson and M. J. Balas, "A Connection Between State-space and Doubly Coprime Fractional Representations," *IEEE Trans. A-C. AC-29*, pp. 831-832, 1984.

- [32] B.C. Chang and A. Yousuff, "Pole Placement and the Observer-based Controller Parametrization," To appear in *IEEE Transactions on Automatic Control*.
- [33] C. A. Desoer and M. Vidyasagar, Feedback Systems: Input-Output Properties, Academic Press, 1975.
- [34] J. C. Doyle and G. Stein, "Multivariable Feedback Design: Concepts for a Classical/Modern Synthesis," IEEE Trans. A-C, AC-26, pp.4-16, Feb. 1981.
- [35] N. A. Lehtomaki, N. R. Sandell, and M. Athans, "Robustness Results in Linear-Quadratic-Gaussian Based Multivariable Control Design," IEEE Trans. A-C, AC-26, pp.75-92, Feb. 1981.
- [36] P. M. Van Dooren, "The Generalized Eigenstructure Problem in Linear System Theory," IEEE Trans. A-C, AC-26, pp.111-129, 1981.
- [37] H. H. Rosenbrock, State-Space and Multivariable Theory, Wiley-Interscience, New York, 1970.
- [38] R.C. Chang, X.P. Li, S.S. Banda, and H.H. Yeh, "Design a Nearly H^∞ Optimal Controller by Using DGKF's State-space Formulae," under preparation.
- [39] J. Doyle, "Analysis of Feedback Systems with Structured Uncertainties," IEE PROC. Vol.129 Pt.D. No.6, pp. 242-250, 1982.
- [40] J. Doyle, "Structured Uncertainty in Control System Design," Proceedings of the 24th Conference on Decision and Control, Dec. 1985.
- [41] M. K. H. Fan and A. L. Tits, "Characterization and Efficient Computation of the Structured Singular Value," IEEE Trans. A-C, AC-31, pp. 734-743, Aug. 1986.
- [42] M. K. H. Fan and A. L. Tits, "m-Form Numerical Range and the Computation of the Structured Singular Value," IEEE Trans. A-C, AC-33, pp. 284-289, Mar. 1988.

- [43] M. G. Safonov and J. Doyle, "Minimizing Conservativeness of Robustness Singular Values," in S. G. Tzefestas (ed.), *Multivariable Control*, D. Reidel Publishing Company, 1984.
- [44] B. G. Morton and R. M. McAfoos, "A Mu-Test for Real Parameter Variations," *Proceedings of the 1985 American Control Conference*.
- [45] R. D. Jones, "Structured Singular Value Analysis for Real Parameter Variations," *1987 AIAA Conference in Guidance and Control*.
- [46] M.G. Safonov and M. Athans, "Gain and Phase Margin for Multiloop LQG Regulators," *IEEE Trans. A-C. AC-22*, pp. 173-179, 1977.
- [47] M.G. Safonov, "Stability Margins of Diagonally Perturbed Multivariable Feedback Systems," *Proceedings of the 20th IEEE Conference on Decision and Control*, Dec. 1981.
- [48] R.E. De Gaston and M.G. Safonov, "Exact Calculation of the Multiloop Stability Margin," *IEEE Trans. A-C. AC-33*, pp. 156-171, 1988.
- [49] R.S.S. Pena and A. Sideris, "A General Program to Compute the Multivariable Stability Margin for Systems with Parametric Uncertainty," *Proceedings of the 1988 American Control Conference*.
- [50] A. Sideris and R. S. S. Pena, "Fast Computation of the Multivariable Stability Margin for Real Interrelated Uncertain Parameters," *Proceedings of the 1988 American Control Conference*.
- [51] V. L. Kharitonov, "Asymptotic Stability of an Equilibrium Position of a Family of Systems of Linear Differential Equations," *Differentsial'nye Uravneniya*, Vol. 14, No. 11, pp. 1483-1485, 1978.
- [52] A.C. Bartlett, C.V. Hollot, and H. Lin, "Root Locations on an Entire Polytope of Polynomials: It Suffices to Check the Edges," *Mathematics of Control, Signals, and Systems*, Vol.1, pp.61-71, 1988.

- [53] M. Fu and B.R. Barmish, "Stability of Convex and Linear Combinations of Polynomials and Matrices Arising in Robustness Problems," Proceedings of the Conference on Information Sciences and Systems, John Hopkins University, 1987.
- [54] S. Bialas, "A Necessary and Sufficient Condition for the Stability of Convex Combinations of Stable Polynomials or Matrices," Bulletin of the Polish Academy of Sciences, Technical Sciences, Vol. 33, No. 9-10, pp.473-480, 1985.
- [55] K.H. Wei and Yedavalli, "Invariance of Strict Hurwitz Property for Uncertain Polynomials with Dependent Coefficients," IEEE Trans. A-C. AC-32, pp. 907-909, 1987.
- [56] L.H. Keel, S.P. Bhattacharyya, and J.W. Howze, "Robust Control with Structured Perturbations," IEEE Trans. A-C. AC-33, pp. 68-78, 1988.
- [57] H. Bouguerra, B.C. Chang, H. H. Yeh, and S. Banda, "Fast Stability Checking for the Convex Combination of Stable Polynomials," To appear in IEEE Transactions on Automatic Control.
- [58] H. Chapellat and S. P. Bhattacharyya, "A Generalization of Kharitonov's Theorem for Robust Stability on Interval Plants," TCSP Research Report #88-004, E.E. Dept., Texas A&M, Jan. 1988.
- [59] B.R. Barmish, M. Fu, and S. Salem, "Stability of a Polytope of Matrices: Counterexamples," IEEE Trans. A-C. AC-33, pp. 569-572, 1988.
- [60] B.C. Chang, O. Ekdal, H.H. Yeh, and S.S. Banda, "Computation of the Real Structured Singular Value via Polytopic Polynomials". Proceedings of the 1989 AIAA GNC Conference, Boston, MA, Aug. 1989.
- [61] L.A. Zadeh and C.A. Desoer, Linear System Theory, McGraw-Hill, New York, 1963.
- [62] A. S. Householder, The Numerical Treatment of a Single Nonlinear Equation. McGraw-Hill Book Company. N.Y. 1970.

- [63] W. V. Lovitt, Elementary Theory of Equations. Prentice-Hall, Inc. N.Y. 1939.
- [64] T. Kailath, Linear Systems, Prentice-Hall, 1980.
- [65] B.C. Chang and A. Yousuff, "A Straightforward Proof for the Observer-based Controller Parametrization," Proceedings of the 1988 AIAA Guidance, Navigation and Control Conference, pp.226-231, Minneapolis, August 1988.
- [66] M. Vidyasagar, "A State-Space Interpretation of Simultaneous Stabilization," IEEE Trans. A-C, AC-33, pp. 506-508, 1988.
- [67] E. A. Jonckheere and M. Verma, "A Spectral Characterization of H_∞ Optimal Feedback Performance and Its Efficient Computation," Systems and Control Letters, 1986.
- [68] Z. Z. Wang, Ph.D. Dissertation: Synthesis of Linear Multivariable Feedback Systems in Infinite Index Norm, supervised by Professor J. B. Pearson, Dept. of E. E., Rice University, Aug. 1984.

APPENDIX A

Proof of Theorems

Proof of Theorem 3.3-2:

Let $N_G(s)D_G(s)^{-1}$ with $\deg |D_G(s)| = n$ and $D_K(s)^{-1}N_K(s)$ with $\deg |D_K(s)| = n+m$ be a right MFD (matrix fraction description) of $G_{22}(s)$ and a left MFD of $K(s)$ respectively [64]. It is well known that the characteristic polynomial of the closed-loop system is

$$\phi_{\text{closed-loop}}(s) = |D_K(s)D_G(s) - N_K(s)N_G(s)| \quad (\text{A1-1})$$

Let $L_K(s)$ be a greatest common left divisor of $D_K(s)$ and $N_K(s)$. That is,

$$D_K(s) = L_K(s)\hat{D}_K(s), \quad N_K(s) = L_K(s)\hat{N}_K(s) \quad (\text{A1-2})$$

where $\hat{D}_K(s)$ and $\hat{N}_K(s)$ are left coprime. It is easy to see that the zeros of $L_K(s)$ are the uncontrollable or the unobservable poles of the controller realization in Fig. 3.2-3. That is,

$$\{ \text{zeros of } L_K(s) \} = \mathcal{P}_{\text{removal}} \quad (\text{A1-3})$$

Plug (A1-2) into (A1-1), we have

$$\phi_{\text{closed-loop}}(s) = |L_K(s) \cdot |\hat{D}_K(s)D_G(s) - \hat{N}_K(s)N_G(s)|| \quad (\text{A1-4})$$

The zeros of $|\hat{D}_K(s)D_G(s) - \hat{N}_K(s)N_G(s)|$ are the poles of the closed-loop system with a minimal controller realization. From Theorem 3.3-1, (A1-3) and (A1-4), we can see that

$$\mathcal{P}_{\text{closed-loop with min. controller}} + \mathcal{P}_{\text{removal}} = \mathcal{P}_{\text{regulator}} + \mathcal{P}_{\text{observer}} + \mathcal{P}_{Q(s)} \quad (\text{A1-5})$$

To complete the proof, we need to show that $\mathcal{P}_{\text{removal}}$ is a subset of $\mathcal{P}_{\text{regulator}} + \mathcal{P}_{\text{observer}}$ when $Q(s)$ is minimal. The dynamic equations of the observer-based controller

in Fig. 3.2-3, i.e., the block diagram inside the dotted-line box, can be written as follows:

$$\dot{\hat{x}} = (A+B_2F+HC_2+HD_{22}F)\hat{x} + \begin{bmatrix} -H & -(B_2+HD_{22}) \end{bmatrix} \begin{bmatrix} y \\ u_2 \end{bmatrix} \quad (A1-6a)$$

$$\begin{bmatrix} u \\ \tilde{y} \end{bmatrix} = \begin{bmatrix} F \\ -(C_2+D_{22}F) \end{bmatrix} \hat{x} + \begin{bmatrix} 0 & -I \\ I & D_{22} \end{bmatrix} \begin{bmatrix} y \\ u_2 \end{bmatrix} \quad (A1-6b)$$

Assume that the added dynamics $Q(s)$ is described by the following minimal realization:

$$\dot{k} = \tilde{A}k + \tilde{B}\tilde{y} \quad (A1-7a)$$

$$u_2 = \tilde{C}k + \tilde{D}\tilde{y} \quad (A1-7b)$$

The controller $K(s)$ is just a combination of (A1-6) and (A1-7). From (A1-6) and (A1-7), we have the dynamic equations of the controller $K(s)$ as follows:

$$\begin{bmatrix} \dot{\hat{x}} \\ \dot{k} \end{bmatrix} = \begin{bmatrix} \alpha_{11} & \alpha_{12} \\ \alpha_{21} & \alpha_{22} \end{bmatrix} \begin{bmatrix} \hat{x} \\ k \end{bmatrix} + \begin{bmatrix} \beta_1 \\ \beta_2 \end{bmatrix} y \quad (A1-8a)$$

$$u = \begin{bmatrix} \gamma_1 & \gamma_2 \end{bmatrix} \begin{bmatrix} \hat{x} \\ k \end{bmatrix} + \delta y \quad (A1-8b)$$

where

$$\beta_1 = -H - (B_2+HD_{22})(I-\tilde{D}D_{22})^{-1}\tilde{D} \quad (A1-9a)$$

$$\beta_2 = \tilde{B} + \tilde{B}D_{22}(I-\tilde{D}D_{22})^{-1}\tilde{D} \quad (A1-9b)$$

$$\gamma_1 = F + (I-\tilde{D}D_{22})^{-1}\tilde{D}(C_2+D_{22}F) \quad (A1-9c)$$

$$\gamma_2 = -(\mathbf{I} - \tilde{\mathbf{D}}\mathbf{D}_{22})^{-1}\tilde{\mathbf{C}} \quad (\text{A1-9d})$$

$$\alpha_{11} = \mathbf{A} + \mathbf{H}\mathbf{C}_2 + (\mathbf{B}_2 + \mathbf{H}\mathbf{D}_{22})\gamma_1 \quad (\text{A1-9e})$$

$$= \mathbf{A} + \mathbf{B}_2\mathbf{F} - \beta_1(\mathbf{C}_2 + \mathbf{D}_{22}\mathbf{F}) \quad (\text{A1-9f})$$

$$\alpha_{12} = (\mathbf{B}_2 + \mathbf{H}\mathbf{D}_{22})\gamma_2 \quad (\text{A1-9g})$$

$$\alpha_{21} = -\beta_2(\mathbf{C}_2 + \mathbf{D}_{22}\mathbf{F}) \quad (\text{A1-9h})$$

$$\alpha_{22} = \tilde{\mathbf{A}} - \tilde{\mathbf{B}}\mathbf{D}_{22}\gamma_2 \quad (\text{A1-9i})$$

$$\delta = -(\mathbf{I} - \tilde{\mathbf{D}}\mathbf{D}_{22})^{-1}\tilde{\mathbf{D}} \quad (\text{A1-9j})$$

Now, assume that the state-space representation (A1-8) of the controller $\mathbf{K}(s)$ is unobservable. Then by PBH test [64], there exists a nonzero vector ξ such that

$$\begin{bmatrix} \gamma_1 & \gamma_2 \end{bmatrix} \begin{bmatrix} \xi_1 \\ \xi_2 \end{bmatrix} = 0; \quad \begin{bmatrix} \xi_1 \\ \xi_2 \end{bmatrix} = \xi \quad (\text{A1-10a})$$

$$\begin{bmatrix} \alpha_{11} & \alpha_{12} \\ \alpha_{21} & \alpha_{22} \end{bmatrix} \begin{bmatrix} \xi_1 \\ \xi_2 \end{bmatrix} = \lambda \begin{bmatrix} \xi_1 \\ \xi_2 \end{bmatrix} \quad (\text{A1-10b})$$

for some eigenvalue λ of (A1-8). Note that it is the eigenvalue λ that is unobservable.

From (A1-10b), we get

$$\alpha_{11}\xi_1 + \alpha_{12}\xi_2 = \lambda\xi_1 \quad (\text{A1-11a})$$

which, by using (A1-9e) and (A1-9g), is rewritten as

$$(\mathbf{A} + \mathbf{H}\mathbf{C}_2)\xi_1 + (\mathbf{B}_2 + \mathbf{H}\mathbf{D}_{22})(\gamma_1\xi_1 + \gamma_2\xi_2) = \lambda\xi_1 \quad (\text{A1-11b})$$

In view of (A1-10a), the above equation reduces to

$$(A + HC_2) \xi_1 = \lambda \xi_1 \quad (A1-11c)$$

which clearly establishes that the unobservable eigenvalue belongs to $\mathcal{P}_{\text{observer}}$.

Proceeding similarly, it can be shown that if (A1-8) is uncontrollable then the uncontrollable eigenvalue belongs to $\mathcal{P}_{\text{regulator}}$.

Note in the above development that $\xi_1 = 0$ contradicts the minimality assumption of $Q(s)$. Thus,

$$\mathcal{P}_{\text{unobservable}} \subset \mathcal{P}_{\text{observer}} \quad (A1-12a)$$

$$\mathcal{P}_{\text{uncontrollable}} \subset \mathcal{P}_{\text{regulator}} \quad (A1-12b)$$

where $\mathcal{P}_{\text{unobservable}}$ is the set of all the unobservable poles of the controller $K(s)$.

$\mathcal{P}_{\text{uncontrollable}}$ is defined similarly. This completes the proof of Theorem 3.3-2.

Proof of Remark 4.2-1:

Clearly, the realization (4.2-4) is controllable if the pair

$$\{(A_2 - L_2 L_2^T X_2)^T, (D_{\perp} W_2 - D_{12} R_D^{-1} B_2^T U_2 X_2)^T\} \quad (A2-1a)$$

is controllable. This pair is controllable if there exists a positive definite \hat{X} such that

$$\begin{aligned} (A_2 - L_2 L_2^T X_2)^T \hat{X} + \hat{X} (A_2 - L_2 L_2^T X_2) \\ + (D_{\perp} W_2 - D_{12} R_D^{-1} B_2^T U_2 X_2)^T (D_{\perp} W_2 - D_{12} R_D^{-1} B_2^T U_2 X_2) = 0 \end{aligned} \quad (A2-1b)$$

Substituting \hat{X} by X_2 , then the left hand side of (A2-1b) can be reduced to

$$A_2^T X_2 + X_2 A_2 - X_2 L_2 L_2^T X_2 + W_2^T W_2 \quad (A2-1c)$$

which is zero according to (4.2-3e).

Proof of Theorem 4.3-7:

Recall that

$$\mu(\gamma) := \inf_{\hat{Q} \in (RH^\infty)^{m \times r}} \| (R_{11} + \hat{Q}) (\gamma^2 I - R_{21}^* R_{21})^{-1/2} \|_\infty \quad (A3-1)$$

The theorem will be proved by a contradiction. Let

$$\alpha = \sqrt{\mu^2(\gamma) \gamma^2 + [1 - \mu^2(\gamma)] c^2} \quad (A3-2)$$

Suppose that (4.3-14) is not true. Then from Theorem 4.3-1, $\gamma_0 < \alpha$ implies that

$$\mu(\alpha) := \inf_{\hat{Q} \in (RH^\infty)^{m \times r}} \| (R_{11} + \hat{Q}) (\alpha^2 I - R_{21}^* R_{21})^{-1/2} \|_\infty < 1 \quad (A3-3)$$

An optimal \hat{Q} for (A3-3) is denoted by \hat{Q}_1 , i.e.,

$$\mu(\alpha) = \| (R_{11} + \hat{Q}_1) (\alpha^2 I - R_{21}^* R_{21})^{-1/2} \|_\infty < 1 \quad (A3-4)$$

Thus,

$$(\alpha^2 I - R_{21}^* R_{21})^{-1/2*} (R_{11} + \hat{Q}_1)^* (R_{11} + \hat{Q}_1) (\alpha^2 I - R_{21}^* R_{21})^{-1/2} < I \quad \text{for all } \omega \quad (A3-4)$$

$$\begin{aligned} \Leftrightarrow (R_{11} + \hat{Q}_1)^* (R_{11} + \hat{Q}_1) &< \alpha^2 I - R_{21}^* R_{21} \\ &= \mu^2(\gamma) \gamma^2 I + [1 - \mu^2(\gamma)] c^2 I - R_{21}^* R_{21} \\ &\leq \mu^2(\gamma) \gamma^2 I + [1 - \mu^2(\gamma)] R_{21}^* R_{21} - R_{21}^* R_{21} \\ &= \mu^2(\gamma) (\gamma^2 I - R_{21}^* R_{21}) \quad \text{for all } \omega \end{aligned} \quad (A3-5)$$

$$\Leftrightarrow (\gamma^2 I - R_{21}^* R_{21})^{-1/2*} (R_{11} + \hat{Q}_1)^* (R_{11} + \hat{Q}_1) (\gamma^2 I - R_{21}^* R_{21})^{-1/2} < \mu^2(\gamma) I \quad \text{for all } \omega \quad (A3-6)$$

$$\Leftrightarrow \| (R_{11} + \hat{Q}_1) (\gamma^2 I - R_{21}^* R_{21})^{-1/2} \|_\infty < \mu(\gamma) \quad (A3-7)$$

which contradicts the fact that $\mu(\gamma)$ is the infimum as stated by (A3-2). Hence,

$$\gamma_0 \geq \alpha = \sqrt{\mu^2(\gamma) \gamma^2 + [1 - \mu^2(\gamma)] c^2} \quad (A3-8)$$

Proof of Corollary 4.3 8:

Denote the right-hand side of (4.3-15) (or (4.3-17)) by β_3 . The function $\mu(\gamma)$ can be considered as a curve in a two-dimensional space. The point $(\gamma_0, 1)$ is the intersection of the curve $y = \mu(\gamma)$ and the horizontal line $y = 1$. Draw a straight line connecting the two points $(\gamma_1, \mu(\gamma_1))$ and $(\gamma_5, \mu(\gamma_5))$. This straight line will cross the horizontal line $y = 1$ at the point $(\beta_3, 1)$. Since the function $\mu(\gamma)$ is continuous, convex, and strictly monotonically decreasing, it is easy to see that

$$\gamma_0 > \beta_3 \text{ if } \mu(\gamma_5) > 1 \text{ and } \gamma_0 < \beta_3 \text{ if } \mu(\gamma_5) < 1.$$

Inequalities (4.3-16) and (4.3-18) can be proved in a similar way.

Proof of Theorem 5.2-3:

Without loss of generality, we will show that α_i 's, $i=0,1,2,\dots,n$, are linear (affine) functions of $\bar{\delta}_1$ while $\bar{\delta}_2, \dots, \bar{\delta}_m$ remain unchanged. Let $m_{ij}(s)$ be the i - j entry of the matrix $M(s)$. Then

$$\det [I + M(s)\Delta]$$

$$= \begin{vmatrix} 1+m_{11}\bar{\delta}_1 & m_{12}\bar{\delta}_2 & \dots & m_{1m}\bar{\delta}_m \\ m_{21}\bar{\delta}_1 & 1+m_{22}\bar{\delta}_2 & \dots & m_{2m}\bar{\delta}_m \\ \vdots & \vdots & \ddots & \vdots \\ m_{m1}\bar{\delta}_1 & m_{m2}\bar{\delta}_2 & \dots & 1+m_{mm}\bar{\delta}_m \end{vmatrix}$$

$$= \begin{vmatrix} 1 & m_{12}\bar{\delta}_2 & \dots & m_{1m}\bar{\delta}_m \\ 0 & 1+m_{22}\bar{\delta}_2 & \dots & m_{2m}\bar{\delta}_m \\ \vdots & \vdots & \ddots & \vdots \\ 0 & m_{m2}\bar{\delta}_2 & \dots & 1+m_{mm}\bar{\delta}_m \end{vmatrix} + \bar{\delta}_1 \begin{vmatrix} m_{11} & m_{12}\bar{\delta}_2 & \dots & m_{1m}\bar{\delta}_m \\ m_{21} & 1+m_{22}\bar{\delta}_2 & \dots & m_{2m}\bar{\delta}_m \\ \vdots & \vdots & \ddots & \vdots \\ m_{m1} & m_{m2}\bar{\delta}_2 & \dots & 1+m_{mm}\bar{\delta}_m \end{vmatrix}$$

$$:= \hat{m}_1(s) + \bar{\delta}_1 \hat{m}_2(s)$$

Here $\hat{m}_1(s)$ that $\hat{m}_2(s)$ are rational functions with real coefficients. Now, we can write

$$\hat{m}_1(s) + \delta_1 \hat{m}_2(s) = \frac{n_1(s)}{d_c(s)d_1(s)} + \delta_1 \frac{n_2(s)}{d_c(s)d_2(s)} = \frac{n_1(s)d_2(s) + \delta_1 n_2(s)d_1(s)}{d_c(s)d_1(s)d_2(s)}$$

where the $\{n_1(s), d_1(s)\}$ and $\{n_2(s), d_2(s)\}$ are coprime polynomial pairs, and $d_c(s)$ is a greatest common factor of the denominator polynomials of $\hat{m}_1(s)$ and $\hat{m}_2(s)$.

The polynomials $n_1(s)d_2(s)$ and $n_2(s)d_1(s)$ can be represented as

$$a_0 s^n + a_1 s^{n-1} + a_2 s^{n-2} + \dots + a_n$$

and

$$b_0 s^n + b_1 s^{n-1} + b_2 s^{n-2} + \dots + b_n$$

respectively. Therefore, the characteristic polynomial is

$$\begin{aligned} & \alpha_0 s^n + \alpha_1 s^{n-1} + \alpha_2 s^{n-2} + \dots + \alpha_n \\ &= (a_0 + \bar{\delta}_1 b_0) s^n + (a_1 + \bar{\delta}_1 b_1) s^{n-1} + (a_2 + \bar{\delta}_1 b_2) s^{n-2} + \dots + (a_n + \bar{\delta}_1 b_n) \end{aligned}$$

i.e.,

$$\alpha_i = a_i + \bar{\delta}_1 b_i \quad i = 0, 1, 2, \dots, n$$

Proof of Theorem 5.2-6:

Recall that $\bar{\mathcal{D}} = \{ \bar{\delta}_i : -1 \leq \bar{\delta}_i \leq 1, i = 1, 2, \dots, m \}$. To complete the proof we need to show that for any $\bar{\delta}^* \in \bar{\mathcal{D}}$, the image of $\bar{\delta}^*$ is inside the polytope $\mathcal{P}(\bar{\mathcal{D}})$ if the mapping is multilinear. Let

$$\bar{\delta}^* = [\bar{\delta}_1^*, \bar{\delta}_2^*, \bar{\delta}_3^*, \dots, \bar{\delta}_m^*]^T \in \bar{\mathcal{D}}$$

and define

$$\bar{\delta}^*(k) = [\bar{\delta}_1^*, \bar{\delta}_2^*, \dots, \bar{\delta}_k^*, \sigma_{k+1}, \sigma_{k+2}, \dots, \sigma_m]^T$$

where $0 < k \leq m$, and σ_i is either $+1$ or -1 , for $k+1 \leq i \leq m$. Note that $\bar{\delta}^*(k)$ represents one of the 2^{m-k} points which associate with $\bar{\delta}^*$ on the boundary hyperplanes of $\bar{\mathcal{D}}$. $\bar{\delta}^*(0)$ is one of the vertices of $\bar{\mathcal{D}}$ and $\bar{\delta}^*(m) = \bar{\delta}^*$. We shall prove by mathematical induction that $\mathcal{I}(\bar{\delta}^*(m)) \in \mathcal{P}(\bar{\mathcal{D}})$.

Assume that the image of the 2^{m-k} $\bar{\delta}^*(k)$'s are all in $\mathcal{P}(\bar{\mathcal{D}})$ and define

$$\bar{\delta}^*(k^+) = [\bar{\delta}_1^*, \bar{\delta}_2^*, \dots, \bar{\delta}_k^*, +1, \sigma_{k+2}, \dots, \sigma_m]^T$$

and

$$\bar{\delta}^*(k^-) = [\bar{\delta}_1^*, \bar{\delta}_2^*, \dots, \bar{\delta}_k^*, -1, \sigma_{k+2}, \dots, \sigma_m]^T$$

Let the line segment connecting $\bar{\delta}^*(k^+)$ and $\bar{\delta}^*(k^-)$ be denoted by λ_k . Obviously, λ_k is parallel to $\bar{\delta}_{k+1}$ -axis, since the only coordinate change from $\bar{\delta}^*(k^+)$ to $\bar{\delta}^*(k^-)$ is along the $\bar{\delta}_{k+1}$ -axis. Therefore, the image of λ_k is also in $\mathcal{P}(\bar{\mathcal{D}})$ by the virtue of Lemma 2.5. Since $\bar{\delta}^*(k+1)$ is a point on λ_k , its image must also in $\mathcal{P}(\bar{\mathcal{D}})$. The fact that the image of $\bar{\delta}^*(0)$ is in $\mathcal{P}(\bar{\mathcal{D}})$ is established by the definition of $\mathcal{P}(\bar{\mathcal{D}})$. This completes the proof.

Proof of Theorem 5.2-7:

The proof is similar to De Gaston and Safonov's [48]. The only difference is that their co-domain is the complex plane while ours is the coefficient space. The roots of the characteristic equation, i.e., the eigenvalues of $A-B\Delta C$ are uniquely determined by the parameter vector $\bar{\delta}$ and therefore so is the coefficient vector α . For any $\bar{\delta}^x \in \bar{\mathcal{D}}_1$, there exists a $\bar{\delta}^y \in \bar{\mathcal{D}}_2$ such that $\bar{\delta}^y = \bar{\delta}^x$ and thus $\mathcal{I}(\bar{\delta}^y) = \mathcal{I}(\bar{\delta}^x)$. Hence $\mathcal{I}(\bar{\mathcal{D}}_1) \subset \mathcal{I}(\bar{\mathcal{D}}_2)$. Since $\mathcal{P}(\bar{\mathcal{D}}_1)$ is the smallest convex set that contains all the points of $\mathcal{I}(\bar{\mathcal{D}}_1)$, (5.2-6) is a direct consequence of (5.2-5).

Proof of Theorem 5.2-8:

Again, the proof is similar to De Gaston and Safonov's [48]. The vertices of $\bar{\mathcal{D}}_1$ and $\bar{\mathcal{D}}_2$ are mapped into $\mathcal{P}(\bar{\mathcal{D}})$ and therefore $\mathcal{P}(\bar{\mathcal{D}}_1)$, $\mathcal{P}(\bar{\mathcal{D}}_2)$, and $\mathcal{P}(\bar{\mathcal{D}}_1) \cup \mathcal{P}(\bar{\mathcal{D}}_2)$ are contained in $\mathcal{P}(\bar{\mathcal{D}})$. Since $\mathcal{I}(\bar{\mathcal{D}}_1) \subset \mathcal{P}(\bar{\mathcal{D}}_1)$, $\mathcal{I}(\bar{\mathcal{D}}_2) \subset \mathcal{P}(\bar{\mathcal{D}}_2)$, and $\mathcal{I}(\bar{\mathcal{D}}_1) \cup \mathcal{I}(\bar{\mathcal{D}}_2) = \mathcal{I}(\bar{\mathcal{D}})$, we have $\mathcal{I}(\bar{\mathcal{D}}) \subset \mathcal{P}(\bar{\mathcal{D}}_1) \cup \mathcal{P}(\bar{\mathcal{D}}_2)$.

APPENDIX B

Real Solution Existence Checking by Using Sturm Theorem

Given a polynomial $P_n(x)$ of degree n and an interval $[a,b]$ on the real axis, find how many roots of $P_n(x)$ are located inside $[a,b]$?

Sturm Sequence:

Let

$$P_n(x) = a_0x^n + a_1x^{n-1} + \dots + a_{n-1}x + a_n \quad (B-1)$$

and

$$f_0(x) = P_n(x) \quad (B-2)$$

$$f_1(x) = \frac{d}{dx} P_n(x) \quad (B-3)$$

Divide f_0 by f_1 and denote the remainder by $-f_2$. Divide f_1 by f_2 and denote the remainder by $-f_3$, continue the process until f_n is a constant. To illustrate,

$$\begin{aligned} f_0 &= Q_1 f_1 - f_2 \\ f_1 &= Q_2 f_2 - f_3 \\ &\vdots \\ &\vdots \\ &\vdots \end{aligned} \quad (B-4)$$

$$\begin{aligned} f_{n-2} &= Q_{n-1} f_{n-1} - f_n \\ f_{n-1} &= Q_n f_n \end{aligned}$$

To actually compute the coefficients of the polynomials f_i , we suggest forming the following table:

a_0	a_1	a_2	a_3	a_4	...
b_0	b_1	b_2	b_3	...	
\bar{c}_0	\bar{c}_1	\bar{c}_2	...		
c_0	c_1	c_2	...		

where the a_i 's ($i=0,1,2,\dots,n$) are the coefficients of the original polynomial $f_0(x)$. The b_i 's ($i=0,1,2,\dots,n-1$) are the coefficients of $f_1(x)$. The \bar{c}_i 's ($i=0,1,2,\dots,n-1$) are given as

$$\bar{c}_i = b_0 a_{i+1} - a_0 b_{i+1} \quad (\text{B-5})$$

and the c_i 's are the coefficients of $f_2(x)$ which are given as

$$c_i = \bar{c}_0 b_{i+1} - b_0 \bar{c}_{i+1} \quad (\text{B-6})$$

Similarly the coefficients of $f_i(x)$ ($i = 3, 4, \dots, n$) can be computed. Once these functions are constructed, it can be shown that they form a Sturm sequence [63] with the following properties:

- i) For any value $x_0 \in [a,b]$ at which $f_i(x) = 0$, we have $f_{i-1}(x_0) \cdot f_{i+1}(x_0) < 0$.
- ii) The last function in the sequence $f_n(x)$ does not vanish for any $x \in [a,b]$. Also, it is required that $f_0(x)$ does not vanish at the end points of the interval $[a,b]$.

Note that any given row of the above table can be multiplied or divided by any nonzero real constant without affecting the properties of the functions $f_i(x)$.

Theorem (Sturm):

Let the functions $f_0(x)$, $f_1(x)$, $f_2(x)$, ..., $f_n(x)$ be a Sturm sequence and let $V(x)$ represent the number of variation of sign of the sequence at x , then the number of real roots in the interval $[a,b]$ is exactly $V(a) - V(b)$ with repeated roots counted only once.

A proof of this theorem can be found in [62].